SCHOOL OF GEOGRAPHICAL AND EARTH SCIENCES

MSc DISSERTATION

Natural and Anthropogenic Factors Controlling Algae Growth in the Ythan Estuary, Aberdeenshire

2014-15

1003524

1003524

University of Glasgow

School of Geographical and Earth Sciences

COVER SHEET FOR DISSERTATION

Declaration of Originality

Name:……

Matriculation Number:……..

Course Name:……..

Title of Dissertation):……..

Number of words……

Plagiarism is defined as the submission or presentation of work, in any form, which is not one's own, without acknowledgement of the sources. Plagiarism can also arise from one student copying another student's work or from inappropriate collaboration. The incorporation of material without formal and proper acknowledgement (even with no deliberate intention to cheat) can constitute plagiarism. With regard to dissertations, the rule is: if information or ideas are obtained from any source, that source must be acknowledged according to the appropriate convention in that discipline; and any direct quotation must be placed in quotation marks and the source cited immediately.

Plagiarism is considered to be an act of fraudulence and an offence against University discipline. Alleged plagiarism will be investigated and dealt with appropriately by the School and, if necessary, by the University authorities.

These statements are adapted from the University *Plagiarism Statement* (as reproduced in the *School Undergraduate Handbook*). It is your responsibility to ensure that you understand what plagiarism means, and how to avoid it. Please do not hesitate to ask class tutors or other academic staff if you want more advice in this respect.

Declaration: I am aware of the University's policy on plagiarism and I certify that this piece of work is my own, with all sources fully acknowledged.

Signed:……

Abstract

The Ythan Estuary in Aberdeenshire is a Site of Special Scientific Interest due to the numerous protected species which incorporate it into their ecosystem. In recent years algae growth in the estuary has been seen to increase, causing concern over the integrity of the estuary as a habitat for wildlife. By examining sediment, river flow, nutrient levels and temperature it is possible to identify the driving factors behind this increased algal growth. Using data gathered in the field as well as historical climate data the contribution of each of these factors to algae growth can be determined.

Acknowledgements

I would like to acknowledge a number of people without whom this study would not have been possible. From SEPA Clare Scanlan and Kirsten Gray provided much of the data that were used through this paper. Kenny Roberts and my fellow postgraduates Khruewan Champangern and Charlie Gilles for their help in fieldwork as well as assistance with analysing the data. Peter Chung, John Gilleece and Les Hill for their help in preparing and imaging my samples. Finally Trevor Hoey who provided assistance, support and helped to make sense of my data when there was none to be seen.

Contents

Chapter 1. Introduction

The problem of algae growth and eutrophication in British waters is being acknowledged as a much more pressing issue as the environmental impact on protected and controlled waterways is understood. This rise in the amount of algae observed as well as its impact on the environments they inhabit can be attributed to human changes in watersheds. Groundwater and overland flow from agricultural areas, as well as direct outputs from industry and urban areas, lead to increased concentrations of nutrients in the waterways (notably nitrates and phosphates) which facilitate algae growth. In order to introduce legislation which will protect these areas from excess algae growth, the links between nutrient input, transport, deposition and output must be understood. This paper considers only the growth of macroalgae in the estuary, and not that of microscopic microalgae, and hypothesises that this growth is controlled by a mixture of natural and anthropogenic factors and the interactions between them, notably sediment type and size; river flow; air temperature and water nutrient concentrations. This study aims to gain a better understanding of how these processes interact, affecting the growth of algal blooms within the environment of the Ythan Estuary in Aberdeenshire. This site was chosen due to its designation by Scottish Natural Heritage (SNH) as a Special Protection Area owing to its use as a nesting ground for protected wildfowl including Terns, Eider and Pink-Footed Geese, and the increased presence of algae in recent years. A map of the site area can be seen in Figure 1.1.

Figure 1.1-Site map of the Ythan Estuary, Aberdeenshire (57°19'N, 1°59'W). Inset shows location of Ythan estuary (blue box) within Scotland (Source: Digimap, 2016)

Image 1.1- View of the Sleek of Tarty, looking upstream from the A975 Road Bridge

Image 1.2- View of upper estuary, looking upstream from the bridge at Kirkton of Logie Buchan

Image 1.3- Macroalgae growth in the Sleek of Tarty

1.1- Aims

Through analysis of sediment samples this study aims to examine each of the above factors individually. This analysis will provide an understanding of the distribution of sediment throughout the Ythan Estuary and the controls on the grain size of sediment deposits. These sediment samples were collected from inter-tidal areas during two separate surveys of the Ythan estuary. Firstly, surface sediment samples were collected by the Scottish Environmental Protection Agency (SEPA) during a survey of algal growth on the estuary in August 2014. Secondly, deep cores were taken during fieldwork in November 2014. Dating of the sediment cores will provide an in-depth understanding of varying deposition rates through the different depositional environments of the estuary. Water samples will be taken to provide an understanding of the nutrient concentrations of water entering, circulating and exiting in the estuary, as well as an understanding of the nature of mixing between freshwater and seawater inputs in the Ythan. Finally, climate data in the form of discharge rates and temperature for the surrounding area will be collected to better understand the impact that changes in seasonal and annual climate have on the year to year algae growth in the Ythan.

1.2- Site Introduction

The Scottish Natural Heritage (SNH) review of the Ythan provides a good description of the physical characteristics of the estuary. The following information on the site is taken from SNH (1996) unless otherwise stated. The total size of the catchment area of the River Ythan and its tributaries is approximately 650 km². The tidal Ythan estuary extends to Waterton, 11km upstream from the mouth of the Ythan river, while the intertidal area covers approximately 1.85 km² (Balls *et al*,1995). The largest intertidal mudflat is found at the Sleek of Tarty on the right bank of the estuary, seen in Image 1.1. A spring tidal range of 3.1m means that the Ythan estuary is classified as mesotidal. The main land use of the catchment is agriculture, covering approximately 95% of the total area. The physical estuary characteristics include a sheltered beach composed of coarse dune sand at the mouth, and an elongated tidal basin. A peninsula at John's Hole Point protects the estuary sediments from most incoming wave energy, as evidenced by the presence of large areas of intertidal mud. The estuary along with the Sands of Forvie at the mouth are designated as nature reserves due to breeding fowl, and as such it remains one of the least modified estuaries in Scotland. The main channel in the estuary has migrated very little during in the documented history. This is believed to be due to a trench or buried channel in glacial deposits which controls the alignment (SNH, 1996).

The sedimentary inputs to the estuary control the characteristics of the intertidal zones. A large, protected dune system, the Sands of Forvie, exists on the left bank near the mouth of the estuary. There is also a system of spit bars at the coast, formed from longshore drift caused by prevailing winds. From these two sources, coarse sediment is spread by aeolian processes over the lower courses of the estuary. As a result, the supratidal and intertidal sediments near the mouth of the estuary are observed to be much coarser than those found

further upriver. Tributary inputs from the Tarty Burn and Burn of Forvie create gravelly lag deposits in deltaic formations which prograde onto the intertidal mudflats. From these inputs finer sediments are also deposited in upstream segments of the estuary. Figure 1.2 shows the sedimentary layout of the Ythan estuary.

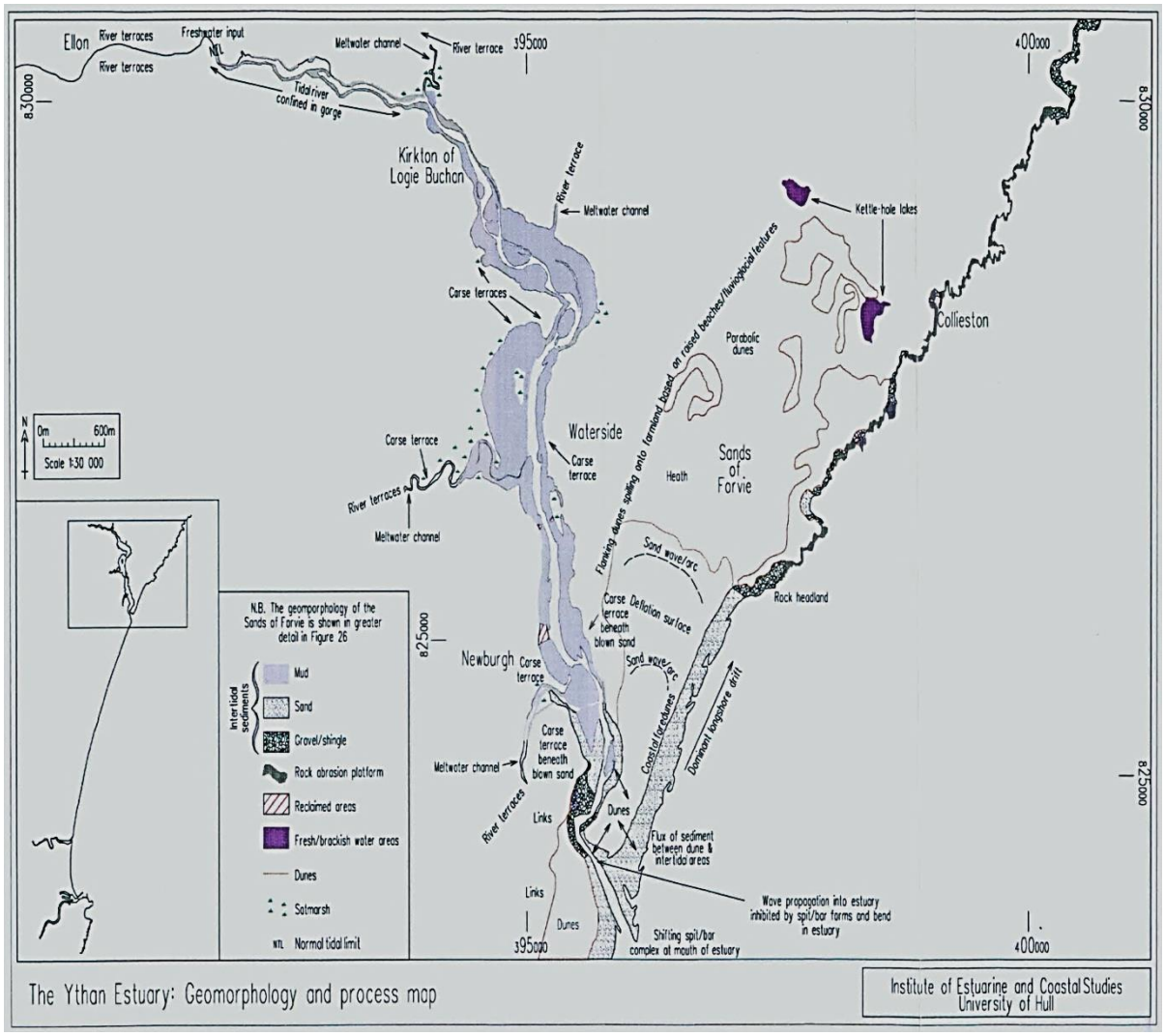

Figure 1.2-Sedimentary map of the Ythan Estuary (University of Hull, via SNH, 1996)

Winds have a limited impact on the Ythan estuary. This is due to the channel running perpendicular to the prevailing wind direction, which data from the nearest weather station at Dyce indicates as WSW. Additionally, the average width of the estuary is around 300m which means there are very few internally generated waves due to a short fetch length, causing minimal redistribution of sediments. However, these winds do lead to the creation of spits, bars and near shore banks at the estuary mouth which act as an important sediment source as they are then redistributed to the estuary and Sands of Forvie.

Though human disturbances to the physical estuary are minimal due to its protected status, it has been designated as a Nitrate Vulnerable Zone (NVZ) due to the growing problem of eutrophication (Domburg *et al*, 1998). From 1959, grazing on the Sands of Forvie has been prohibited, allowing growth of anchoring flora. There is also an on-going issue with siltation, leading to channel constriction, upstream of the Waterton Bridge, where sediment flow is obstructed by the bridge supports. Inputs in the water of the estuary include sewage treatment works at Ellon which have been using the Ythan River as an output since 1978. An upstream poultry factory also releases liquids and organic waste which are transported into the estuary. During periods of high slack water, the sewage outputs and poultry effluent combine in the upper reaches of the estuary. These inputs result in the addition of nitrates, silicates and phosphates into the estuary, with concentrations for each peaking at different times of year depending on their time of application. Pugh (1993) created a nutrient budget for the estuary, stating that 48% of P and 2% of N input to the estuary occurred as a result of the sewage treatment works at Ellon. This figure in 1967 was 10% for P and 1% for N. The budget also stated that the majority of N sources were diffuse, from atmospheric and terrestrial inputs. Figure 1.3 below, from Balls *et al* (1995), shows the increasing nutrient

concentrations in the estuary over time. These increases coincide with the national increase in the use of chemical fertilisers over that time, including a 6 fold increase in nitrogen fertilisers across the UK (Balls *et al* 1995).

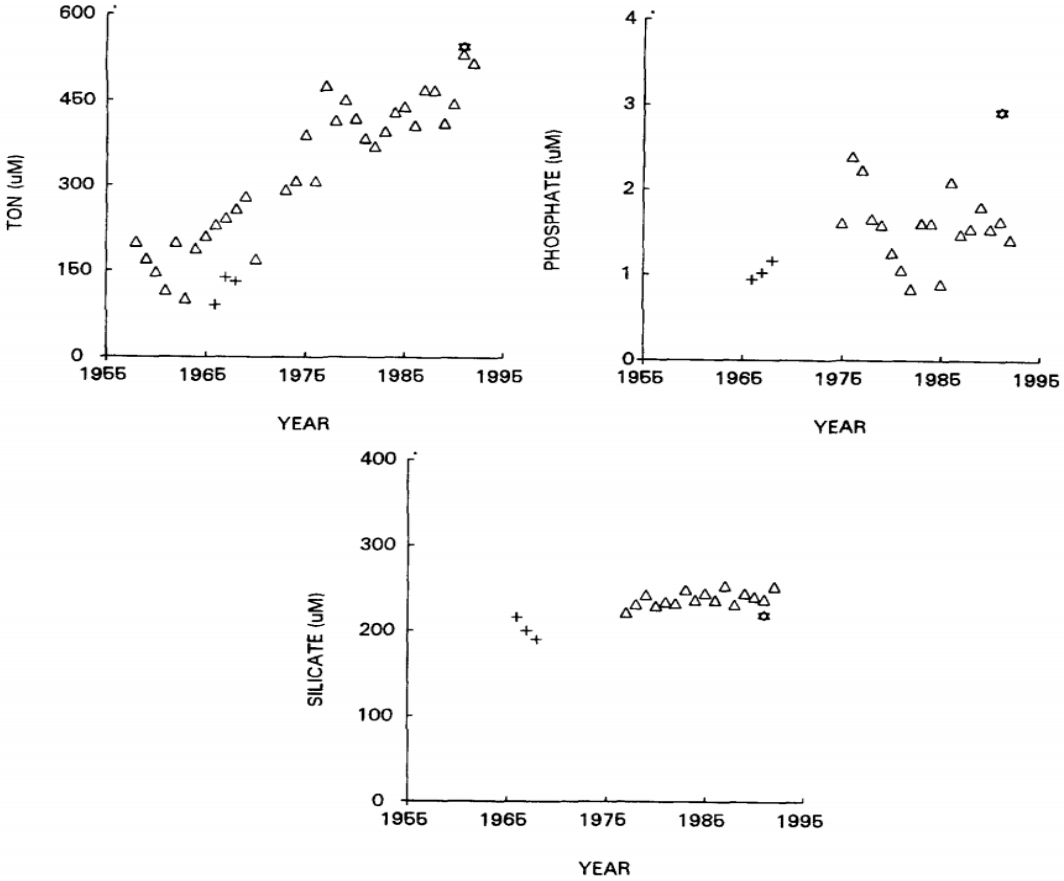

Figure.1.3- Nutrient concentrations in the Ythan estuary 1955-1995 from Leach (1969)-△ - and NERPB- + -(Balls *et al*, 1995)

Rafaelli (1999) and Balls *et al* (1995) are authors of two papers which describe the current state of eutrophication and algae growth in the Ythan estuary. Balls *et al* (1995) state that, due to the agricultural nature of the catchment, the River Ythan has some of the highest concentrations of nitrate in any major Scottish river. Organic N concentrations in the Ythan river have increased from "…ca 100-15µM in the late 1960s to ca 500-550 µM in the early 1990s." (Balls *et al.* (1995). Surveys conducted by SEPA on the estuary, as well as the paper by Rafaelli (1999) describe "…three main types of green macro-algae on the Ythan estuary mudflats: *Enteromorpha* spp., *Ulva lactuca* and *Chaetomorpha linum". Enteromorpha* is explained to occur throughout the estuary, while the other two types are found mainly in the middle-to-upper reaches. The findings in Rafaelli (1999) regarding the location and extent of macroalgae in the estuary are examined by Green (2005) who uses geospatial analysis of the colour photographs used by in the original study to confirm these, though he does state that density and species data need to be collected by field studies. This distribution is explained in the paper as being a result of mixing of fresh and sea water, along with the tolerances of each type of algae. In the Ythan, algae in the upper reaches are exposed to freshwater and its associated high nutrient concentrations for a much longer period over the tidal cycle, while algae closer to the estuary mouth will experience freshwater contact for much less time, varying from day to day according to tidal and weather conditions (Figure 1.4).

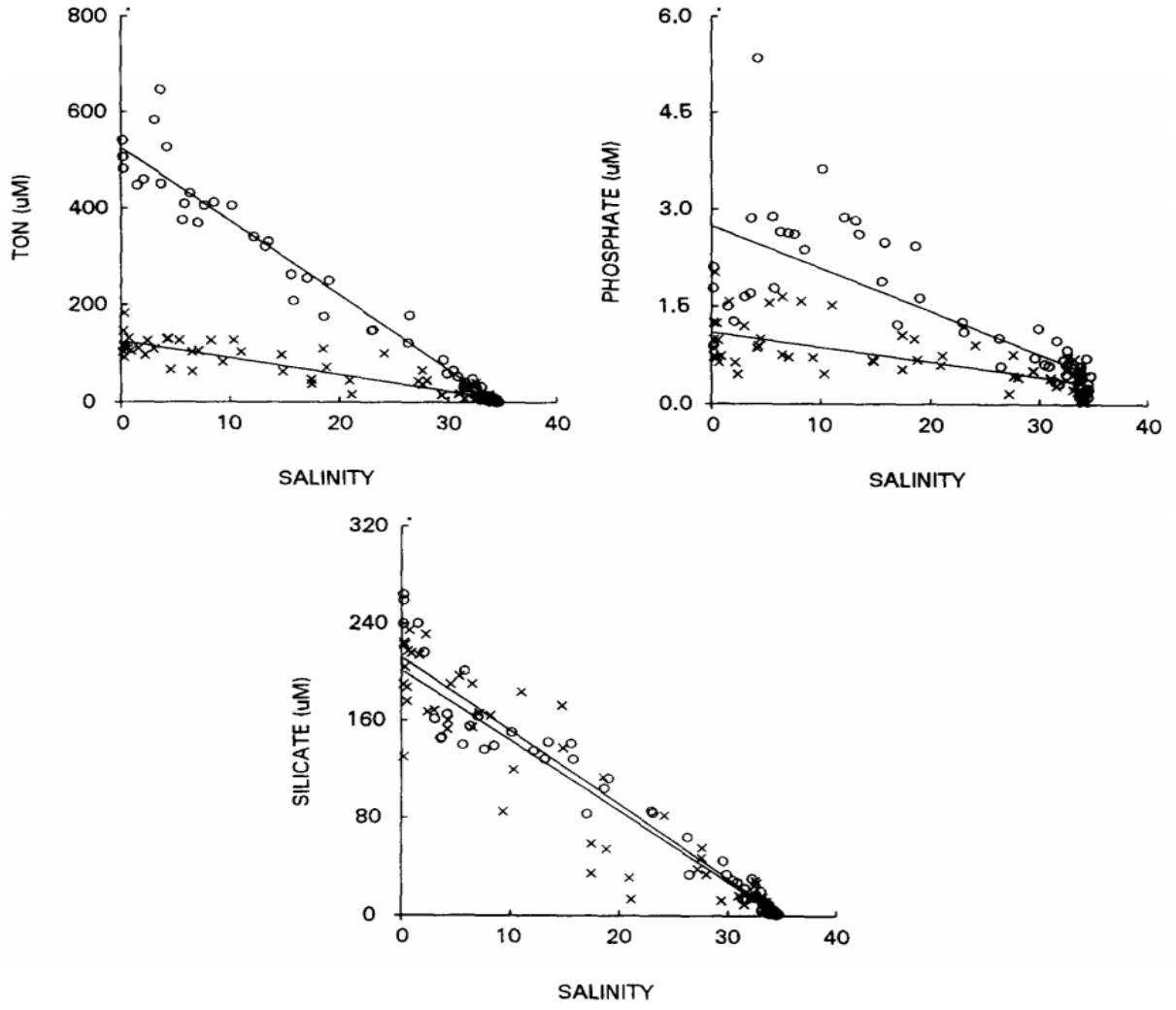

Figure 1.4-Nutrient concentrations versus Salinity for 1967- x - and 1991/92- o - (Balls *et al*, 1995)

Rafaelli (1999) states that the algae begin to grow in April, while peak algal biomass in the estuary occurs around August. The study concludes by stating that "…the three most frequently cited explanations for blooms of macro-algae in shallow waters are excess nitrogen, excess phosphorus and changes in the estuary's bathymetry and hydrography." However, there is little evidence of large-scale phosphorous change in last 30 years, while the bathymetry has remained unchanged since the earliest recordings in the 1880s. The paper states that the most likely scenario for the observed increase in algal biomass would be a shift in farming practices towards more N-demanding crops, with a greater rate of application of N to these crops. This would then result in an increase in N levels in the river and the estuary which would explain the increase in the biomass and distribution of macro-algal mats. One anomalous season detailed in the study occurred during 1996, where occurrences of algal mats were much depleted from the previous year. Rafaelli (1999) hypothesises that flooding in the previous autumn removed much of the algal material in the estuary that, while in decline, would provide the basis for the algal blooms in the coming spring.

Chapter 2- Literature Review

2.1-Estuaries

The term estuary describes an environment where marine and fluvial processes mix, so in order to understand the active effects in the Ythan estuary, this environment must be better understood. Estuaries are defined as semi-enclosed and coastal bodies of water which can communicate freely with the ocean, and in which the ocean water is diluted by freshwater of a terrestrial origin (Cameron and Pritchard, 1963). However, within this definition, estuaries vary greatly and thus can be further categorised based on their water balance, geomorphology, vertical salinity structure, and hydrodynamics (Valle-Levinson, 2010). The morphological changes in estuarine environments are described in Karunarathna *et al* (2007), who state they exist as "complex physical systems" where sediments are subject to waves, tides and river flow. As such, the morphology is controlled by the response of the shore and sea bed to these mixed forces, as well as the local sediment characteristics and geology.

Time scales of evolution in estuaries can vary from hours to millennia. The post-glacial Ythan estuary has been altered due to changing conditions over varying time periods. A bathymetric study in Karunarathna *et al* (2007) shows alternating periods of accretion and erosion in outer and middle regions of the estuary, which is important to consider when observing rates of deposition in the Ythan during this study. Temmerman *et al* (2012) also provide insight into short-term changes in estuarine evolution. The paper describes the effect that changes in platform vegetation can have on flow rates and transport in estuaries. Results in this article describe how removal of platform vegetation led to a 2-4 times

increase in flow velocities across the platform, while channel velocities were seen to reduce by a factor of 3. As a result, platform sedimentation drops while channel infilling increases. The results of Temmerman *et al* (2012) are relevant to this study as changing vegetation would be expected to impact upon the deposition of sediment, and therefore nutrients, in the estuary. D'Alpaos *et al* (2007) model the changing morphologies of estuarine systems. This model relies on rates of sediment erosion and deposition and the presence of vegetation as well as tidal forces and changing sea levels. Longer term scales of evolution in the estuary, as a result of post-glacial recovery, should also be considered. The first factor to acknowledge would be sea level rise. Since the end of the last ice age (16kY BP), sea levels have risen steadily. Shennan *et al* (2002) describe known relative sea levels around Britain since the last glaciation. The site with the nearest and most relevant available data to the Ythan estuary is Wick. The Wick graph from Shennan *et al* (2002) is used in this instance due to the long time period shown as well as the similarities between sea levels at Wick and Aberdeen observed in recent measurements, as shown in Rennie and Hansom (2011). The data show that there has been a near-steady rise in relative sea level since 16kY BP at Wick (Figure 2.1). This is due to the greater availability of water being released from terrestrial sources such as ice caps and glaciers. This rise has slowed and can be seen to be in decline since 4k ya as isostatic rebound has caught up to and overtaken rising sea levels.

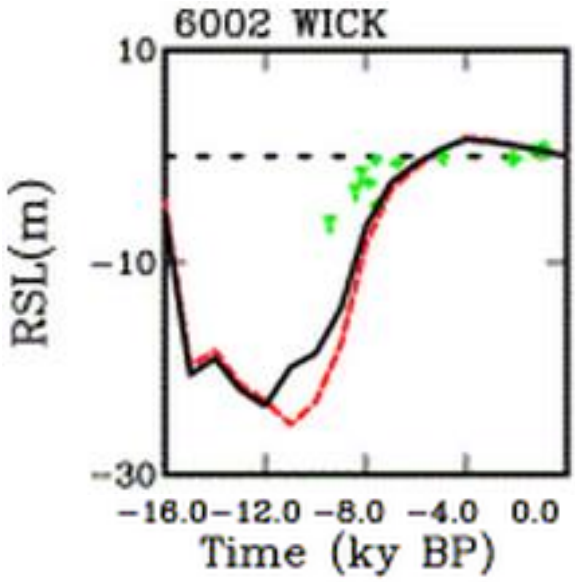

Figure 2.2-Sea level rise at Wick (16k ya-present)

Maier *et al* (2008) state that estuaries are among the marine systems most at risk from eutrophication as they have very little interaction with the adjoining pelagic waters. Due to this, many studies have tried to quantify the rate of change in nutrient concentrations in global water bodies. Jaworski *et al* (1997) estimate that "…human activities have increased N fluxes to coastal rivers of the NE United States by 5 to 14 times their natural rates." Heathwaite *et al* (1996) state that N and P levels of water bodies in many areas of Europe and the UK are now greater than 20 times the background concentrations while Conley (2000) estimates that P loading to estuarine systems has increased by 2-6 times since 1900. Retrospective analyses are further discussed in Conley (2000), showing that a first wave of the coastal eutrophication problem may have occurred during the 19th century, when industrial activities increased the input of N and P into river systems in Western Europe. Nitrogen loading is examined in conjunction with algal biomass and is found to account for only 36% of variance, therefore the paper concludes that N loading alone cannot be used as a predictor of algal growth. An example used in this paper is the case study of the

Chesapeake and San Francisco Bays. San Francisco Bay is seen to have higher P and comparable N to Chesapeake Bay, but much less chlorophyll activity and no problems with hypoxia/anoxia. Cloern (2001) also examines the problem of predicting algae growth using nutrient input data. The paper describes a simple model, produced by Vollenweider (1976), which modelled P vs Chlorophyll in lakes, accounting for lake morphometry and hydraulic residence time. This model was found to describe 75% of all observed variability in chlorophyll concentrations. However, Cloern (2001) also describes the attempted modelling of algal biomass as a function of N input through landuse by Meuuwig (1999) in 15 Canadian estuaries. The study concluded that chlorophyll yield, per unit N delivery, was found to be 10 times lower than predicted in comparable lake systems. These studies, among others, highlight the issues with trying to model nutrient-driven algae growth in estuarine systems.

2.2- Sedimentation

Rates of sedimentation in estuaries vary through differing timescales, from long-term sea level and sediment availability changes and by shorter term physical and biological factors. Deposition sequences can be identified which point to post-glacial sea level rise as the main factor. In a longer timescale, Schlager (1993) states that stratigraphic sequences, and the systems tracts which divide them, can be interpreted as the result of glacial sea-level cycles superimposed on a steady rate of subsidence. He further mentions that factors such as short-term variations of subsidence, climate and sediment supply are to be regarded as modifiers rather than the dominant controlling processes in producing the sequences.

In order to understand the sedimentary environments of the Ythan estuary, we must first investigate the processes by which sediment is transported and deposited through estuarine environments. Some texts which deal directly with these processes include Allen *et al* (1980), Dronkers (1986) and Officer (1980). The confluence of fresh and saline water in estuaries is an important driver of sedimentation, since it provides the longitudinal and vertical density gradients during mixing, which in turn generate the estuarine density-driven circulation. Mixing of fresh and saline water is affected by turbulence, which intensifies diffusion. This turbulence is generated by currents arising from river flow, tides, or both (Allen *et al*, 1980, Dronkers, 1986). Tidal influences can also impact deposition of sediment as described in Allen *et al* (1980). This effect is caused by the change in ratio of river flow to tidal volume during the spring-neap tidal cycle. During spring tides, a residual accumulation of water, and therefore deposition of sediment, is observed. The time of sampling will be important to consider when testing water from the Ythan as the turbidity and suspended material is known to change based on the tidal cycle (Uncles et al, 2002).

Widdows *et al* (1998) cover the deposition of sediment in intertidal mudflats, using a portable, *in-situ* annular flume to measure rates of biodepostion, sediment erosion and re-suspension. The controls on deposition include "…particle size and density, water and organic content, cohesiveness of sediment, depositional history, air exposure and biological activity." (Widdows *et al.* (1998)). The study focuses primarily on biological activity, splitting macrofauna into two groups, and shows how sediments can be alternatingly fixed, by benthic organisms, or destabilised. Results from this study show a clear correlation between erodibility of sediments and bioturbation. This destabilisation was further monitored and shown to be highest in pools and gullies, where bioturbation is high during low tides. Grabowski *et al* (2011) further examine the erodibility of sediments. This is an important area to understand in relation to the Ythan, as nutrients are fixed within deposited sediment, which is shown in the mineralogical analysis undertaken by Stove (1978) which highlights the ability of certain minerals in the Ythan Estuary to form flocs and consolidate, particularly in the upper part of the Middle Ythan Estuary. Grabowski *et al* (2011) describe erodibility as an attribute of the sediment itself, which is dependent on sediment properties which control "…resistive forces in the sediment, such as gravity, friction, cohesion, and adhesion". Average particle size is widely used as a predictor of erodibility and is summarized in the Postma diagram found in Appendix 1. However, shear stress is a more reliable measure of erodibility due to the muddy nature of estuarine sediments, and this is shown in Figures 2.2 and 2.3 below. Figure 2.2 shows how eroding pressure increases with grain size while Figure 2.3 describes the non-linear relationship between eroding pressure and critical shear stress for suspension. The article states that "adding clay to a sand bed makes it more resistant to erosion, up to a maximum erosion threshold at 30–50% clay". Density of sediment beds is

negatively correlated with erodibility. Dense sediment beds are seen to have lower erosion rates, up to 100 times lower and higher erosion thresholds, up to 5–8 times higher than less dense beds.

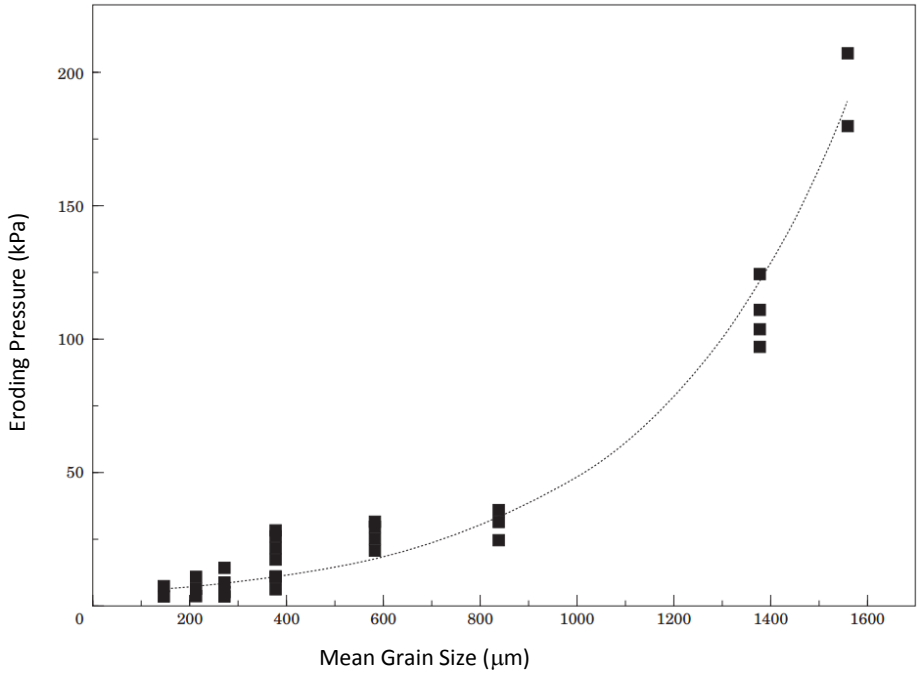

Figure 2.2-Mean grain size vs. Eroding Pressure (from Tolhurst *et al*, 1999)

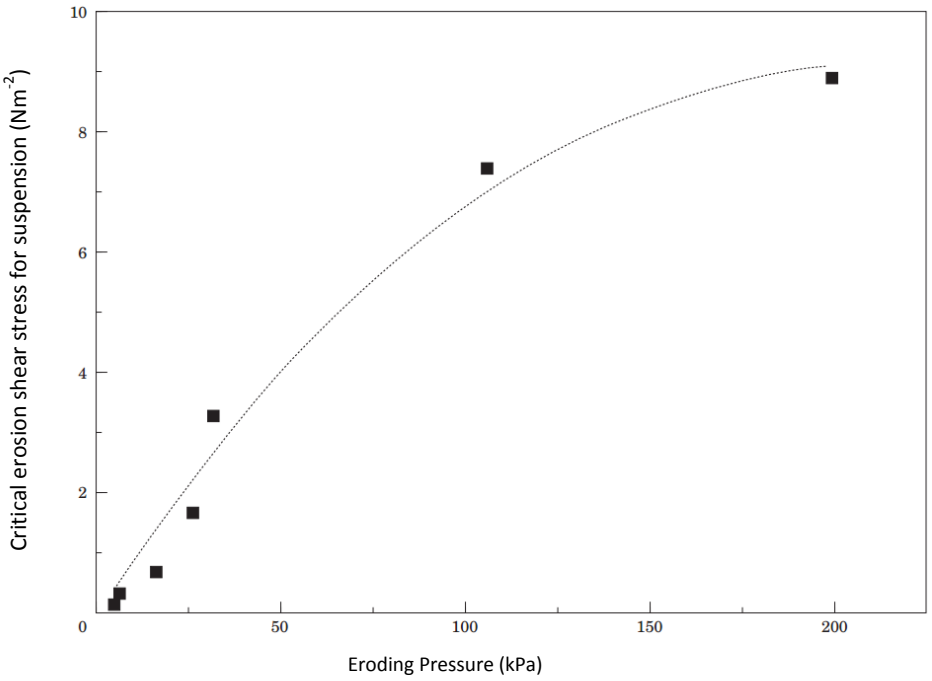

Figure 2.3- Relationship between eroding pressure and shear stress (from Tolhurst *et al* 1999)

However, the article then goes on to describe the impacts that other factors have on erodibility. Multiple studies have been conducted which link erodibility with changes in temperature. Kelly and Gularte (1981) shows that erodibility increases by a factor of 3 with a change in temperature from 10°C to 30°C. There are two hypotheses as to why this happens. Firstly, increasing temperature may cause a weakening of inter-particle bonds, resulting in higher erodibility. Secondly, temperature increases may cause a lower viscosity of pore water, leading to a higher permeability of the sediments and greater velocities at the bed surface (Grabowski *et al*, 2011). Finally, the paper refers to other factors which may, but have not been conclusively shown to, affect erodibility. These include salinity, pH and presence of metals in the sediment.

2.3- Eutrophication and Algae Growth

The focal point of this study is the growth of floating algal mats in the Ythan estuary. Algae, along with bacteria, are one of only two organisms in aquatic systems which rely solely on the transport of dissolved substances through the water (Jansson, 1988). Among these substances, many different forms of dissolved N and P (mainly orthophosphates) are utilised by algae for growth. Flindt *et al* (1999) provides good information on the occurrence of algal mats. The paper describes algae growth as a "self-accelerating system", whereby algal mats begin by growing on the bed in estuaries with photosynthesis controlled by light availability. However, in instances where there is low light, respiration is greater than the oxygen generated by photosynthesis, thus creating anoxic conditions which kill algae and invertebrates in the surrounding area, adding nitrogen and phosphorous to the cycle and leading to increased algal growth. This removal of species also aids algal advance in two ways. Firstly, bare bottom sediment has higher phosphate concentrations than in vegetated areas, where there is uptake by plant roots as oxygen is released. Secondly, the loss of invertebrates removes potential grazers from the growth area.

Pihl *et al* (1999) also provide a good insight into this area. The paper examines the distribution of algae mats in the Swedish Skagerrak archipelago in relation to nutrient sources. This three-year study, which looked at nutrient input and used aerial photography to observe algae cover (defined as cover of ≥5%), took place from 1994-1996, and found that the distribution of algae was similar over the observed period, and seemingly unrelated to nutrient inputs from point sources and tributaries. The study instead found that the main factor controlling this growth was exposure to wind, waves and water exchange as nutrient loads among the embayments were essentially unlimited. The paper also states that "…in

shallow coastal areas with limited water exchange, such as the Swedish Skagerrak, organic matter from decomposed algae can accumulate and…constitute the basic pool for future algal production". Because of this, growth of algal mats on soft bottoms could be self-regenerating.

This self-accelerating, unchecked algal growth is of concern due to the anoxic and eutrophic conditions that they create. Cloern (2001) describes eutrophication as "…the myriad biogeochemical and ecological responses, either direct or indirect, to anthropogenic fertilisation of ecosystems at the land-sea interface." Boesch (2002-1) describes how algal growth is controlled in this instance by a greater availability of N and P nutrients, increasing primary production of phytoplankton. Rafaelli *et al* (1998) describe how N concentrations are often attributed as the most limiting factor to algae growth, due to its low availability in coastal waters compared to other nutrients. However, changes in P concentrations as well as changes in hydrography are also shown to increase the proliferation of algal blooms. This increase reduces the clarity of the surrounding waters and results in a higher amount of organic material being deposited into bottom waters and sediment. Decomposition of this increased organic matter results in a depletion of dissolved oxygen (hypoxia) in stratified bottom waters to levels too low to sustain fish and invertebrates, leading to decreased species diversity. Lower levels of water clarity may also eliminate seagrass and microalgal meadows that provide important habitats. Boesch (2002-2) further explains that "…in shallow coastal waters with ample light penetration, eutrophication can cause proliferation of macroalgae which smother benthic organisms and decompose to reduce oxygen levels". Another factor raised in Rafaelli (1998) is that of seasonal flow. The paper explains that in a case study, low algal mat coverage was recorded in the summer of 1996. It then goes on to hypothesise that this low coverage is thought to be due to a major hydraulic event the

previous October (1995) where a period of heavy rainfall increased river flows dramatically leading to widespread flooding within the catchment. Macroalgae are in their decline phase in October, leaving substantial amounts of material normally overwinter in order to provide the impetus for the next summer bloom. However, it is predicted that the flooding removed much of this overwintering biomass, decreasing the amount of material which would normally begin a new algal population in the summer. This factor will be further examined in this study to see whether it has had any impact on the observed algae growth in the Ythan Estuary.

2.4- Nutrient Budget

Nutrient budget and fluxes are important to understand when considering algal growth in the Ythan Estuary. Domburg *et al*. (1998) discuss the specific nutrient budget of the Ythan estuary. The study states that, due to changes in farming practices in the watershed over the monitored period, NO_3 concentrations in the River Ythan have increased from 2.5 mg/l in the 1960's to 7.5 mg/l by 1995. D'Elia *et al* (1985) describe how primary productivity in freshwater environments is generally P limited, while productivity in marine waters is generally N limited. Estuaries, however, provide an interesting mix of marine and freshwater influences which make the impact of nutrient flux harder to quantify. Nutrient and material exchanges between subsystems (intertidal, sub-tidal and marginal) in tidal salt marsh estuarine systems are linked by the tidal creek water column, as shown in Figure 2.4 below.

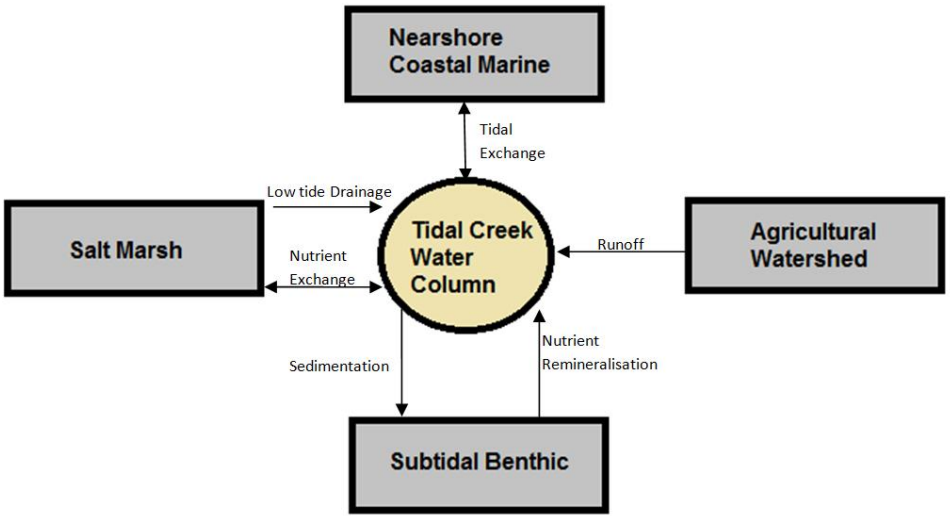

Figure 2.4-System exchanges in Estuaries, after Childers *et al* (1993)

Results from Childers and McKellar (1987) show that water column processes which relate to phytoplankton production and N cycling account for much of the seasonal variability seen in phytoplankton biomass and inorganic N concentrations (Figure 2.4). The specific driver of

these transfers between the tidal creek water and other subsystems is tidal hydrology, and thus the amount of transfer is dependent on the tidal forces specific to each site. Nutrient inputs into the tidal creek water system are controlled by incoming forces of freshwater and marine systems. Typically, in spring and winter months the systems experience high freshwater input, carrying a surplus of N relative to P compared to that of typical phytoplankton needs. During late summer in low-flow conditions, nutrient cycling plays a much more important role in supply, and the nutrients derived from sediments are quantitatively more important, and have a surplus P to N concentration relative to phytoplankton needs (D'Elia, 1985).

In many estuarine systems, such as the Ythan, the surrounding land is primarily used for agriculture and therefore the watershed is subject to many non-point inputs of P and N nutrients. Carpenter *et al* (1998) describe how farming practices impact nutrient flux. The paper states that nutrient flows to aquatic systems are directly related to animal stocking densities, while excess fertilisation and manure production causes a build-up of P and N in the soil which is in turn transported into the river systems. Vanni *et al* (2001) also examine the impact that agricultural land use has on the nutrient budget of an adjacent freshwater system. It is stated in the paper that in agricultural areas, most P is transported in particulate form, while N is mostly present as nitrates, as shown in Gallagher *et al* (2007), where 99% of observed N in groundwater is present as nitrates. Gallagher *et al* also state that this is due to the chemical properties of the nitrates used in fertilisers, which have high solubility and negatively charged ions to allow greater infiltration through the soil matrix. Further, nitrate concentrations can persist in groundwater for long periods due to high

dissolved oxygen levels and limited microbial denitrifier populations which "…combine to impede dissimilatory nitrate reduction."

Gallagher *et al* (2007) undertook a study in the Chesapeake Bay watershed where agriculture accounts for 36% of landuse, which is comparable but lower than in the Ythan watershed. Groundwater velocities were observed to range from 6 to 200mm/day, so travel time of nutrients would be on the scale of weeks to years, meaning that the discharge of degradable pesticides is much less prevalent than that of inorganic nitrogen compounds. The paper states that approximately 6% of pesticides entering the estuary are as a result of groundwater, while the remaining 94% comes from much more direct overland flow. N fluxes in this study were observed in the order of 1-10mg/m²/hr while pesticide fluxes were calculated to be much lower, at 0.1-1 µg/m²/hr. This high concentration of dissolved N is important to seasonal nutrient flux, as dissolved N can enter into river systems in groundwater during baseflow conditions (Gallagher *et al*, 2007 state that groundwater accounts for 60% of flow in non-tidal streams) while the particulate P is much more dependent on overland flow from storm conditions. N levels in groundwater in the Chesapeake Bay watershed have been found in many cases to exceed the 10 mg/l for acceptable drinking water defined by the US Environmental Protection Agency. However, Vanni *et al* (2001) also state that nutrient fluxes were observed to vary greatly even between watersheds of similar climate and land use, making it difficult to cross-compare systems.

Chapter 3- Methods

3.1-Sampling

Fieldwork was conducted on the estuary in late November 2014. The primary purpose of this was to collect sediment cores from strategic areas of the Ythan estuary. These sediment samples were necessary for data on: a) the nature of sedimentation, i.e. continuous or episodic; and; b) analysis of the sediment layers' nutrient status. The sampling locations were chosen based on maps of algal mat growth (Figure 3.1).

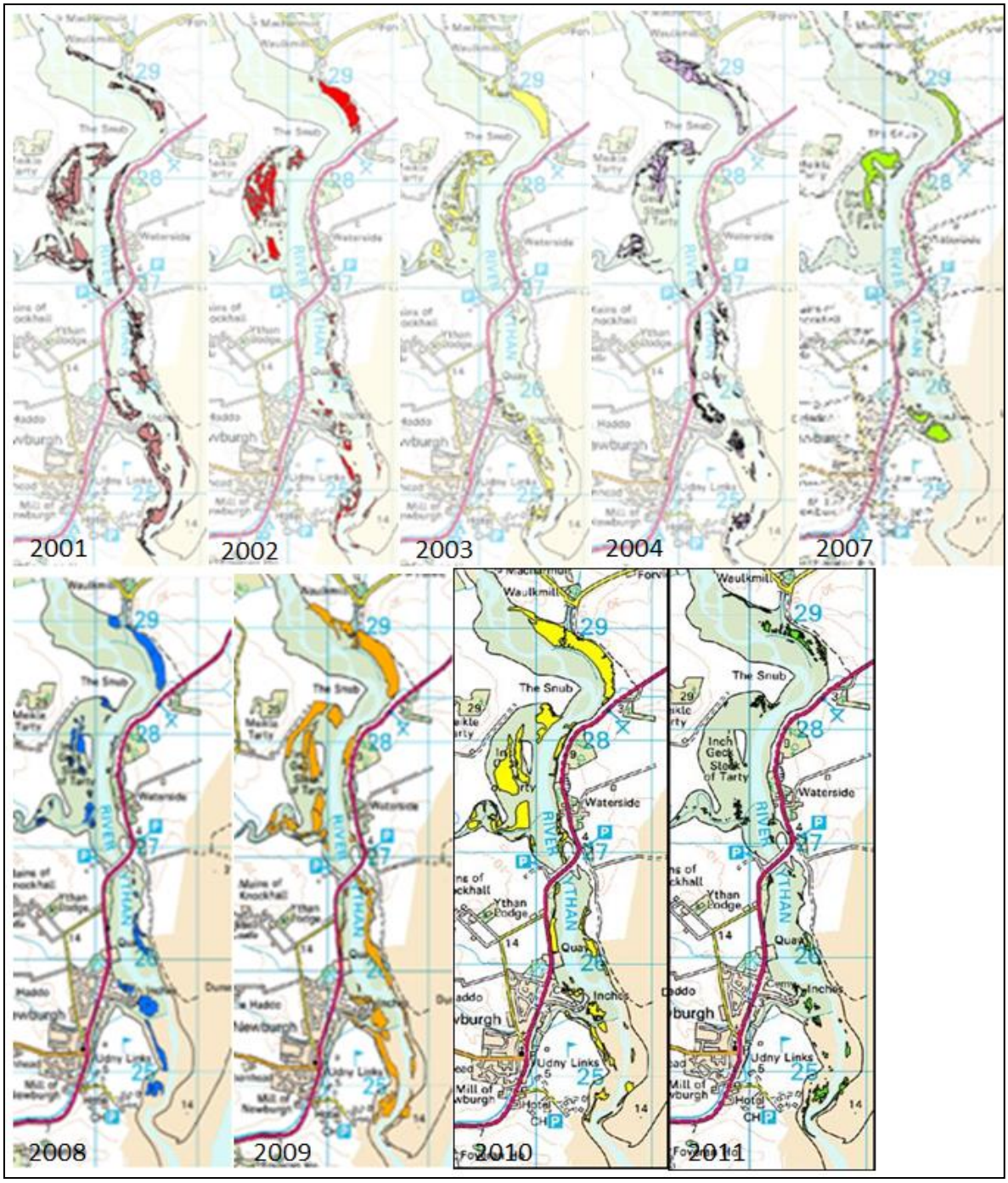

Figure 3.1-Algal Mat Locations by year 2001-2004, 2007-2011 (sepa.org). Different colours are used for different years for clarity.

The maps shown in Figure 3.1 were analysed to find areas with consistent algal growth through the observed period. Further core locations were chosen in areas that experienced little or no algal growth over the observed period in order to compare and contrast the sedimentary characteristics as well as the water quality of these areas. The final sample locations are shown below (Figure 3.3, Table 3.1). Cores were taken using a D-Section (Russian) corer. Coring can have some negative impacts on the integrity of samples. These include core compaction and smearing of surface sediment down the core, as described in Wrath (1936). Jackson (1986) further describes limitations of the coring method including horizon disturbance and sample depth. Due to the fine and cohesive nature of the sediments in the Ythan estuary, coherent cores were able to be taken to adequate depths, and care in removal and storage of the cores ensured minimal horizon disturbance.

The sampling method, described in Vleeschouwer *et al* (2010), involved coring in 0.5m sections through the sediment. Cores of different depths were taken from a different, adjacent hole in order to preserve the natural integrity of the sediment layering. Additionally, each successive core was sampled 50mm above the base of the previous core, leaving an overlap which ensures the data from the ends of cores were replicated in case of damage during transport (Figure 3.2).

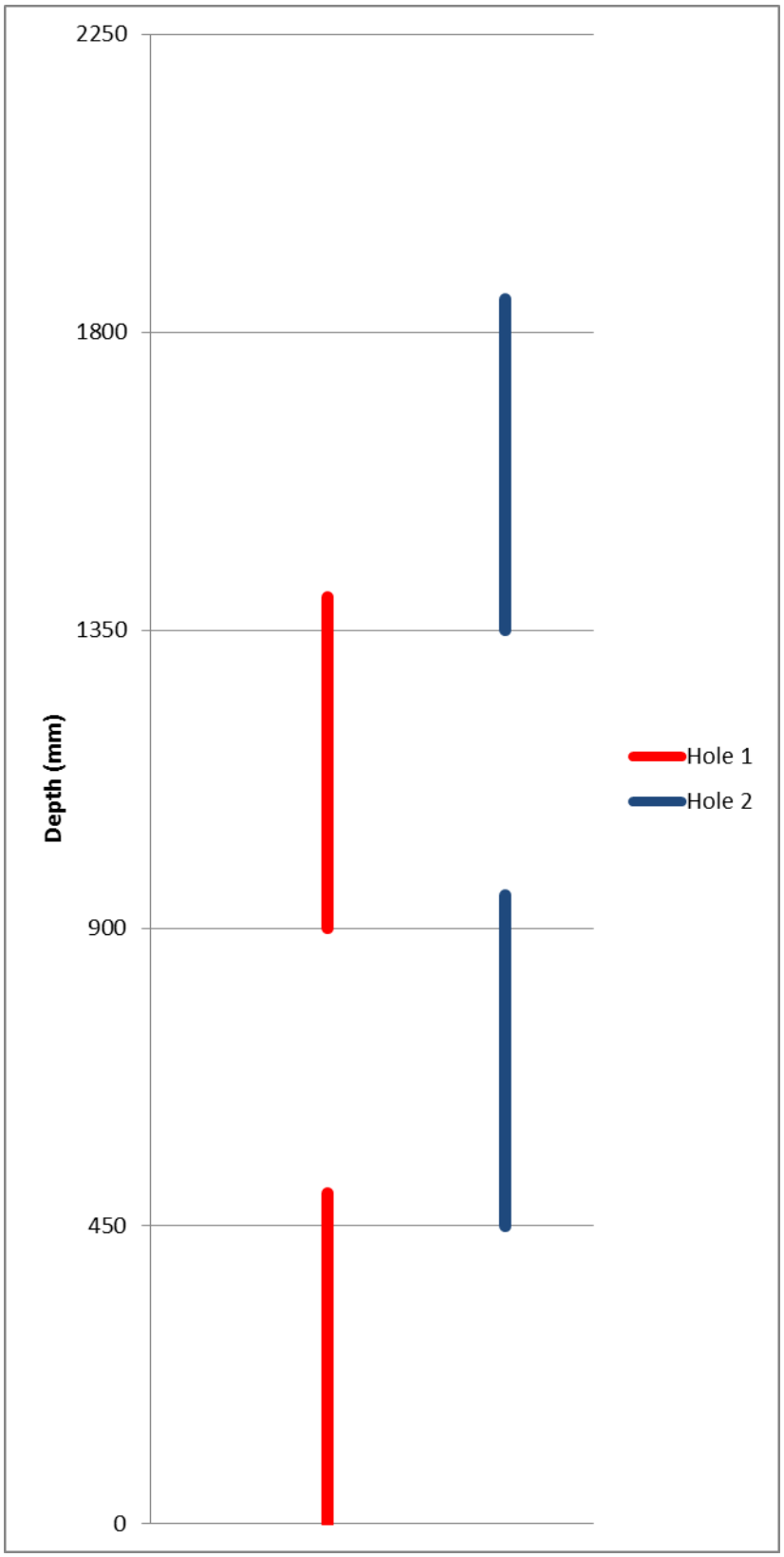

Figure 3.2- Two hole method of sampling with D-section corer

Each core location was sampled to the maximum depth possible. This depth was controlled by the resistive forces in the sediment becoming too great to pass by hand. This sample collection was carefully performed in order to preserve “in situ” conditions of the sediment and ensure it was undisturbed through the sampling process (Baxter *et al*, 1981). This care was necessary to maintain the stratigraphic and chemical integrity of the cores. After sampling, the cores were wrapped in Clingfilm, and the top end of each core marked. They were then wrapped in a protective layer of tinfoil and stored in semi-circular PVC half-tubes for transport. The samples were then returned to Glasgow and kept refrigerated. The sampling locations for each core are shown in Figure 3.3.

Core	Coordinate	Depth (mm)	Surface
L1	57°21'87"N 1°59'72"W	500	Mud
L2	57°21'34"N 2°0'56"W	1750	Mud
L3	57°19'57"N 1°59'43"W	500	Mud
R1	57°20'8"N 2°0'32"W	450	Mud w/pebbles
R2	57°20'40"N 2°0'19"W	950	Mud
R4	57°18'49"N 1°59'37"W	275	Sand

Table 3.1- Coordinates, depths and surface material for 6 cores from the Ythan Estuary

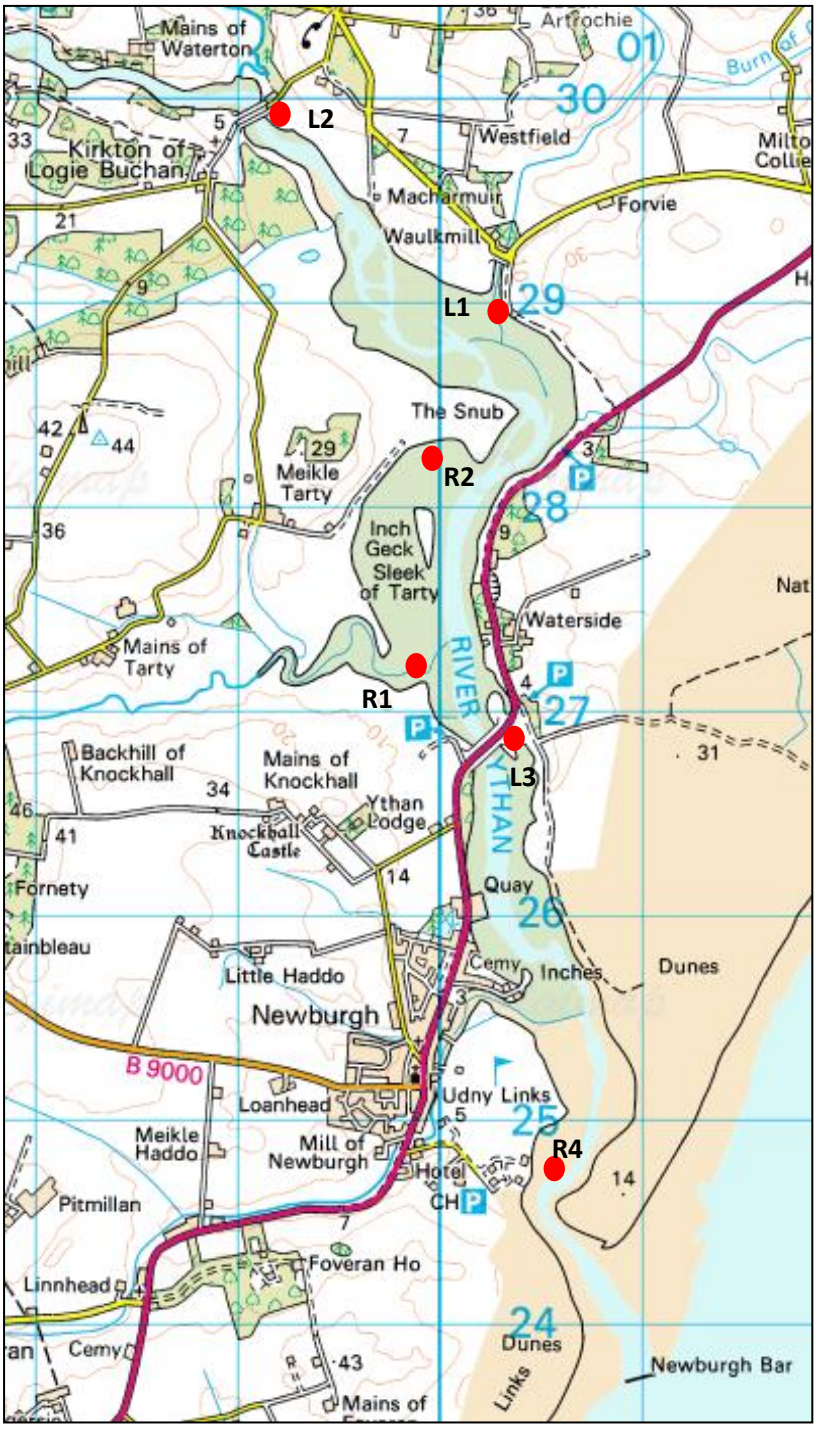

Figure 3.3-Location of sediment cores (1:40,000 OS background map provided by EDINA Digimap)

3.2-Sediment Analysis

Each core was individually photographed and these photographs were then analysed to identify specific layers of interest. Upon viewing, individual layers were identified. Specific layers were sampled, chosen based on either an observed change in colour of the sediment or a change in the grain size. Depending on grain size, the Laser Diffraction (Coulter) analysis method described below can require varying amounts of sediment. To ensure that enough sample was removed for this analysis, a 10mm wide cross section was taken through half of the core, leaving half of the sediment in that layer for future analysis. Each individual sample was labelled according to the core and depth at which they were sampled. These samples, along with surface sediment samples provided by SEPA (Kirsten Gray, August 2014), were further analysed. The SEPA samples were stored in a cool box and collected from SEPA offices in September 2014.

3.3- Organic Content

The first step in analysing the samples was to establish organic content by measuring the percentage loss on ignition (LOI%) of the sediment samples. The samples were placed in labelled crucibles, the individual weight of which had been previously measured, and an initial "wet" weight was measured using a Mettler Toledo AG204 precision scale (readability 0.1mg). They were then dried in an oven at 110°C for a minimum of 24 hours to ensure all mass as a result of moisture in the sediment could be discounted. The dry weight of each sample was then measured and they were submitted to a further 5 hours in a furnace at 450°C. This ignition temperature was necessary to burn off all of the organic content in the samples, while not being too high as to lose CO_2 from carbonates in the sediment, as described in Gale and Hoare (1991). As the samples were estuarine, they were considered likely to contain high levels of $CaCO_3$. The weight after ignition was noted, and the difference from dry weight calculated to give LOI. This was then calculated as a percentage of the original dry weight to give the LOI% which is taken as the organic content %. These results can be seen in Table 4.1.

In between drying and ignition of the sediments, samples were stored in sealed desk jars of a self-indicating silica gel desiccant. This ensured that no mass was gained from moisture in the air after drying.

3.4- Grain Size Analysis

To prepare samples for measurement, each individual sample was stirred with a mortar and pestle to break up aggregates. Following this, the sample was passed through a 2mm sieve, which did not affect the majority of the samples but removed up to 5% of the material in the coarsest samples, and then prepared in a Calgon/water solution to prevent grains from aggregating when in solution. The samples were then placed in an ultrasonic bath for 3 minutes to further disperse individual grains. Once this process was completed, the prepared samples were subjected to analysis using a Beckman-Coulter LS230 laser diffraction particle size analyser, as described in McCave *et al* (1986). Three measurement runs were completed for each sample. The outputs from each run were stored in separate files for each core, and labelled by their depth and run number. To ensure no interference between samples, the analyser was pumped at the end of the 3 runs, and the background intereference measured before a new sample was added. The instrument provides output in the form of a percentage volumetric composition of the total sample, broken into 117 size classes from 4μm to 2mm. Mean grain size of the particles is provided, calculated as $Xc*Nc/\sum Nc$ where Xc is the weighted centre of the channel and Nc is the percentage of particles in the channel (Beckman Coulter, 2011). Percentiles of the grain-size distribution (e.g. D_{16},D_{50},D_{84}) were calculated in Excel, along with sediment sorting (standard deviation) $(D_{84}/D_{16})^{\mathbf{0.5}}$.

Further analysis of sediments was undertaken using both light and electron microscopy. Core L2 was chosen for this as it was the longest core available, and the coarsest and finest layers from this were then selected. The sediment from these layers was placed into a resin, fixed on viewing slides and polished to 30 μm thicknesses. Samples were photographed under both plane and cross polarised light and these were then annotated. Samples were

then coated in carbon for viewing under the Scanning Electron Microscope (SEM) and attached to aluminium stubs using double sided carbon tabs. A FEI Quanta 200F Environmental SEM was used for the imaging. The same samples were analysed and photographed under varying levels of electron magnification.

For the surface sediment samples collected by SEPA, the mean sediment grain size of each sample was mapped and interpolated in ArcGIS using kriging (Figure 4.1). Mean grain size for these samples was also plotted against elevation, which was determined using a Digital Elevation Model produced from LIDAR data. Samples from the identified layers in the sediment cores were analysed using the same methods as for the surface sediment samples. For each core, mean and median sediment grain size, standard deviation and LOI% were plotted against depth. Two examples of these figures, produced for the cores taken at sites R2 and L2, are shown in the results section (Figure 4.5).

3.5- Quantifying algal cover

A factor which is hypothesised to have an impact on algal growth is the amount of river discharge on a seasonal scale, as explained by Rafaelli (1998). In order to analyse this effect, the volume of algae in the estuary in a given year had to be quantified. This was done by geo-referencing the algal cover maps of the Ythan provided by SEPA to a basemap of the estuary in ARCGIS. Using the ARCGIS software, each area of algae shown was traced with a polygon. The total area of the polygon shape file was then taken as the area cover of algae in that year. Total cover was then plotted against the discharge from the River Ythan in various formats in order to examine hypotheses that different aspects of river flow conditions (i.e. total or mean flow; seasonal mean flows over the previous 12 months; maximum flows) control algal growth. Figure 4.9 in the results section shows the total discharge for each season over the study period.

3.6- River Flow

The flow data were gathered by a data request from the NRFA (National River Flow Archive, ww.nrfa.ceh.ac.uk) which provided daily flow rates for the River Ythan at a monitoring station upriver, located in the midpoint of Ellon, 3.5 km upstream of the map extent in Figure 3.3. These data were reformatted to extract maximum, minimum, mean and median flows on annual, monthly and seasonal scales. Seasons were divided by hydrologcial year, so Spring was taken to be January-March and so on. Finally, these values were plotted against the total algal cover. Due to missing data it was only possible to plot the discharge for the Ythan up to and including the year 2009.It is important to note that the fieldwork to determine the algal cover was undertaken in Autumn, allowing a more accurate hypothesis about which antecedent seasonal conditions will have had the most impact on the observed growth.

3.7-Nutrient Analysis

A second round of fieldwork was conducted on the Ythan estuary on the 23rd August, 2015. Water samples were collected at strategic locations around the estuary in order to analyse the Nitrate and Phosphate concentrations throughout the estuary. The sampling locations were again chosen by examining algal distribution throughout the estuary, as well as at well-spaced sections of the estuary, to gain an understanding of the flow of water through the channel and how nutrients are transported and deposited through the estuary. Additionally, samples were taken from locations upstream on the River Ythan as well as in the tributaries to gauge the nutrient content of freshwater entering the main estuary, and a pure sea water sample was taken from a sampling location to the north to understand the nutrient content of the saltwater entering the estuary from its mouth. Samples were taken during low-tide conditions to ensure the greatest influence of freshwater. Figure 3.4 below shows the sample locations within the estuary. Not shown are the upstream sample from the River Ythan, which was taken at Ythan Terrace in Ellon, 3.4km upstream from the top of the estuary, and the seawater sample which was taken at Collieston Harbour, 5.5km north of the estuary mouth. In order to ensure there was minimal decomposition of nutrients, samples were stored in a coolbox immediately after collection, and were filtered on the day of sampling. After filtering, sampled were stored in a refrigerator for one night and nutrient analysis was carried out the following day.

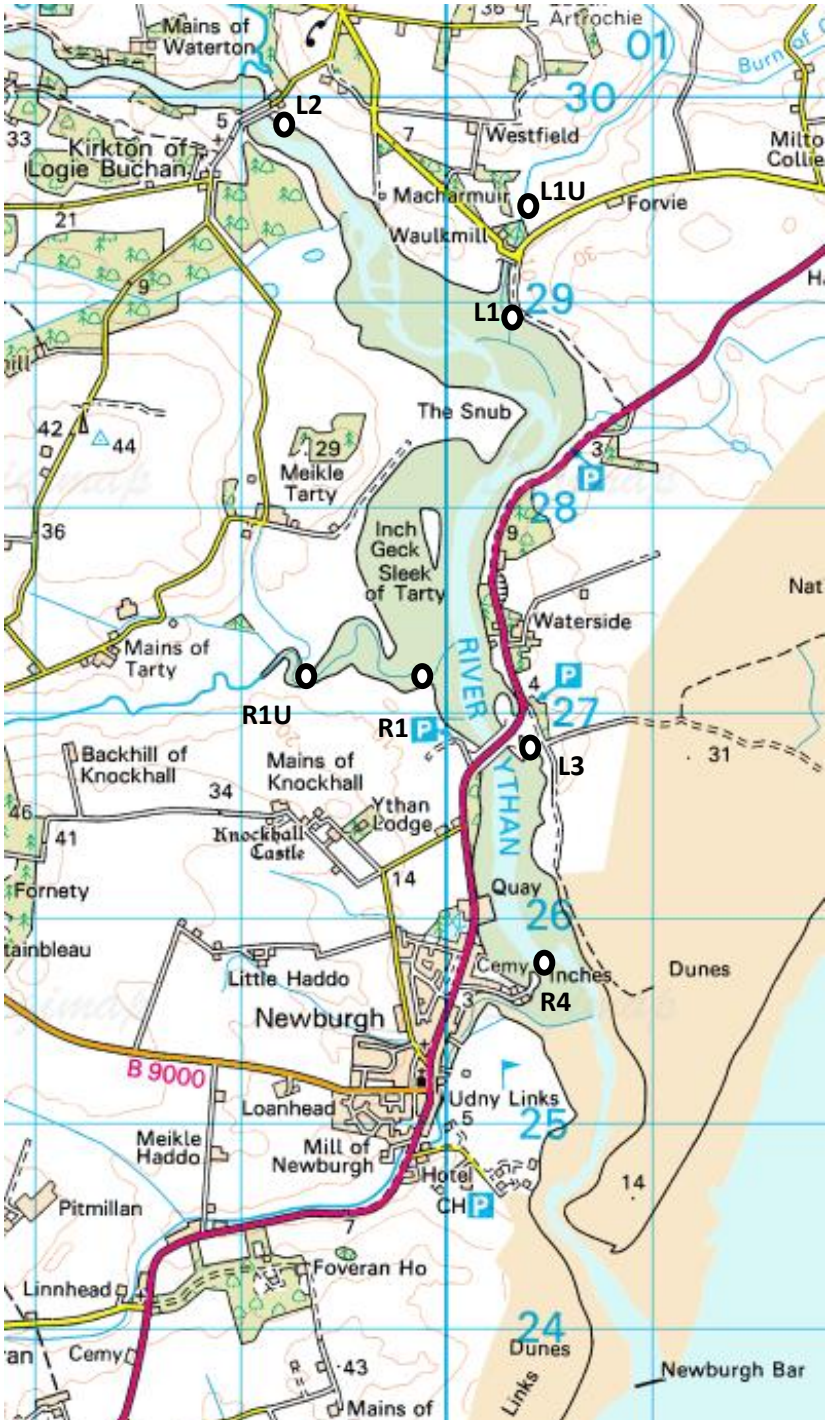

Figure 3.4-Water Sample Locations. U denotes upstream sample. (1:40,000 OS background map provided by EDINA Digimap)

Nutrient analysis was carried out using a Technicon Autoanalyser II system, a continuous flow automated analyser, as described by Montel and Oudot (1988). The system conducts a colorimetric analysis of colours produced from water samples. Which colour is produced during the process is dependent on the nutrient being analysed and the reagent used. For the phosphate analysis, soluble reactive phosphorous (SRP) was measured. This is calculated by adding antimony to the sample to produce phosphomolybdate, which has a faint yellow colouring. Ascorbic acid is then added to reduce this further, producing a blue colour with a wavelength of 690nm in the presence of phosphomolybdate which is then picked up by the automated colorimetry analysis. The sampling range was set as 0 to 100μg/l, which was based on figures provided by SEPA. For analysis of nitrogen in the water samples it was necessary to measure total oxidised nitrogen (TON), as the Greiss reagent used in the preparation process reduces nitrate to nitrite meaning that the method measures nitrate plus nitrite. The reagent used in this process produces a pink colour in the presence of nitrites in the sample with a wavelength of 530nm which can then be picked up by the properly calibrated colorimetric system. The sampling range for this analysis was set as 0-5mg/l.

Several measures were taken in order to reduce the error in the process. Firstly, “zeroed” samples of fresh deionized water were run through the analysis to ensure there were no faulty measurements, and that the system was correctly calibrated. “Blank” samples of deionized water were also prepared in the filtering process, in between samples, in order to ensure there was no cross contamination between samples. Standard samples were prepared with high nutrient readings of a known value, which further ensured the system

was correctly calibrated. Finally, each sample was analysed twice with a deionized water rinse between them, and an average concentration value was then taken.

3.8- Temperature

The final factor which is expected to have an impact on algae growth is the air temperature in the area, as this will be correlated with water temperature and also sunlight. The same algal cover maps of the Ythan were used as in the flow analysis. Temperature data were gathered from the Met Office website from the closest active station available, at Braemar (90km southwest of Newburgh) which provided maximum and minimum mean temperature on a monthly scale. These data were then reformatted so that data were also available on a seasonal scale. The resultant monthly and seasonal values were plotted against the area of total algae cover and trends were analysed. The data was reformatted and placed into a table which can be seen in Table 4.4.

Chapter 4. Results and Analysis

4.1-Sediment Grain Size

The samples collected by SEPA were all processed using Laser Diffraction as explained in Section 3.4. Appendix 2 shows the sample locations and Appendix 3 shows a map of their median grain size.

Figure 4.1 shows some clear patterns in the size of sediment over the estuary. The coarsest mean sediment grain size is found on the left bank near the mouth, adjacent to the Sands of Forvie. This large dune system provides an input of relatively coarse (silt-sand) sediment. This coarse sediment continues inland and across both banks to the area of the estuary level with the Foveran Burn, just south of the town of Newburgh. Upstream of this point, the effect of the sands of Forvie is much less apparent. The other areas with coarse sediments (>90μm) are observed in the estuary immediately downstream of the mouths of the two tributaries, at the Tarty Burn and the Burn of Forvie. This is interpreted as resulting from input of coarse sediment from the tributaries, and so a similar coarsening would be expected downstream of the Foveran Burn, but the wind-blown sediment from the Sands of Forvie may be obscuring this effect. The finest material observed in Figure 4.1 is found in the northern part of the Sleek of Tarty, and on both banks immediately below the A975 road bridge (not shown in Figure 4.1) in the area of standing water on the left bank and the exposed bank area opposite, at the northern edge of Newburgh. Finer sediment can also be seen to be deposited at the downstream edge of the bridge at Kirkton of Logie Buchan, at the inland edge of the estuary.

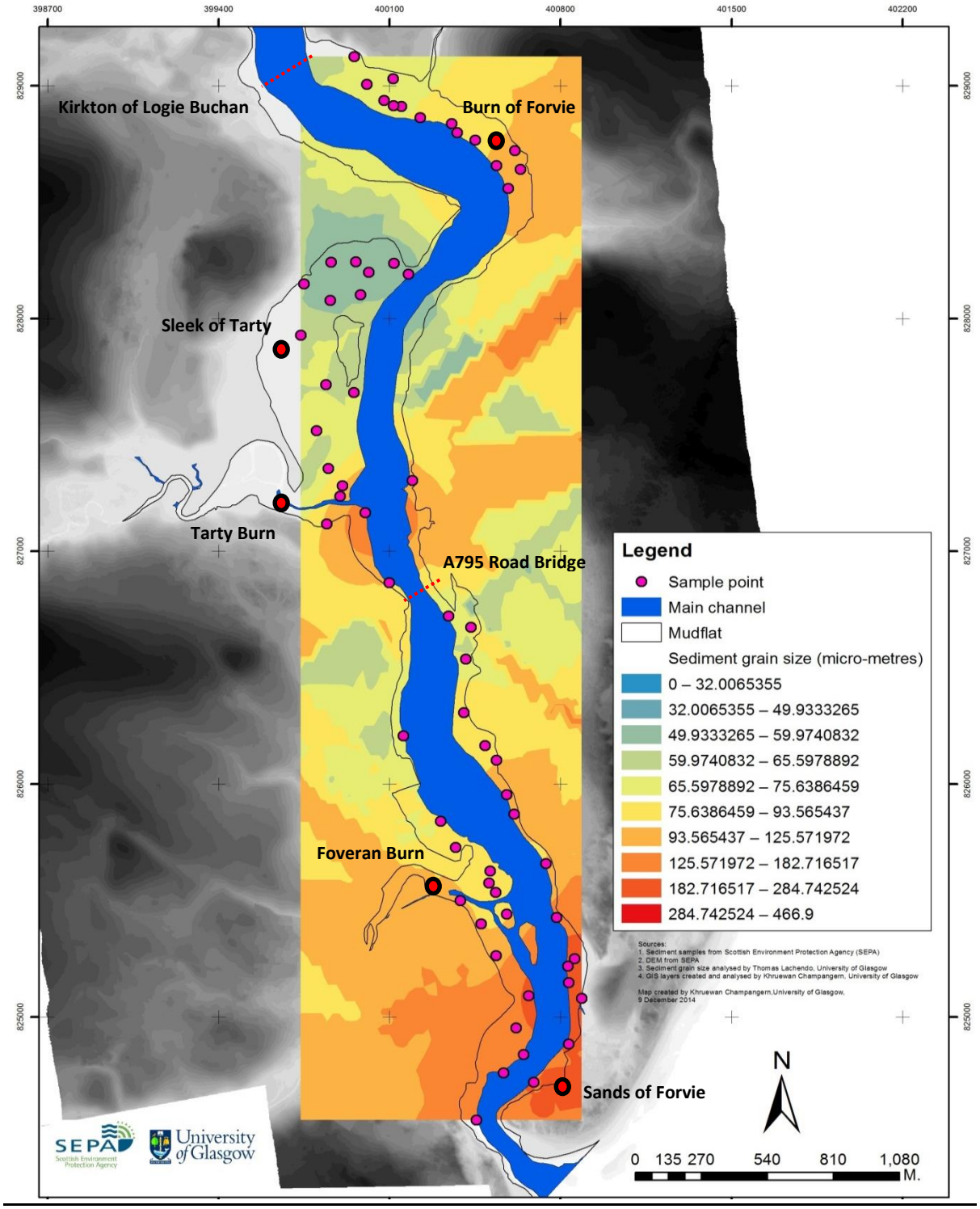

Figure 4.1-Mean grain size of surface sediment samples interpolated using kriging. Samples collected by SEPA.

Background image was created using a DEM of LIDAR images.

Figure 4.2 shows both mean and median grain size against distance from the mouth of the estuary. This graph allows a better understanding of how sediment is deposited as it is transported through the estuary, as well as the extent of the influence of aeolian transport from the sands of Forvie.

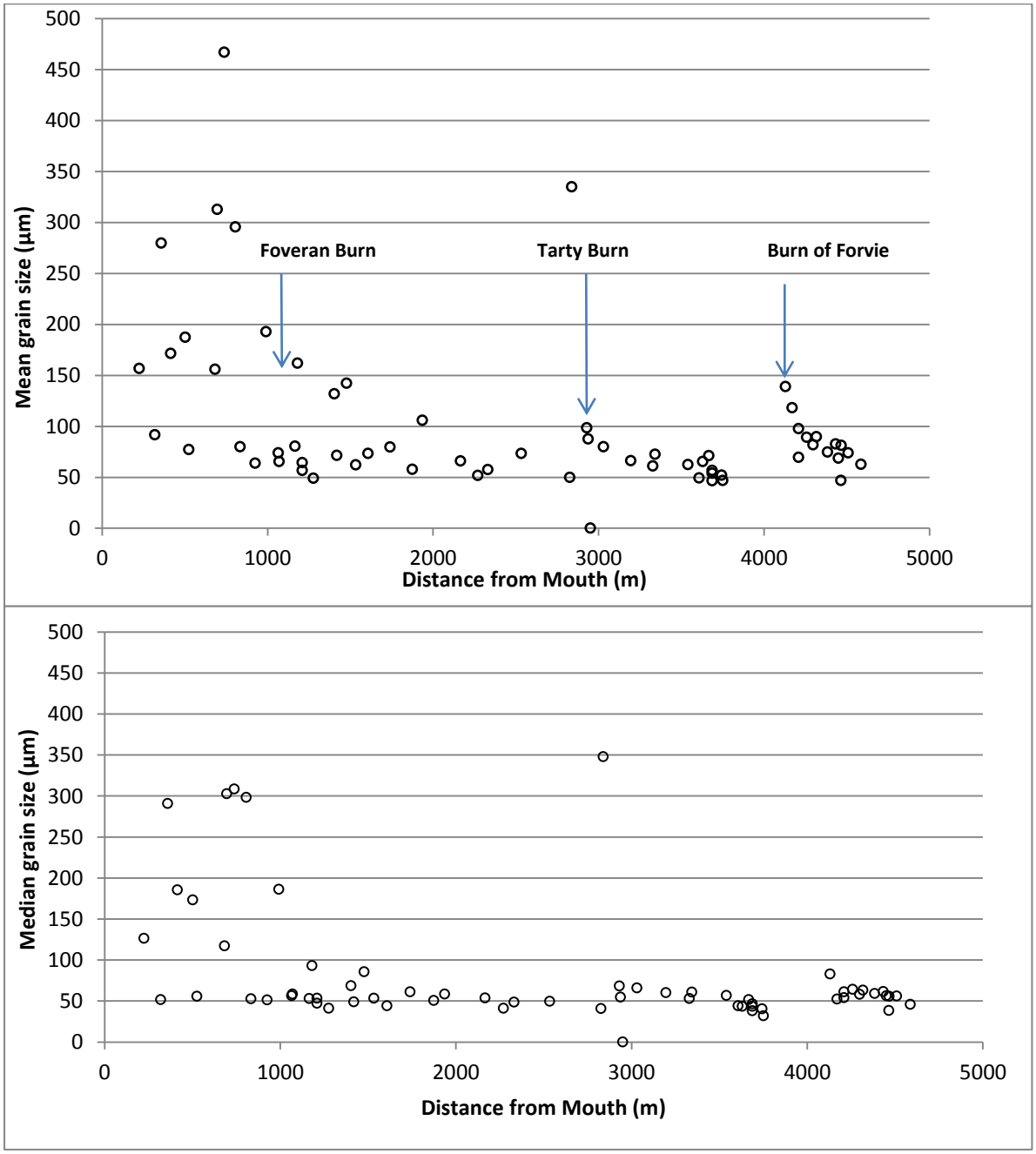

Figure 4.2-Median (b) and mean (a) grain size as a function of distance from the estuary mouth. Approximate locations of tributary inputs are indicated.

Figure 4.2 shows that most samples are in the 30-100μm range, with coarser (sand) material becoming more common closer to the estuary mouth, seen between 2000m and 1000m from the mouth. After 1000m the sediment grain size remains high for the remaining section of estuary as the deposits are increasingly dominated by wind-blown materials from the Sands of Forvie. The one coarse sample visible at 3000m is thought to be related to the deposition of coarser materials as the Burn of Tarty enters the main estuary. The two graphs tend to represent the data in a similar fashion, though the median (Figure 4.2(b)) displays a greater range between samples above 2000m from the estuary mouth.

Sediment grain size was also plotted against elevation, which is a function of both distance from the mouth and distance from the main channel, to provide more in-detail information on sediment distribution in the estuary (Figure 4.3). By comparing these data to Figure 4.2 it is clear that the distance from channel has little impact on mean grain size, as the correlation between variables (p=0.005) is not seen to be improved compared to Figure 4.2.

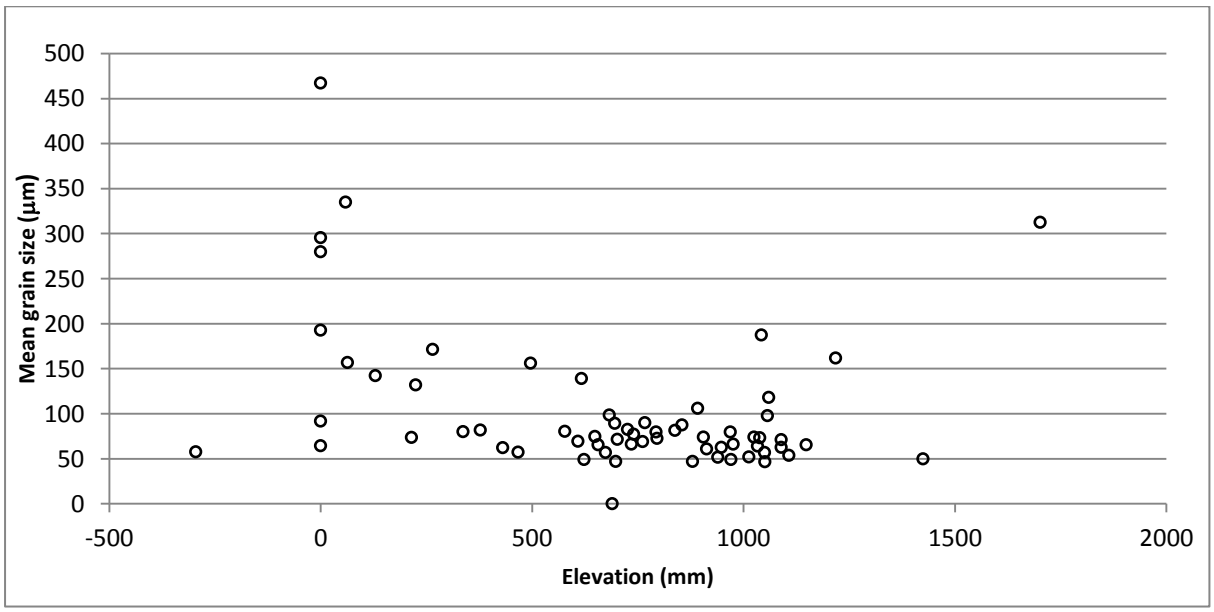

Figure 4.3-Mean grain size against elevation. Sample elevation (relative to mean sea level) was determined using a DEM produced from LIDAR data

Finally, sediment sorting represented by standard deviation $(D_{84}/D_{16})^{0.5}$ was plotted against distance from the mouth of the estuary (Figure 4.4). This showed no significant correlation between the two variables (p=0.46).

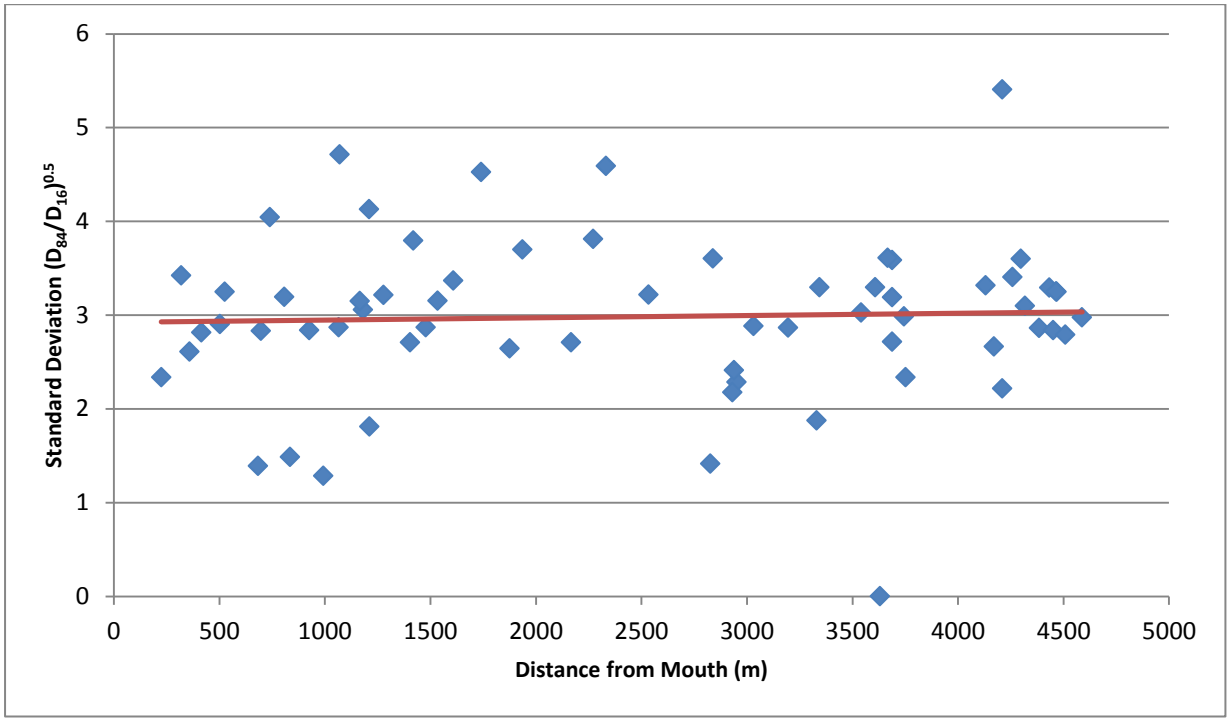

Figure 4.4- Standard Deviation vs Distance from mouth (m). Trend line shows lack of correlation between variables.

4.2- Sediment Core Data

As described in section 3.4, two of the sampled sediment cores were analysed and the results plotted against depth. The two cores are taken from two distinctly different environments, and therefore display separate characteristics. R2 is from a tributary mouth in the middle reaches of the estuary while L2 is from a mudflat in the very upper extent of the estuary. Figure 4.5(a), displaying the data from core R2, shows an upward-coarsening pattern, with the largest grain size seen in the top 100mm. The coarsest layer has a mean grain size of 251µm, and is seen at 65mm depth. This pattern in grain size is also reflected in

the LOI% data, which has the lowest values mirroring the coarsest layers. The sorting of the layers remains fairly constant throughout the core, with one anomalous layer. This layer, at 475mm, is reflected across all three plots for this core. There is a rise in mean and median grain size, mirrored by a drop in LOI% and a rise in the standard deviation of the sample. Deeper than this layer there is little to no variation between layers in any of the three data sets.

Figure 4.5(b) represents the layer data from a longer core, located at site L2. The layer generally contains much finer sediments than those observed in the R2 core, and there is much less variance in the size of sediment down the core. Grain size is seen to be generally constant through the core with the exception of two layers where it rises drastically. These layers, at 875mm and 1415mm depth, display a large spike in the mean grain size of the section accompanied by a lesser increase in median grain size. The highest mean grain size is 102µm seen at 875mm depth. As in core R2, there appears to be a correlation with LOI% data seen to mirror the grain size plot. The lowest values for LOI% are seen to occur in layers with the highest mean grain size. An exception to this trend can be seen in the layer at 415mm depth, where there is a very low LOI% compared to a grain size which appears to be average in relation to the rest of the core. Sorting along the cores seems to also remain constant with the exception of the coarsening layers seen in the grain size data. One anomalous layer can be seen at 1615mm where mean and median grain size both increase while standard deviation remains constant.

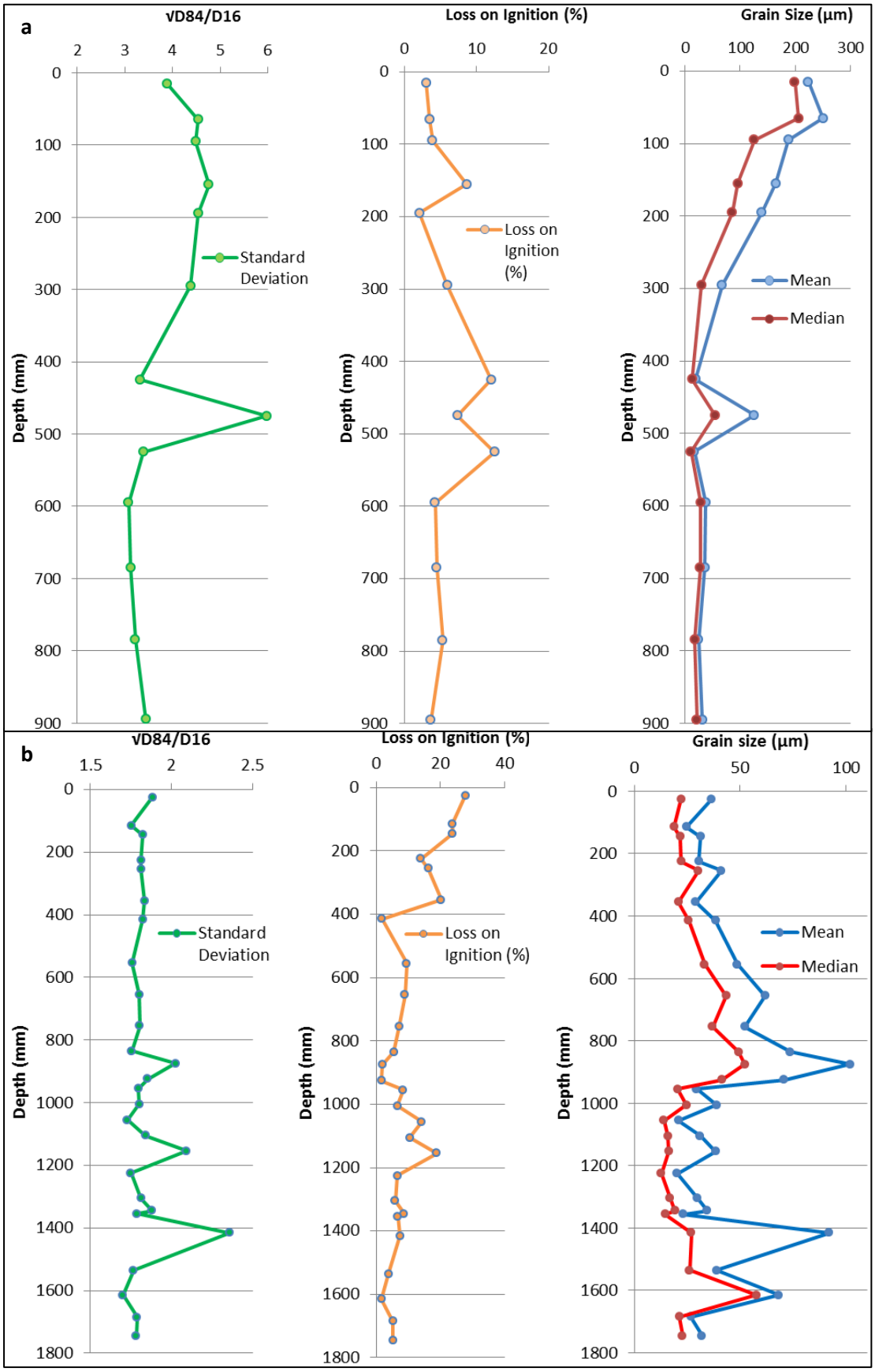

Figure 4.5-Plots of Standard Deviation, LOI% and Grain Size vs Depth for cores L2 (b) and R2 (a)

4.3- Microscope Analysis of sediment cores

SEM and light microscope analysis was undertaken to better understand the changes in composition from fine to coarse layers. The sediment samples used in this imaging were the same samples previously used during LOI% calculation, which results in no visible organic content in the SEM images. Image 4.1 and Image 4.2 contrast light microscope images taken from the finest (1225mm depth) and coarsest (875mm depth) layers in the L2 sediment core. Image 4.3 contains pictures from the SEM analysis of the same samples. From the light microscope images in Image 4.1 and Image 4.2 individual grains sizes and compositions can be identified. The SEM images contained in Image 4.3 further emphasises the individual mineralogy of the two samples as well as contrasting grain sizes at increasingly higher, levels of magnification. Backscatter electron imaging was also used to determine the percentage composition of the two samples.

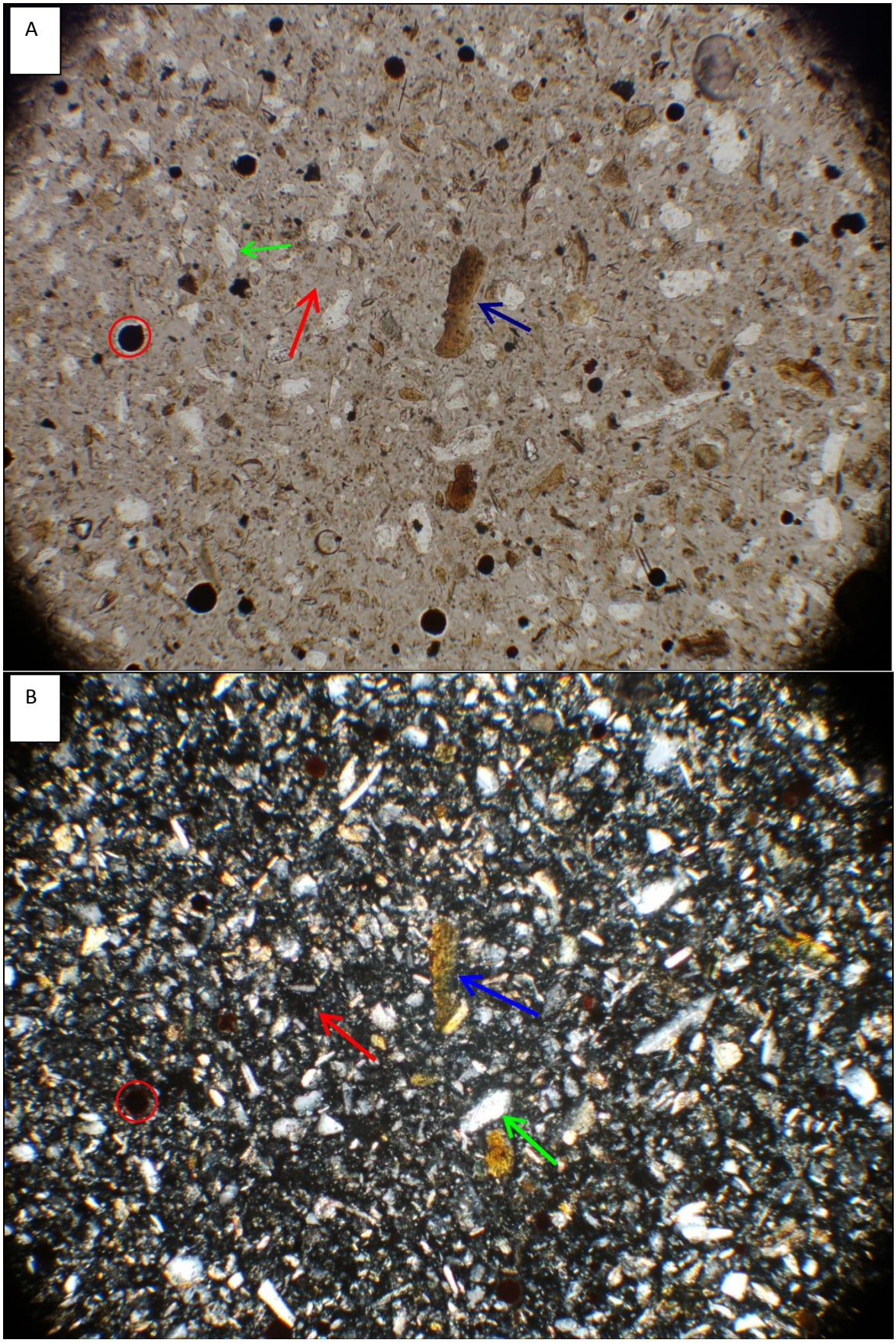

Image 4.1-Light microscope images of L2 sediment layer at 1225mm depth in (A) Plane and (B) Cross polarised light. 20 x magnifications, 1mm field of view.

Image 4.1 (A) shows the finest sediment, from 1225mm depth, in plane polarised light. The important material in the layer is highlighted. Blue arrow shows a dark brown, lath-shaped crystal of biotite mica, approximately 15μm by 5μm. Red arrow indicates the fine, pale-grey clay matrix which comprises much of the layer. The green arrow points to a colourless, high-relief quartz grain, approximately 5μm by 2μm in size. The red circle surrounds a clay aggregate with a diameter of 2-3μm. Image 4.1 (B) displays the same sediment sample in cross polarised light. The same labelling scheme is used in this image to highlight the composition of the sample. The biotite grain demonstrates brown interference colours with straight cleavage patterns. The clay matrix now appears with dark grey/opaque interference colours and the individual grains are more clearly defined. Low-interference quartz grains exhibit no cleavages and their sub-angular shape is highlighted in the cross polarised light. The densely packed clay aggregate appears opaque, allowing no light through the section. Further analysis of this sample using SEM imagery reveal it to be composed of approximately 40% clays in the form of a matrix, the remaining 60% of the layer being composed of mineral fragments of which 65% are quartz grains, 5% are feldspars, 5% are lithic fragments and 25% are micas.

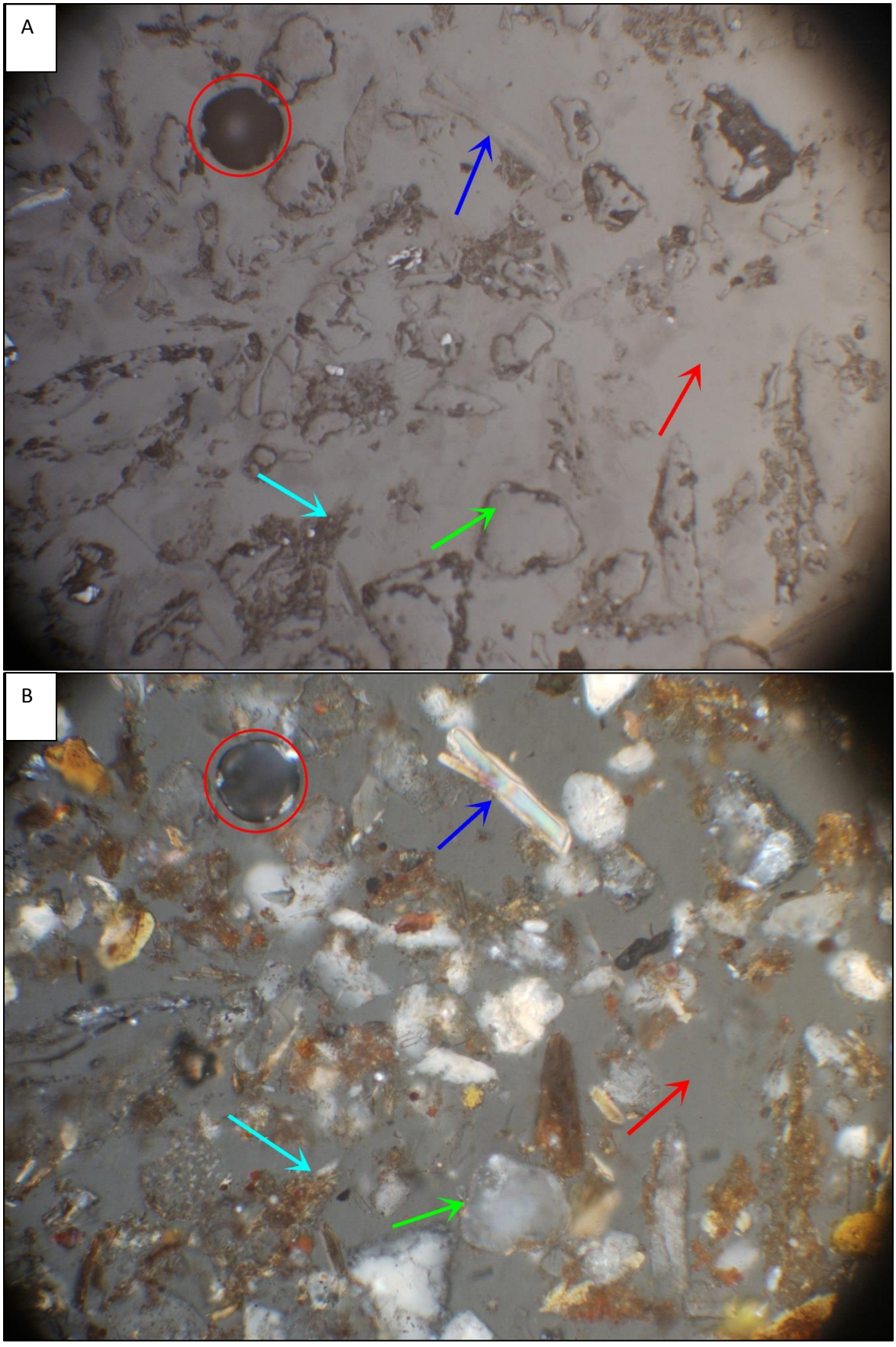

Image 4.2- Light microscope images of L2 sediment layer at 875mm depth in (A) Plane and (B) Cross polarised light. 20 x magnifications, 1mm field of view. Samples had been pre-heated to remove organic material.

Immediately apparent upon viewing this sample is the increase in grain size throughout the entire sample when compared to Image 4.1. Image 4.2 (A) shows sediment from the coarsest layer in L2, from 875mm depth, in plane polarised light. The important material in the layer is again highlighted. Dark blue arrow and light blue arrow show lath-shaped crystals of mica, approximately 20μm by 5μm. Red arrow again indicates the fine, pale-grey clay matrix which is present through the sample. The green arrow points to a colourless, sub-rounded, high-relief quartz grain, approximately 5μm by 2μm in size. The red circle surrounds a resin bubble which should be disregarded. Image 4.2 (B) displays the same sediment sample in cross polarised light. The same labelling scheme is used in this image to highlight the composition of the sample. The high interference colours and basal cleavage patterns of the mica grain indicated by the dark blue arrow identify this as muscovite mica. The light arrow highlights biotite mica, indicated by its dull brown interference colours. The clay matrix again appears with dark grey interference colours and the individual grains are more clearly defined. Low-interference quartz grains can be identified by their lack of cleavages. From analysis of this sample under both light and electron microscopy, the composition is seen to be approximately 55% clays in the form of a matrix, with the remaining 45% composed of mineral fragments of which 60% are quartz, 10% are feldspars, 10% are lithic fragments and 20% are micas.

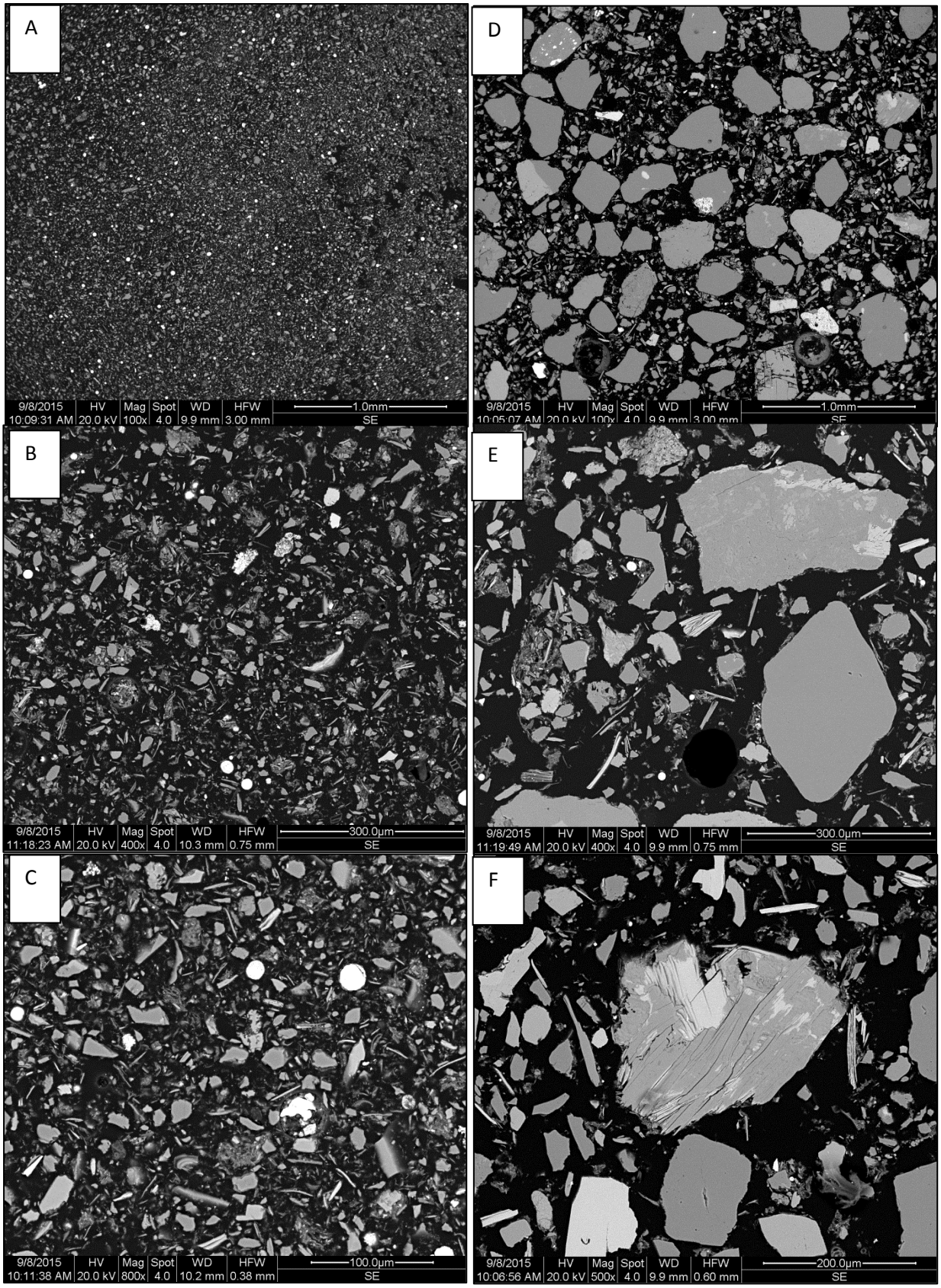

Image 4.3- SEM images of L2 sample at 1225mm depth at (A) 100x (B) 400x and (C) 800x magnification and for L2 sample at 875mm depth at (D) 100x (E) 400x and (F) 500x magnification.

4.4-Distribution of Organics

Using the samples collected by SEPA, percentage Loss on Ignition (LOI%) was calculated as described in Section 3.3, shown in Table 4.1 below. The LOI% for each sample was then mapped (Figure 4.6). The same method was also used on the individual layer samples from the sediment core data, though these are not shown on the Figure.

Figure 4.5 displays some clear trends in the distribution of organic content in the estuary. The greatest concentrations are seen in the middle reaches of the estuary, particularly in areas downstream from tributary mouths. These areas include the left bank of the estuary, from the northern edge of the Sleek of Tarty down to the A975 road bridge, and the right bank next to the town of Newburgh, both downstream from the Burn of Tarty. Further areas of high organic content are seen at the mouth of the Foveran Burn, the northern area of the Sleek of Tarty, and in the upper reaches of the estuary near the bridge at Kirkton of Logie Buchan, downstream of Auchmacoy Burn. The areas which display the lowest organic content tend to be in the lower reaches of the estuary, where grain size is known to be coarser. These areas include both banks in the final reaches of the estuary near the mouth, and in the upper portion of the estuary, low organic content can be seen in the area immediately surrounding the mouth of the Burn of Forvie. A small area of lower organic content is also seen on the left bank just above the Foveran Burn.

Crucible	Weight	Sample	Depth	Wet	Net Wet	Dry	Net Dry	Loss	Ignition	Net Ignition	LOI	LOI(%)
18	13.32	R1/A	350-360	21.26	7.94	18.16	4.84	3.10	17.91	4.59	0.25	5.17
17	12.89	R1/A	290-300	19.48	6.59	17.06	4.17	2.42	16.87	3.98	0.19	4.56
7	13.41	R1/A	130-140	17.98	4.57	15.53	2.12	2.45	15.25	1.84	0.28	13.21
6	10.81	R1/A	50-60	15.20	4.39	12.58	1.77	2.62	12.29	1.48	0.29	16.38
10	12.56	L1/A	400-410	18.00	5.44	15.64	3.08	2.36	15.47	2.91	0.17	5.52
3	13.93	L1/A	320-330	19.45	5.52	17.90	3.97	1.55	17.79	3.86	0.11	2.77
2	13.24	L1/A	280-290	18.60	5.36	16.57	3.33	2.03	16.40	3.16	0.17	5.11
4	12.88	L1/A	260-270	17.54	4.66	16.07	3.19	1.47	15.96	3.08	0.11	3.45
13	18.53	L1/A	240-250	23.38	4.85	22.15	3.62	1.23	22.05	3.52	0.10	2.76
15	13.30	L1/A	220-230	18.10	4.80	16.41	3.11	1.69	16.27	2.97	0.14	4.50
11	13.24	L1/A	205-215	17.62	4.38	16.94	3.70	0.68	16.90	3.66	0.04	1.08
16	13.33	L1/A	190-200	18.36	5.03	16.64	3.31	1.72	16.44	3.11	0.20	6.04
9	15.05	L1/A	170-180	29.76	14.71	28.71	13.66	1.05	28.63	13.58	0.08	0.59
14	27.10	L1/A	145-155	30.45	3.35	29.31	2.21	1.14	29.22	2.12	0.09	4.07
22	15.11	L1/A	130-140	19.72	4.61	18.38	3.27	1.34	18.26	3.15	0.12	3.67
24	25.85	L1/A	110-120	30.93	5.08	29.31	3.46	1.62	29.21	3.36	0.10	2.89
121	24.85	L1/A	100-110	30.60	5.75	28.52	3.67	2.08	28.39	3.54	0.13	3.54
141	13.36	L1/A	60-70	16.79	3.43	14.98	1.62	1.81	14.85	1.49	0.13	8.02

Table 4.1 -Weights of Samples in LOI% testing

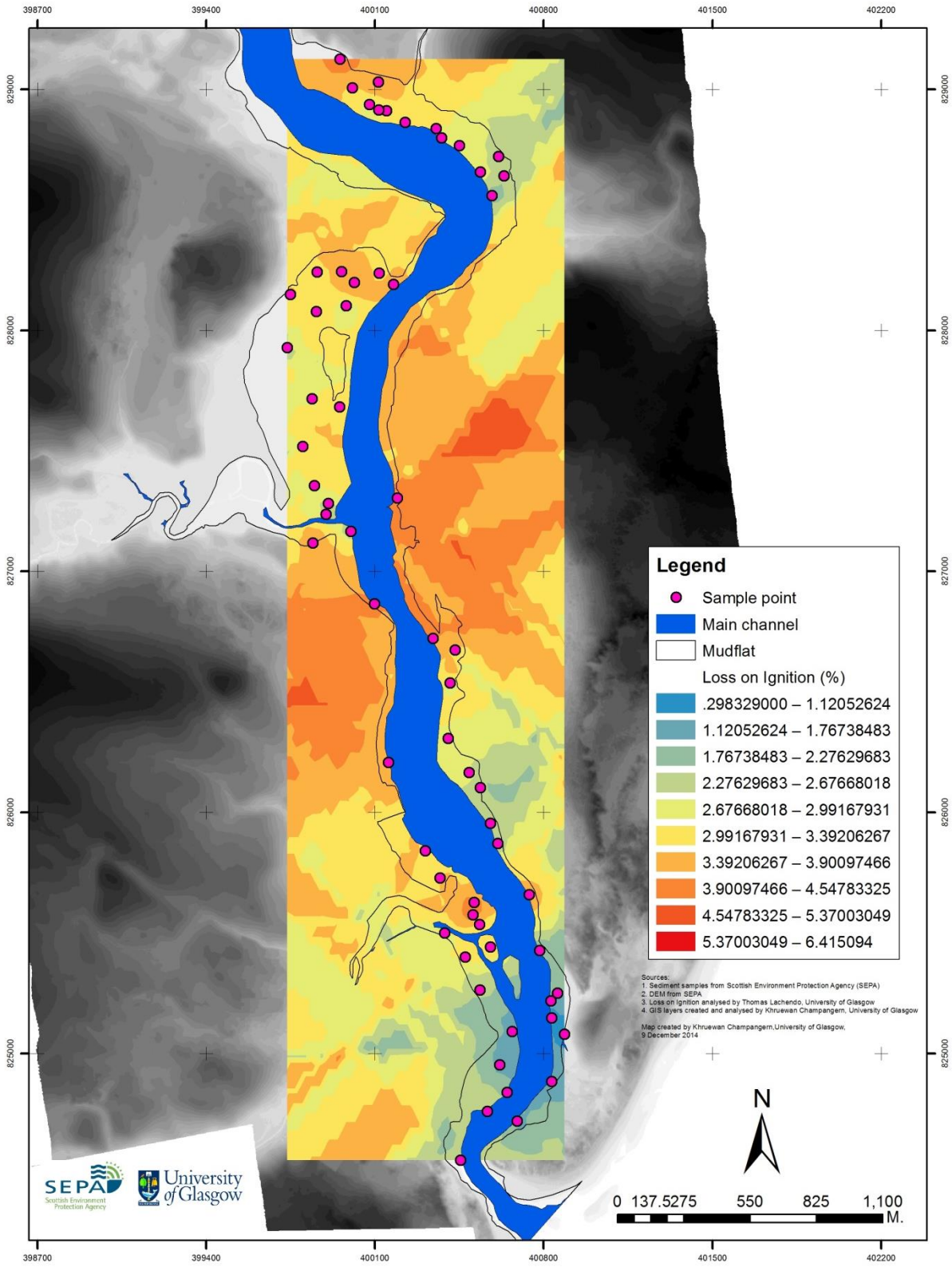

Figure 4.6- Percentage loss on ignition interpolated using kriging. Samples collected by SEPA. Background image was created using a DEM of LIDAR images.

LOI% was also plotted against distance from the mouth of the estuary (Figure 4.7).

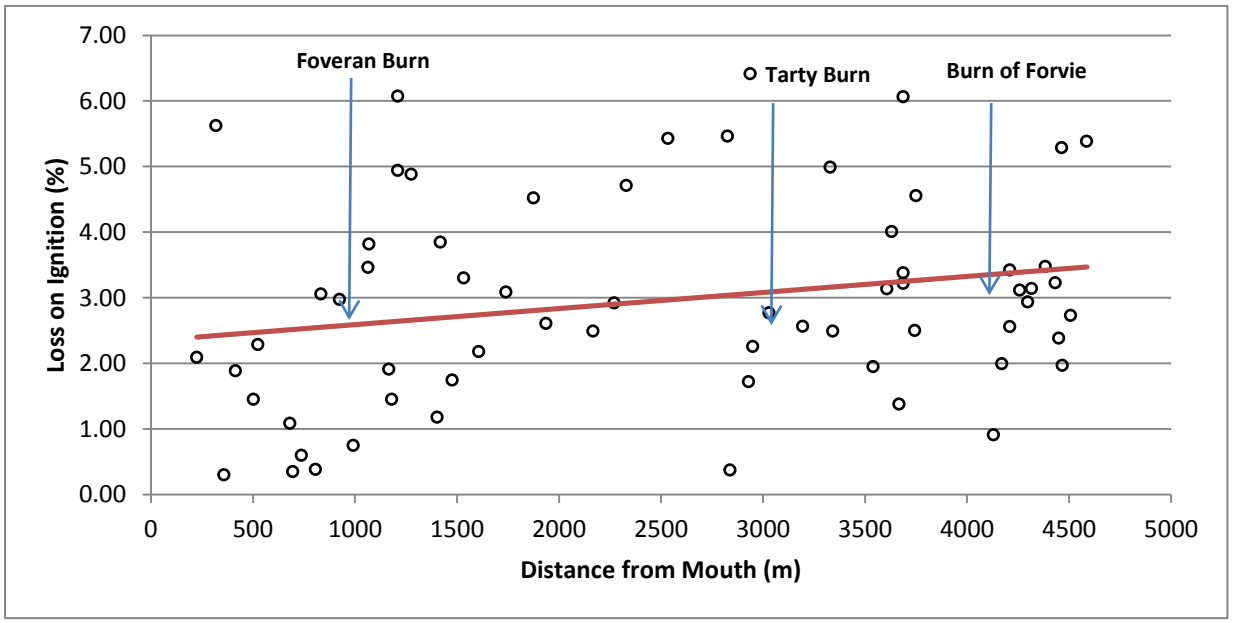

Figure 4.7- Percentage Loss on Ignition vs Distance from Mouth. Trend line is present showing general increase in LOI% upstream.

Figure 4.7 shows a weak general trend for LOI% to increase up estuary (p=0.074). As in Figure 4.2, there appears to be a change in characteristics from around the 1500m mark, where the areas of lowest LOI% are concentrated, where the majority of instances of low LOI% (below 2%) are concentrated while above this mark there are much fewer instances of low LOI%. However, the distance from the mouth of the estuary is not predicted to be the primary driving factor in LOI%. This hypothesis can be further emphasised by combining some of the information from Figures 4.2 and 4.7 in order to clarify the controls on LOI%. LOI% against grain size (Figure 4.8) shows strong correlation between organic content and mean grain size.

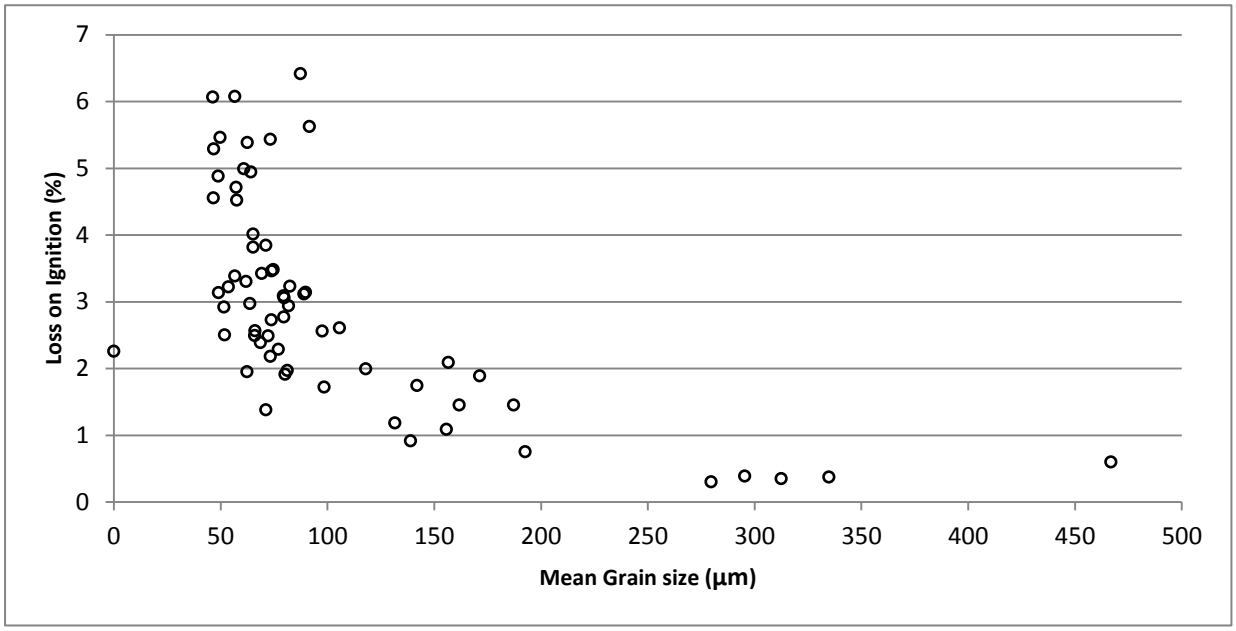

Figure 4.8-Percentage Loss on Ignition vs Mean Grain size.

Figure 4.8 shows a significant correlation (LOI%=4.306 – 0.0128 D_m p<0.0005) between the size of sediment in the estuary and the amount of organic content in that sediment. The samples with the highest mean grain size, above 250µm, contain <1% organic material (LOI%). The highest LOI% is seen only in sediments where the mean grain size of the sample is below 100µm. From 100-250µm there is a cluster of points which have intermediate mean grain size for the observed scale, and display some amount of organic content. However, there are no data points in this range which have an LOI above 2.1%, indicating that the mean grain size is still too high to allow a noticeable accumulation of organics. As LOI% is being used in this study as a proxy for algae growth, Figure 4.8 supports the hypothesis that algae growth in the estuary is to some degree controlled by the existing sediment characteristics and thus by transportation and deposition processes that have already been active in the estuary for its recent history.

4.5- Impact of river flow conditions on algal growth

As described in Section 3.5, total algal cover was calculated from the data provided by SEPA. Figure 4.9 plots these data against the total discharge for each season over the study period.

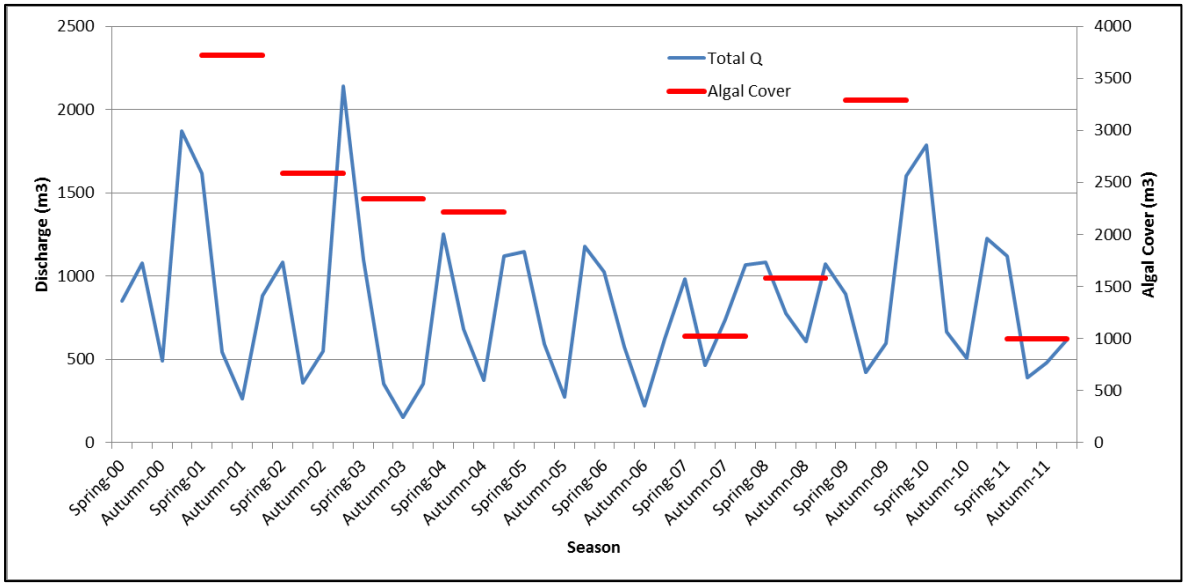

Figure 4.9-Total seasonal discharge vs Autumn Algal Cover for years of known algal cover (2001-2004, 2007-2009).

Figure 4.9 shows clear seasonality in discharge. The periods of highest discharge are seen in winter, with the largest values in 2000, 2009 and a high of 2141m^3 in winter 2002. Lowest total seasonal discharges are seen in summer and autumn, notably in 2001 and 2006 with the lowest observed value in autumn 2003 at 149m^3. There is also clear inter-annual variability in the algae data with total area varying from 3725m^2 in 2001 down to 998m^2 in 20011. As both algae growth and discharge vary greatly, the hypothesis that these variables are correlated was investigated. However, upon analysis there appears to be very little link between the two variables. The lack of association becomes clear when examining the two years with the highest algae cover which have little similarity in the antecedent flow conditions. From the results in the case study proposed by Rafaelli (1998) it would be expected that periods of low algae cover were preceded by low autumn and winter

discharges and vice versa. However, Figure 4.9 suggests that this is not the case. The high coverage in 2009 could be attributed to the low winter discharge in 2008, but the high 2001 coverage followed particularly high mean winter discharge. Additionally the periods of lowest algal cover, in 2007 and 20011, have among the lowest antecedent winter flows. In an attempt to clarify the correlation between the two factors, Figure 4.10 shows the total seasonal flows from spring, summer, previous winter and previous autumn against the algae cover upon which it should be impacting.

Figure 4.10 further demonstrates no significant correlation between algal growth and antecedent seasonal mean flows. Most notably, the highest algae growth is seen to have occurred after high discharges in the spring and previous winter, though the highest previous winter value, which coincides with the second highest spring discharge, was followed by an average amount of total algal cover. One of the lowest algal covers observed (2007) would be expected to have high flow in the previous winter or autumn, but instead displays the opposite, with values among the lowest observed in both categories. Through this analysis, it is clear that no correlation can be observed between discharge and algal growth (Table 4.2).

Regression analysis of the two sets of data further shows this lack of correlation. Algal cover was examined alongside total seasonal discharge in the same year as well as lagged (1 year) discharge for autumn and winter. This analysis produced no significant correlations between these factors. The most significant variable was spring discharge ($p=0.265$, $R=0.489$). This lack of correlation is highlighted by Figure 4.9.

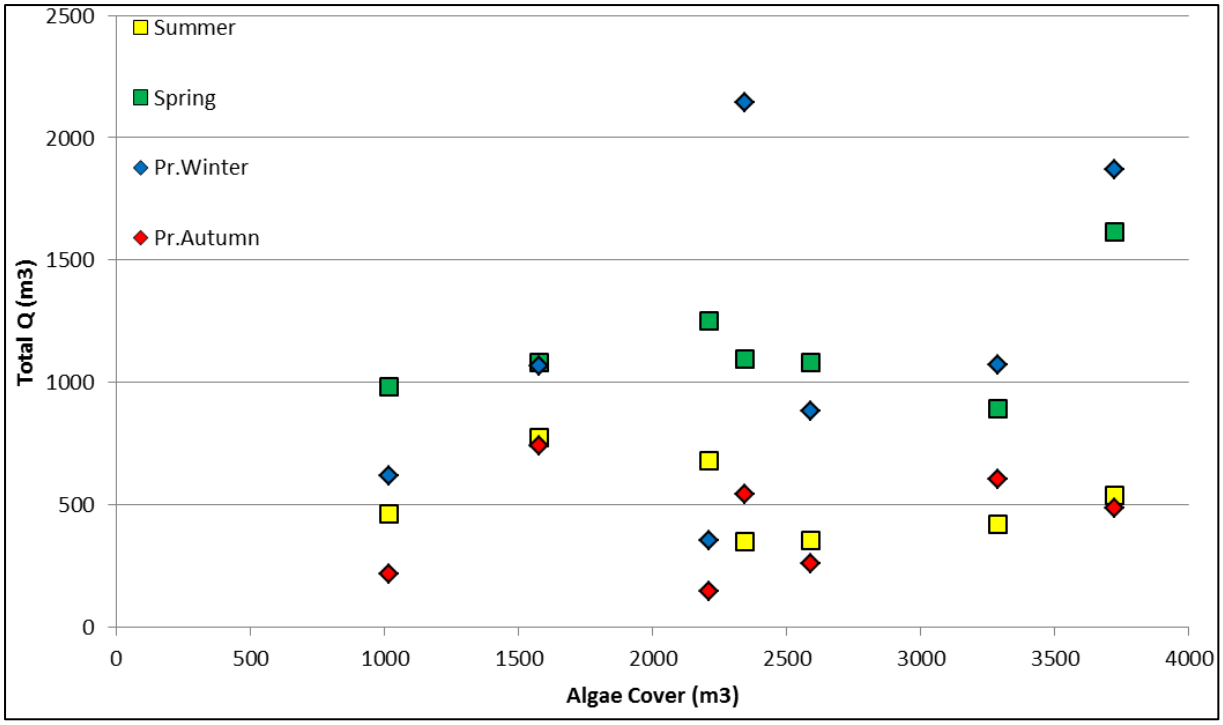

Figure 4.10-Seasonal Discharge vs Algae Cover Seasons were defined using the hydrological year (Oct-Dec for winter etc.)

	Spring	Summer	Previous Autumn	Previous Winter
P-value	0.265	0.559	0.622	0.275
R^2	0.240	0.073	0.052	0.231

Table 4.2- P-value and Coefficient of Determination (R^2) for Algal growth and seasonal discharge.

4.6- Nutrient Analysis

Water samples were collected and analysed for nutrient content as described in Section 3.7. The resultant outputs are in the form of concentrations of nutrient (Table 4.3). Concentrations were also plotted onto a map of the estuary using proportional circles to better communicate the data (Figure 4.11). The data from the estuary water are plotted in the locations that the samples were taken at, while the tributary water data are plotted on the nearest available section of tributary. The upstream Ythan sample and the sea water sample are plotted in the extreme corners of the map as the sample locations are not included. The exact sampling locations can be found in Figure 3.4.

The water samples were taken from a mixture of tributary, upstream, estuary and sea water locations to provide an overview of the nutrient cycling occurring in the estuary. The water samples which yielded the highest nitrate concentrations are the upstream samples at YU, L1U and R1U. A further high nitrate concentration is seen in the estuarine water sample at R1. Lowest nitrate concentrations are seen in water samples from L3 and the sea water sample. Phosphates follow a similar trend, with the highest concentrations seen in the upstream samples at R1U and L1U. The upstream sample at YU, however, does not display the same high concentrations as in the nitrate data. Again the lowest concentrations are found in the estuarine sample L3 and the sea water sample.

Sample Number	YU	L1U	L2	R1U	L1	L3	R1	R4	C
	Nitrate (mg/l)								
Test 1	4.75	2.95	4.53	3.20	2.60	0.37	3.03	1.80	0.29
Test 2	4.60	2.94	4.52	3.17	2.64	0.35	3.04	1.80	0.25
Average	4.68	2.95	4.53	3.19	2.62	0.36	3.04	1.80	0.27
	Phosphate ($_u$g/l)								
Test 1	44.80	62.80	52.40	77.40	97.50	45.40	65.00	48.20	14.90
Test 2	45.00	63.10	52.20	77.50	98.20	46.30	65.30	48.10	14.80
Average	44.90	62.95	52.30	77.45	97.85	45.85	65.15	48.15	14.85

Table 4.3- Concentrations of Nitrates and Phosphates from water samples.

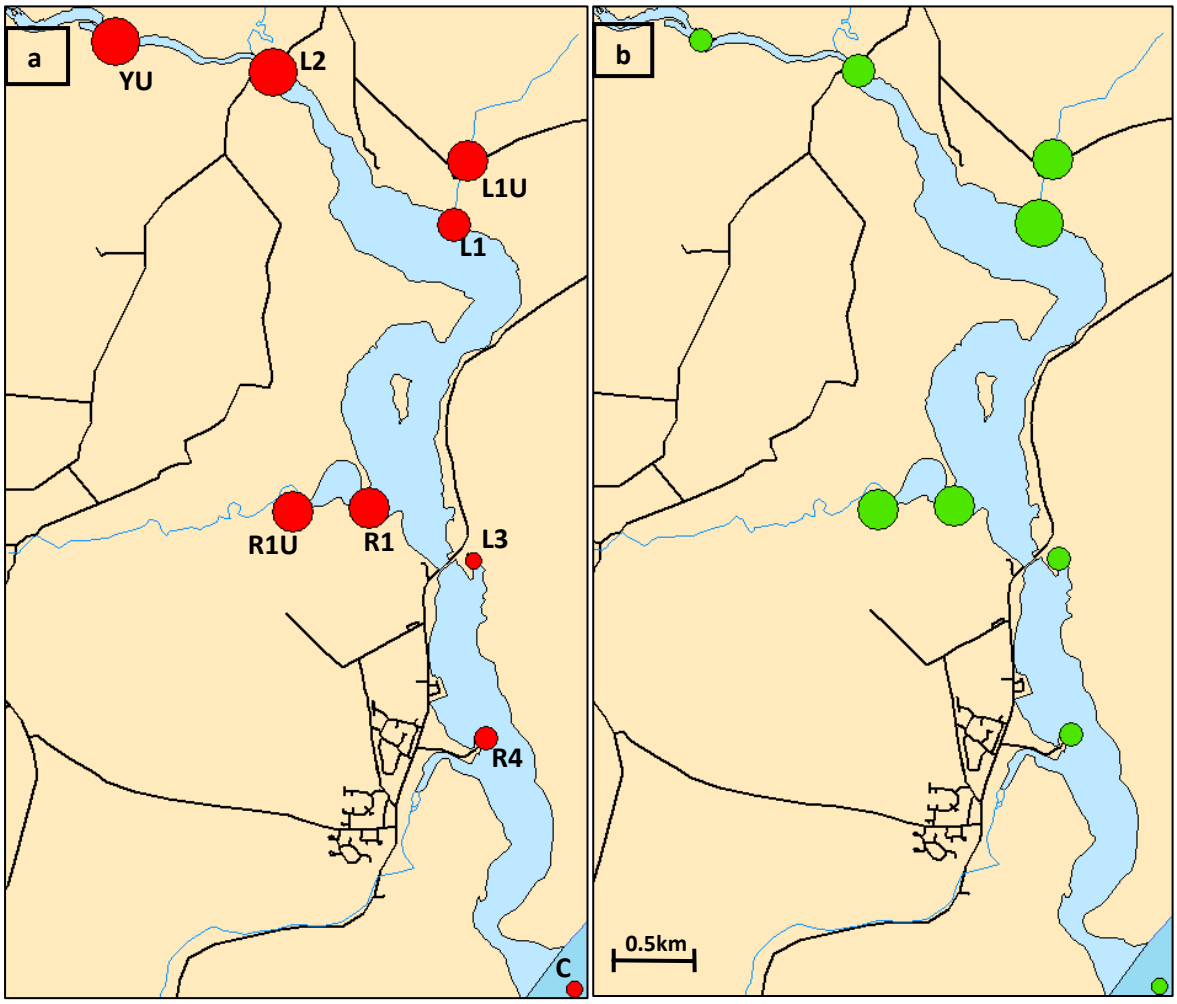

Figure 4.11- Proportional circles showing concentrations of Nitrates (a) and Phosphates (b). Larger circles represent greater concentrations (See Table 4.3 for values).

4.7- Temperature

From Met Office data, monthly mean temperatures were gathered for Braemar in north-east Scotland (Table 4.4). These data were then reformatted to produce seasonal averages and plotted against the total algal cover data as in the flow analysis in Section 4.5 (Figure 4.12). For a graph of monthly temperatures against algal cover, see the graph in Appendix 4.

As with the discharge data, there appears to be little correlation between seasonal temperature and algae growth. Initial hypothesis predicted that algal cover would be partially controlled by temperate climates, facilitating growth. From this, it would be expected that the lowest algal cover would be observed in the years following particularly cold winters and springs. However, upon viewing the data it can be seen that one of the periods of lowest algal growth recorded, in 2007, were in fact preceded by an average daily-low temperature of 0.4°C, which is among the warmest winter/spring periods shown. Conversely, a high spring/summer temperature would be predicted to facilitate algae growth and be observed next to a high total algae cover in the same year. This effect is observed in 2007, where both maximum and minimum temperatures are seen to be comparatively low in summer/spring and total algal growth is at the lowest observed level. However in 2000 a similarly low spring/summer period is observed but produces the highest algal cover, while higher temperatures in the same seasons over the following 3 years see a decline in algal cover.

This influence of temperature on algal growth was subjected to regression analysis in the same way as flow and which further reinforces the lack of correlation seen in Figure 4.12. Regression analyses of algae cover against seasonal temperatures from the same year as well as lagged (1 year) autumn and winter temperature were examined. A weak negative

correlation was found between algal growth and the average daily maximum spring temperatures (p=0.047, R= -0.761), giving a trend $A= -651t_{spring}+6358$ (Figure 4.13). Average daily spring minimum temperatures also displayed a weak correlation with algal cover (p=0.068, R= -0.720).

Finally, multiple regression analyses were run including both temperature and discharge against algal growth in the Ythan. These analyses used all variables in a best sub-sets regression, but in no cases was any second term statistically significant. The best of all combinations combines the most significant correlation, spring temperature (p=0.047), with summer discharge, but the regression was not improved (p=0.119). Full tables of correlation coefficients and significance can be found in Appendix 5.

Max Temperature													Seasonal Max			
	Jan	Feb	Mar	Apr	May	Jun	Jul	Aug	Sep	Oct	Nov	Dec	Spring	Summer	Autumn	Winter
2000	6.5	5.8	8.9	8.7	14.8	15.2	17.6	17.8	14.8	10.6	6.2	5	7.07	12.90	16.73	7.27
2001	3.1	3.8	4.6	8.4	16.2	14.6	17.4	16.8	13.4	12.8	8.5	4.3	3.83	13.07	15.87	8.53
2002	6.2	5	7.8	11	13.6	15.3	16.7	18.5	16	8.7	7.7	4.3	6.33	13.30	17.07	6.90
2003	4.9	5.4	10.9	12.8	12.6	17.5	19.4	19.8	15.7	10.3	8.9	6.1	7.07	14.30	18.30	8.43
2004	5	5.6	7.7	10.6	14.9	15.9	16.4	18.4	15.2	9.7	8.5	7.3	6.10	13.80	16.67	8.50
2005	6.8	4.5	7.8	10.1				17.6	15.9	12.1	7.1	5.7	6.37	10.10	16.75	8.30
2006	4.5	5	4.1	9.3	13	17.8	22	17.7	17.3	12.7	8.2	6.1	4.53	13.37	19.00	9.00
2007	6.7	6.1	8.4	14.3	12.8	15.8	16.4	16.5	14.1	12.9	8	5.2	7.07	14.30	15.67	8.70
2008	5.2	7.9	5.7	8.2	15	15.4	18.4	16.5	14.4	9.9	6.8	4.4	6.27	12.87	16.43	7.03
2009	4.3	5.2	8.3	11.9	13.6	16.6	17.8	17.2	16	11.8	7.4	2.7	5.93	14.03	17.00	7.30
2010	2.1	2.3	6.5	10.9	12.7	17.3	17	16.6	14.2	10.7	4.2	0.8	3.63	13.63	15.93	5.23
Min Temperature													Seasonal Min			
	Jan	Feb	Mar	Apr	May	Jun	Jul	Aug	Sep	Oct	Nov	Dec	Spring	Summer	Autumn	Winter
2000	0.4	-0.4	1.1	0.9	3.4	6.1	7.6	8	7	4.3	1.1	0.7	0.37	3.47	7.53	2.03
2001	-2.8	-2.3	-2.4	0.9	4	6.3	9.2	8.3	7	7.9	1.4	-2.1	-2.50	3.73	8.17	2.40
2002	-0.2	-0.2	0.5	1.9	4.5	7.9	8.9	10.2	6	2.6	2.5	1.3	0.03	4.77	8.37	2.13
2003	-1.5	-2.8	-0.1	1.7	5	8.6	10.4	9	5.1	1.8	2.2	-1.6	-1.47	5.10	8.17	0.80
2004	-0.5	-1.9	-0.1	2.9	4.4	8.1	8	10.1	7.1	4.1	2	-0.2	-0.83	5.13	8.40	1.97
2005	0.2	-0.1	1.1	1.5				8.4	7.6	5.8	-0.6	-0.3	0.40	1.50	8.00	1.63
2006	-1.4	-1.6	-1.8	0.1	3.1	8	9.4	8	7.7	5.2	2.6	-0.3	-1.60	3.73	8.37	2.50
2007	1.2	0.1	0.1	3.3	3.7	7.2	8.7	7.9	5.9	4.1	1.9	-2.4	0.47	4.73	7.50	1.20
2008	-1.1	-1.3	-1	0.1	4	6	9.8	9.5	6.8	2.6	0	-2.5	-1.13	3.37	8.70	0.03
2009	-2.3	-1.7	0.2	1.9	3.1	6.4	8.2	9.1	7.5	4.8	0.7	-6.5	-1.27	3.80	8.27	-0.33
2010	-5.2	-5.8	-2.7	1.2	1.9	7	8.9	7.3	6.3	3.6	-1.8	-8.1	-4.57	3.37	7.50	-2.10

Table 4.4- Reformatted monthly average maximum and minimum temperatures. (Data from Met Office)

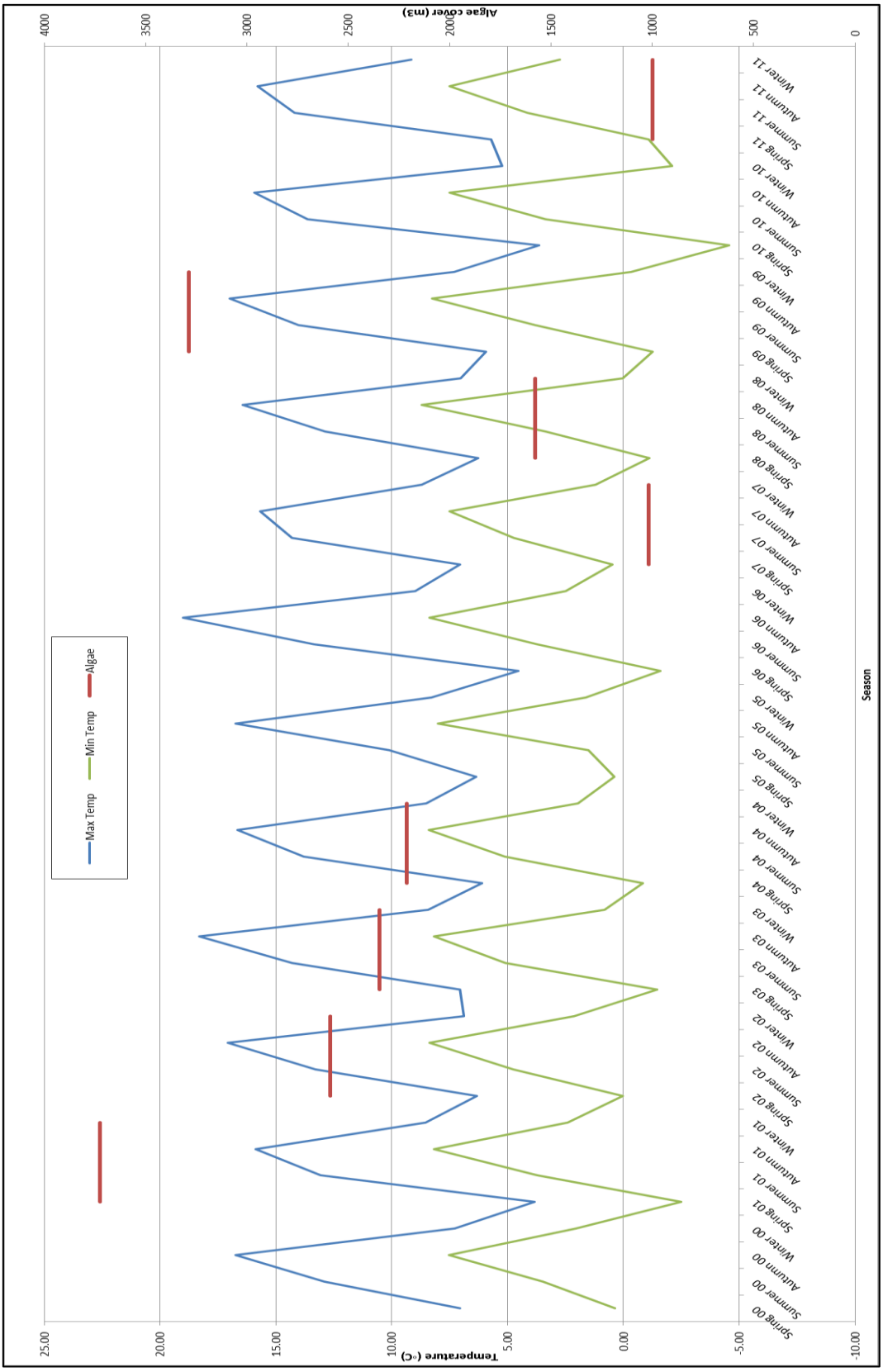

Figure 4.12- Maximum and Mean seasonal temperature vs Algae Cover.

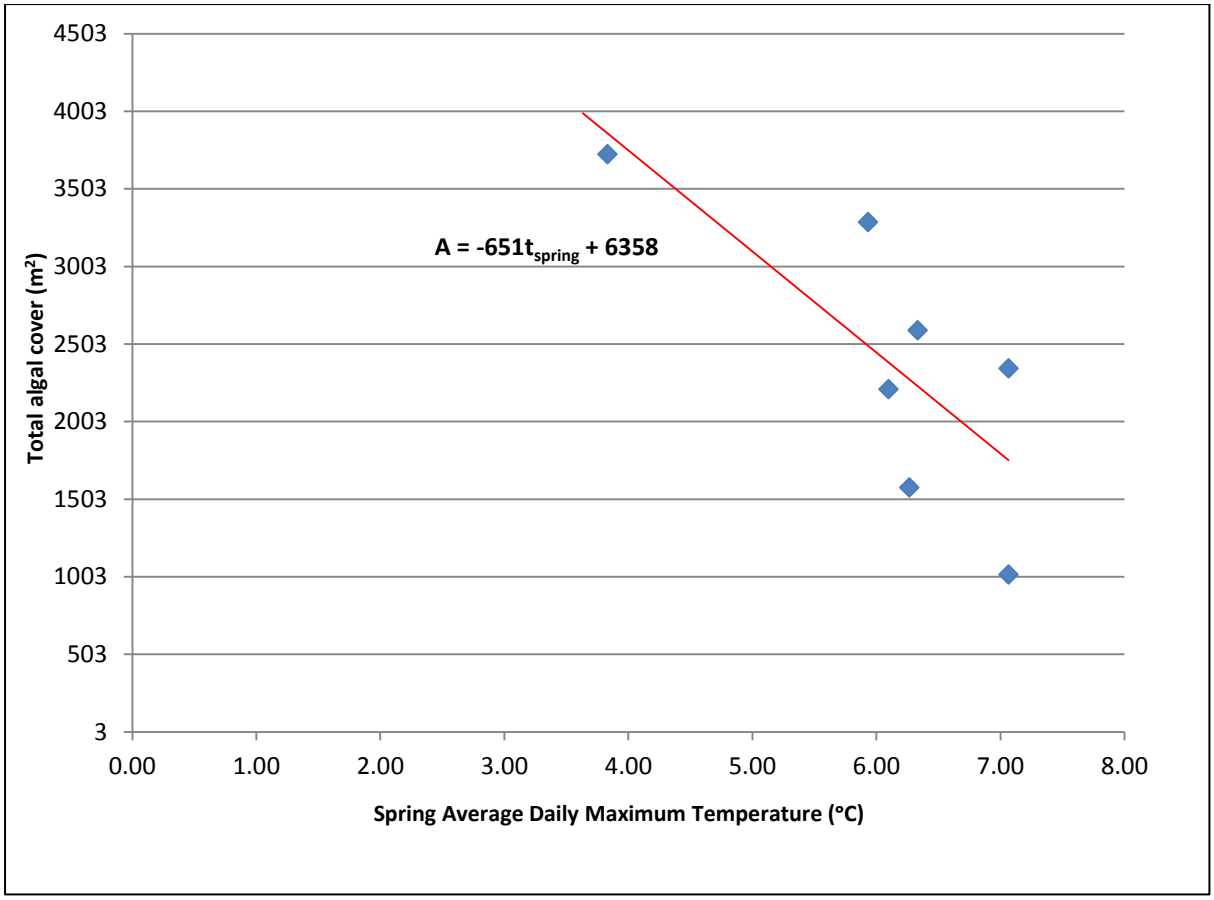

Figure 4.13- Spring (Jan, Feb, Mar) Average daily temperature vs Algal Cover.

Chapter 5. Discussion

5.1- Surface Sediment Data

The distribution of sediment within the estuary as detailed in Chapter 4 can be explained by understanding the various sedimentary inputs into the estuary system. The mean size of the sediment that is transported through the estuary tends to be in the range of 30-100μm (Figure 4.1). As well as the main River Ythan, there are other sediment inputs which account for the changes in grain size observed in Figure 4.1. The coarsest sediment has two main sources: aeolian transport from the Sands of Forvie and fluvial input from the small rivers entering the estuary. The impact of the Sands of Forvie can be seen in Figure 4.2, where there is a coarsening of bed material near the mouth of the estuary. This wind-blown sediment extends to approximately 1000m upstream of the estuary mouth. Additionally, fluvial sediments from tributaries increase the grain sizes found close to the tributary mouths where they enter the estuary. This effect is also visible in Figure 4.2, specifically at 1400m, 3000m and 4200m where there are inputs of sediment from the Foveran Burn, Tarty Burn and Burn of Forvie, respectively. These inputs are identified by an increase in the mean and median grain size followed by a tapering back down to the base grain size downstream towards the estuary mouth (Rice, 1998). The comparative size of these peaks could be attributed to either the relative energy of each tributary relative to the main river, as the higher energy for transport will allow larger sediments to be brought to the estuary, or the influence of the environments through which these rivers are flowing, specifically rock-type and land use, on sediment grain-size and volume (Ferguson *et al* 2006; Rice *et al* 2007). This sorting of tributary inputs is better highlighted in Figure 5.1 below, taken from Dawson (1987). Stove (1978) also shows the influence of tidal forces on sediment size near

the estuary mouth, stating that debris consisting of parts of a wrecked fishing vessel indicate the strong negative (inland) transportation of sediments, which would also add to the coarse sediments seen in the grain size data.

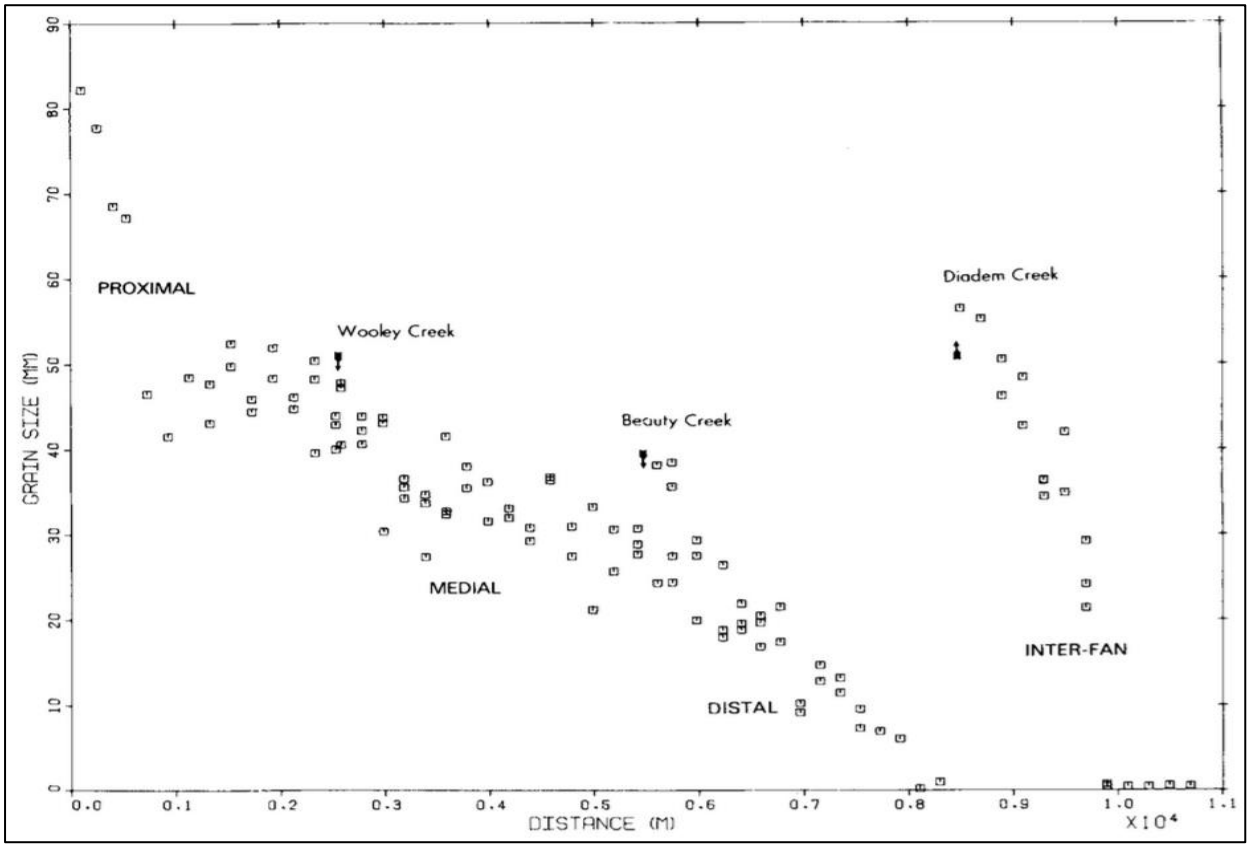

Figure 5.1- Size-Distance graph of grain size in the Sunwapta River, Canada (Dawson, 1987).

The effects of tributary inputs on the deposited sediment in the Ythan estuary extend over a scale of around 150-250m which reflects the size of the tributary relative to the main river, where size is defined in terms of sediment load, and sediment calibre and/or transporting power of the flow (Ferguson *et al* 2006; Rice 1998). Conversely, the areas which have the finest sediment deposits, notably the Sleek of Tarty and upper areas of the estuary, generally occur away from areas of direct sediment input and away from the main river flow, and instead occur in areas which would typically have low flow velocities and shallow

depths. There are two main areas in the upper estuary which display this fine sediment, and both occur on the inside bends of meanders where flow rate will be reduced and sediment can be deposited. The Sleek of Tarty also acts to slow down flow as water enters and is diverted around the curved shape, again depositing some of the fine transported sediment. These fine sediments are most likely deposited as flocs, as described by Stove (1978), with finer clay grains binding to form larger aggregates which are too large to remain in suspension in the reduced flow conditions. These aggregates can be seen clearly in the images in Image 4.3. The dominance of very fine (clay) sizes in the sediment grain size data in this area may be a result of the preparation process for the Coulter analysis, as sediment samples are prepared in a Calgon solution and placed in an ultrasonic bath both of which break up these aggregates. In this way, the measurements represented in the grain-distribution plots may not represent the size distribution of material in transport, instead representing the sediments as being finer than the aggregates which occur naturally (Maroulis and Nanson, 1996). This process is also important to consider when analysing nutrient adsorption into the sediment as aggregates of sediment would have a reduced surface area compared to the individual grains, meaning that adsorption may be lower than the Coulter output data would suggest. Christiansen *et al* (2000) quantifies this relationship for a mesotidal salt marsh, stating that 70-80% of sediments deposited within 8m of a tidal creek are done so in aggregated form. The remaining deposited sediment was composed of coarser individual grains, generally 20μm or larger. The lack of sorting shown in Figure 4.4 can also be attributed to the multiple sources of sediment to the estuary as the overall length of the study area is quite short, and there are four separate inputs over that scale, meaning that the sediments are likely to remain imperfectly sorted as they are transported to the estuary mouth.

5.2- Sediment Core Data

Further understanding of sediment transport and deposition in the estuary can be made through analysis of the sediment core data. The first factor to consider when examining these cores is that of deposition rate, and therefore the relative age of each sampled layer. It was intended in the planning of this study that the cores would be subject to radio-isotope dating, either in the form of ^{210}Pb or ^{137}Cs, the method for which is described in Madsen *et al* (2005). Due to time constraints and availability of facilities this was not undertaken. Therefore, in order to understand deposition rates in relation to this study, previous research in similar environments was consulted to constrain the potential rates of sedimentation in the Ythan. Nielsen and Nielsen (2002) state that the average rate of accumulation in established salt marsh surfaces is approximately 3mm/year, with rates of 9mm/year considered to be relatively high, while Sheffield *et al* (1995) discuss rates of 0.1mm/year, considered particularly low. By considering these rates of accumulation, it is suggested that the 900mm long core from R2 represents sediment deposited over between 100-9,000 years. Similarly, the 1800mm long core from site L2 would represent 200-18,000 years' worth of depositional history. However, from information gathered about the specific sample locations, these ranges can be narrowed down. The core at R2, being from a tributary mouth, would be expected to exhibit relatively fast deposition rates, in the range of 5 to 10mm/year. Deposition rates from the site at L2 are anticipated to be much lower, as historical records of channel position (Champangern, pers comm 2015) show very little change in the past 150 years. From this deposition rates are assumed to be at the lower end of the reported range at 0.5 to 1mm/year.

The first core, R2, comes from the Sleek of Tarty at the mouth of the Tarty Burn. This core comes from an area of mostly coarse sediment, with a mean grain size of over 200μm in the shallowest measured layer, at 15mm depth. The surface sample taken by SEPA at an adjacent location confirms this grain size. The sediment is much coarser than in other sites around the estuary due to its location at the mouth of a major tributary, as explained in Section 5.1. The upwards-coarsening trend seen from 400mm depth is interpreted to represent a change in the sediment supply from the watershed of the Tarty Burn, either as a result of changing land use or water management. Using the above estimate of sedimentation rate, the onset of this change is suggested to be 50-100 years ago. Possible explanations could be manipulation of the river channel or changes in farming practices around that period. The sharp rise in grain size at 475mm depth associated with a clear layer in the core can be attributed to an event, which may be a major weather event or an anthropogenic effect due, for example, to construction or forest removal. Little change between layers of relatively uniform coarseness from the 475mm event to the bottom of the core suggests the input of sediment from the tributary was un-inhibited over this period.

The data for L2 comes from a sediment core taken in the upper edge of the estuary, near the bridge at Kirkton of Logie Buchan. The mean grain size in the shallowest layer is 36μm at 25mm depth, confirmed by the SEPA surface samples (Figure 4.1). The observed fine grain size is typical of an intertidal mudflat area such as this. The two distinct layers at 875mm and 1415mm depth are quite varied in their impacts on the sediment characteristics of the cores and therefore are interpreted as being caused by quite separate events. The event at 1415mm sees a substantial jump in grain size, but recovers rapidly back to the background level. This pattern indicates a high energy event which rapidly deposited a layer of coarse

sediment, followed by a return to normal conditions, again depositing finer sediments. If, as hypothesised, deposition rates in this part of the estuary are very low then this event could be up to 15,000 BP. There is considerable uncertainty on this age, but is potentially of late Glacial or early Holocene age. The other coarse layer at 875mm depth again sees a rise in mean and median grain size, but at a much more incremental rate. This can be seen in the gradual change in grain characteristics in the core. Above the layer, there is a steady decline back to background sediment grain size. This record in the sedimentary log is typical of an addition of coarser material into the river environment which has then been reworked though the estuary over time until the system returns to its normal conditions, resulting in the slow recovery observed. However, it could also reflect a change in river flow or climate. In the case of both of these layers, further interpretation is dependent on reliable dating of the coarse material which should be a priority for further work.

5.3- Distribution of Organics

The distribution of organic material is inferred from the LOI%, and its link to the physical algal growth observed in the estuary by SEPA. To do this, the areas where the algae are observed are overlaid on the LOI% plot in Figure 4.5 in order to see if there is a link between areas of algal growth and areas of high LOI% (Figure 5.2).

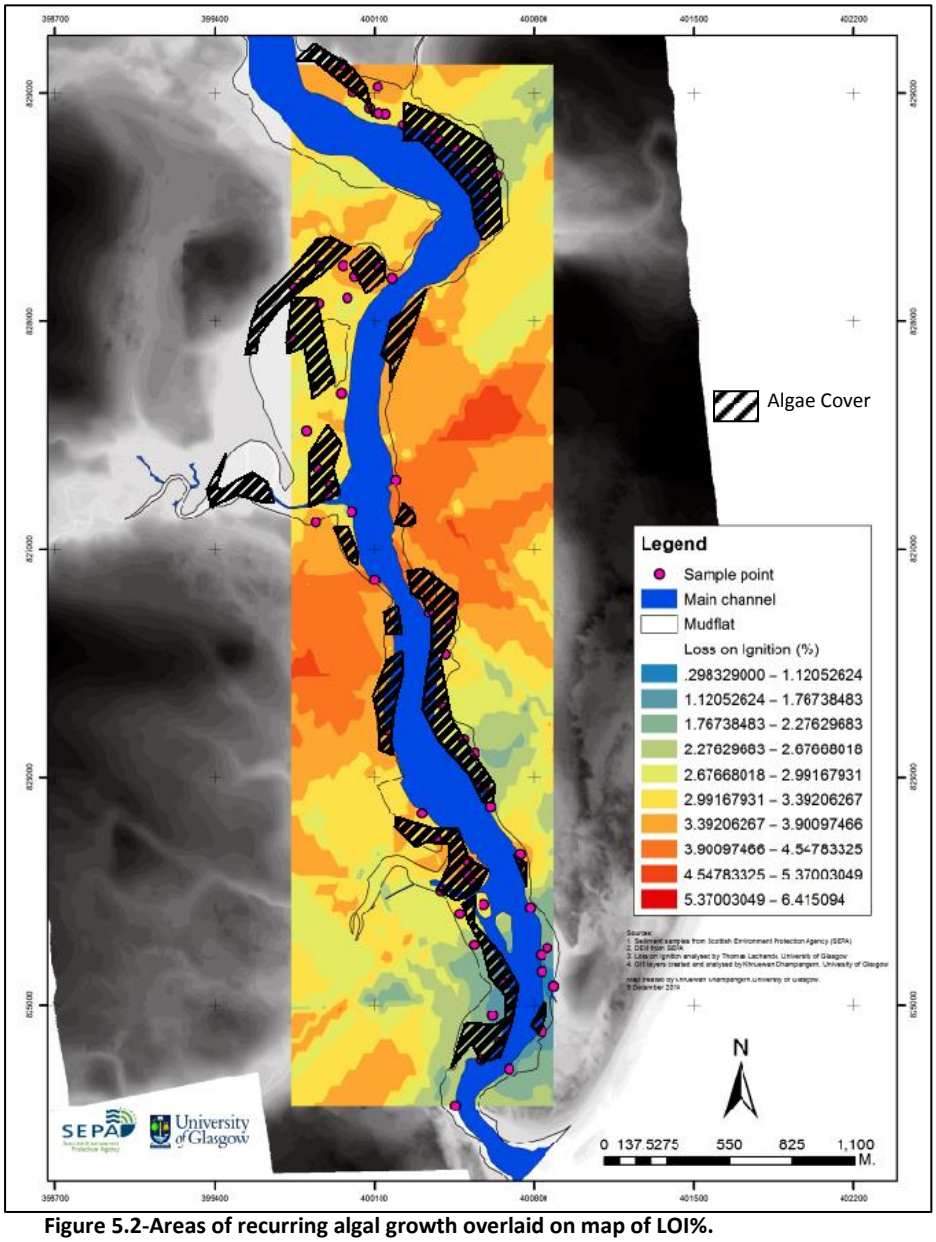

Figure 5.2-Areas of recurring algal growth overlaid on map of LOI%.

Figure 5.2 shows a weak spatial correlation between algal growth and LOI%. The areas identified in the results chapter as having the highest LOI%, the upper area of the Sleek of Tarty and the tributary mouths, all show consistent algal growth through the available years of data. There are, however, some areas which do not show this link, where LOI% was determined to be low but algae growth is seen in at least 5 of the 7 years recorded. These areas include the left bank at the Sands of Forvie as well as the area immediately surrounding the mouth of the Burn of Forvie. Quantitative analysis of the LOI% also shows a weak correlation. Samples which were within the areas determined to have consistent algae growth (Figure 5.2) were found to have a mean LOI% of 0.44 ± 0.025 (N=46) while those samples which lie out-with the areas of consistent algae growth had a mean LOI% of 0.38 ± 0.053 (N=16). These means are not significantly different (one-tailed t-test; $p = 0.14$), but for given LOI% classes the probability of algae being present increases steadily from 0.25 to 0.88 over the range of LOI% observed. The exceptions to this trend are for the lowest LOI% class which had only one observation, and for LOI% of 0.28% (Appendix 6).

One potential cause of a difference between the observed algae and calculated LOI% is due to potential error in the LOI% method of determining organic content. As explained in Hoskins (2002), oven-drying a sample may not be sufficient to remove all moisture from samples which are rich in clays. If this effect were true in this study, it would mean that the LOI% figures for the areas with higher clay compositions could in fact be over-estimating the algae content, and that the difference in algae content between samples is not as great as the figure indicates. Therefore, while LOI% does appear to give a general indication of algal growth in the estuary, LOI% alone should not be used as a direct measure of algal presence.

The distribution of organics in the estuary can be explained by a number of factors. As mentioned in Section 4.2, some of the highest concentrations of algal growth are found in the areas immediately surrounding and downstream of tributary mouths. Rice *et al* (2008) details a study of the impacts of tributaries in this way in the Cascade Mountains, USA, showing that in the areas immediately surrounding tributary mouths algal chlorophyll concentrations are much higher than elsewhere in the system (Figure 5.3).

Figure 5.3 shows clearly that concentrations of algae rise sharply, by 5-50x normal rates, at tributary inputs into a system. The figure shows that the reaches of the system immediately surrounding the tributary also experience this effect, with the impact seen from 0.1 SDUs (standardized distance unit- the distance between a measurement transect and the tributary divided by the inter-transect distance) upriver and extending down up to 2 SDUs downstream. This effect is different from that seen in seen in Pihl *et al* (1999), where there is stated to be no relation between nutrient point sources (mainly tributaries) and algal biomass. The data for the Ythan sediments, where LOI% is seen to be higher from the upstream edge of a tributary mouth and extends a substantial distance downstream, agree much more with the data shown in Figure 5.3, from *Rice et al* (2008). This is likely due to the fact that in the Ythan the main estuary is protected from wave action by the bend at John's Hole Point, while Pihl *et al* (1999) hypothesise that their lack of correlation is due to an altered state of nutrient dynamics from marine influences.

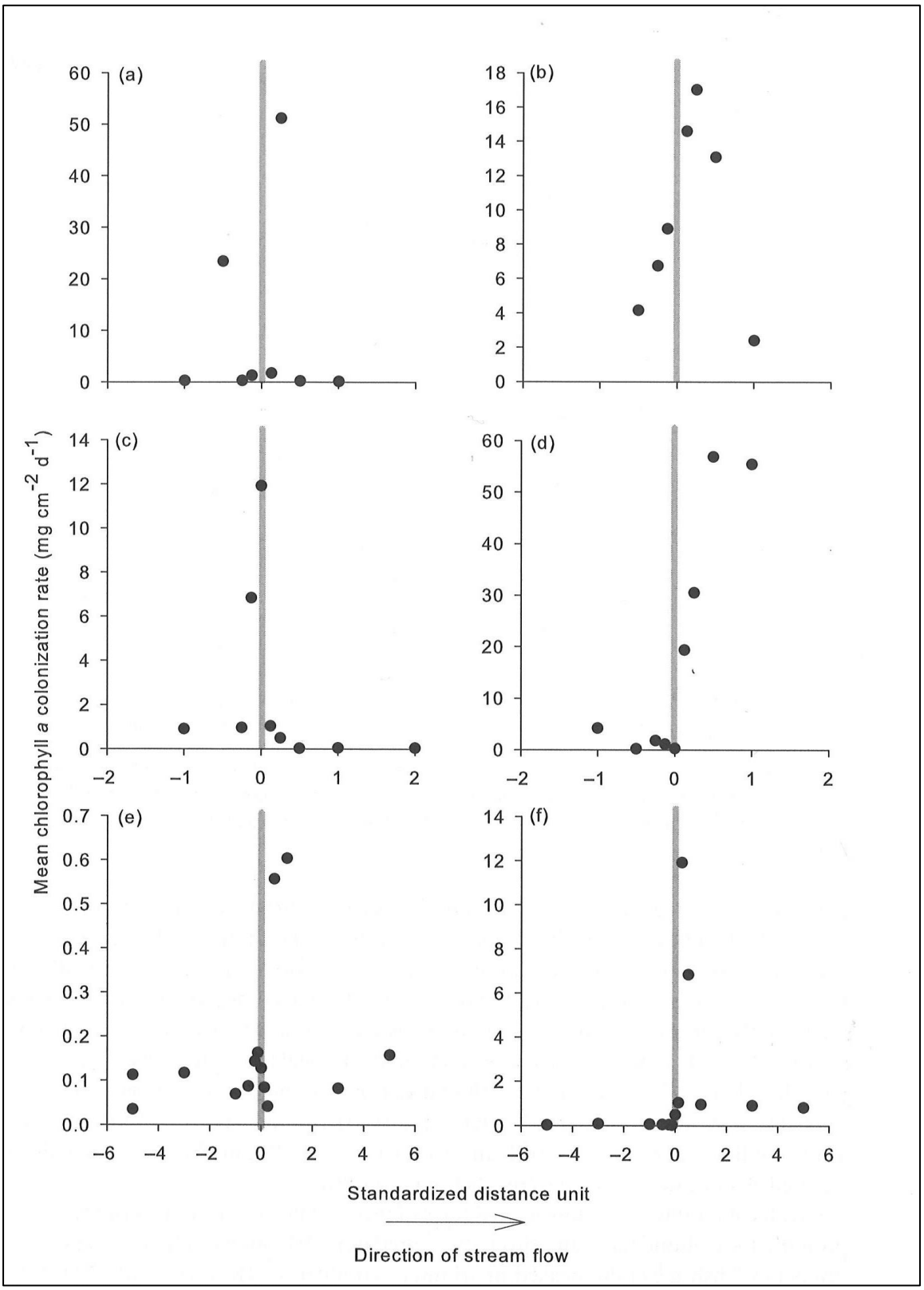

Figure 5.3-Scatterplots of algal chlorophyll accruing on ceramic tiles averaged over a five-week colonization period vs SDUs for the a)Rock, b)Williams, c)Taylor and d)Steele Creek confluences on the Cedar River and the e)Jumbo and f) Falls Creek confluences on Bacon Creek (Rice *et al*, 2008).

Section 4.2 also highlights high LOI% at the backwater below the A975 road bridge and in the upper reaches of the estuary near Kirkton of Logie Buchan. Due to the similar positioning of both of the above sites, it could be hypothesised that the impact of the bridge supports on the surrounding hydrology is helping to facilitate this growth. As suggested by Rafaelli (1998), high flows during certain times of the year could potentially remove the algal biomass required to re-colonise a river in spring. It is possible that the bridges are acting as a buffer, sheltering these areas from the direct energy of these high flow events, resulting in the high algae concentrations observed.

Areas of lowest LOI% are also identified in Section 4.2. These areas are mostly confined to the mouth of the estuary, where sediment is coarser. This pattern is investigated in more depth in Section 5.6. The areas of low LOI% on the left bank, at the mouth of the Burn of Forvie and the left bank just above the Foveran Burn, stand out as not adhering to the pattern of algal growth shown in Figure 5.2 as both of these areas have documented algal growth in multiple years over the observed time period. These data may be explained by non-representative sampling or error in the LOI% process.

Figure 4.5 allows further analysis of LOI% data, showing a significant negative correlation between mean grain size (D_m) and LOI%. The coarser sample at R2 has LOI% between 0-12 while the finer sediments in L2 have LOI% values from 0-30. LOI% values are seen to mirror the grain size (LOI = 22.75 - 0.236 D_m p=0.007) through the L2 data series to a depth of 1200mm while LOI% values in the R2 data correlated (LOI = 10.38 - 0.031 D_m p=0.049) to a depth of 475mm. Deeper than these points, however, there is very little change in LOI% despite high variance in grain size. One hypothesis for this change in the relationship can be explained by the age of the sediment below this depth. This explanation assumes that there

is sufficient decomposition of organics in these layers to destroy the fluctuations that would have been observed in line with the changing grain characteristics. Conversely, the LOI% data from the core at R2 demonstrate a correlation throughout the core, with the strongest correlation in the top 475mm of the core as previously discussed. This absence of evidence of decomposition can be attributed to two factors. Firstly, the core was taken to a shallower depth than at L2, and secondly the rate of deposition is much faster, meaning that the layers are comparatively much younger than in L2. The shallowest layer in the core from R2, has an LOI% of approximately 3% which agrees with the surface sediment samples taken from the same area. The shallowest layer in the L2 core data displays a much higher LOI% than surface samples taken from a similar area. This could be attributed to non-representative sampling or the visible inclusion of plant roots into the core due to the sampling method.

5.4- Impact of temperature and river flow conditions on algal growth

To understand the impact that changing climates have on year to year algal growth, temperature and flow will be discussed jointly. As explained in Section 4.5, there is very little correlation between algal growth and antecedent flow conditions. The further regression analysis detailed in Section 4.5 confirmed this assertion.

The negative correlation between temperature and algal growth shown in Section 4.7 contradicts the proposed hypothesis that increased spring and summer temperatures would facilitate increased algal growth. One possible explanation for this effect is that nutrients are held in the frozen soil at lower temperatures and released when temperatures begin to rise again, leading to a high concentration of nutrients during periods of algal blooming. Figure 4.12 shows that the average daily minimum temperature over the study period often falls below freezing temperature, making this a viable assertion. This is somewhat reinforced by Melillo *et al* (1984) who stated that changes in water temperature can impact the nitrogen immobilization rate.

5.5- Nutrient Analysis

Figure 4.10 and Table 4.2 show varying nutrient concentrations throughout the estuary. For both nitrates and phosphates the highest concentrations are seen in the freshwater inputs and the areas immediately surrounding tributary mouths. Rice *et al* (2008) also show this relationship (Figure 5.4). As with the algal growth plot from the same study, there is an impact seen from 0.1 SDUs upstream, extending up to 6 SDUs downstream. The difference in concentrations can be explained using a simple mixing model to calculate ratios of seawater: freshwater. These ratios can be found using the mixing model formula:

$$Q_f/Q_s = (C_t - C_s)/(C_f - C_t)$$

Where Q_f/Q_s is the volumetric ratio of freshwater to seawater, C_t is the measured concentration, and C_f and C_s are the respective concentrations in the fresh and sea water samples. Results are displayed in Table 5.1. N concentrations were used to produce the ratios as P concentrations did not follow predicted patterns (see below).

Sample	**Ratio (fresh:sea)**
L1	7:1
L2	28:1
L3	1:5
R1	18:1
R4	1:2

Table 5.1-Ratios of Freshwater to Seawater using N concentrations. Freshwater concentrations taken from nearest freshwater source.

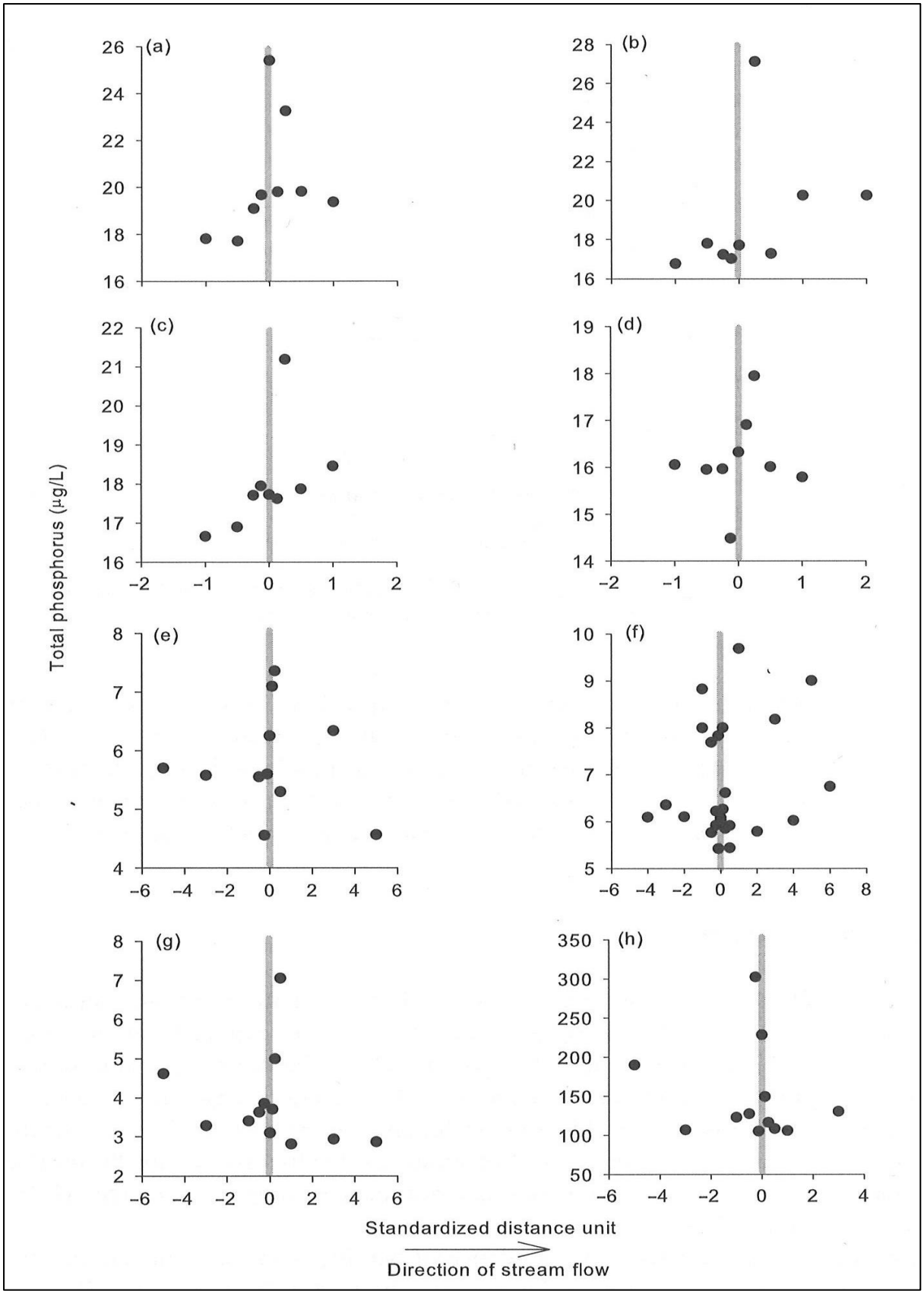

Figure 5.4-Scatterplots of total phosphorous vs. SDUs for the a) Rock, b) Taylor, c) Williams, d) Steele confluences on the Cedar River, e) Ruxell, f) Quartz and Hatchery confluences on Finney Creek and g) Jumbo and h) Falls Creek confluences on Bacon Creek (Rice *et al*, 2008).

Table 5.1 shows a wide range of freshwater concentrations throughout the estuary. There is increasing seawater mixing downstream shown by sites L2 and R4, with the former comprised of mostly freshwater while the latter sees the dominance of the marine inputs. The concentrations at L3 are noteworthy as they have a greater ratio of seawater to freshwater than R4 despite being higher upstream. As this site is located in a backwater and the samples were taken in low tide, it suggests that seawater dominates the intertidal areas when the tide is low.

The concentration data for phosphates also require some interpretation. In sites L1, R1 and L3, the nutrient concentration is higher than in the freshwater or seawater sources. It is possible that this is due to the large populations of seabirds that nest in these intertidal areas (SNH, 1996) when at low tide which could be adding phosphates in the form of waste, increasing them beyond the levels of the tributary inputs.

From these concentration data, it can be seen that the greatest nutrient concentrations are found in areas with the greatest influence of fresh water. P and N concentrations in the freshwater samples were generally higher than those of estuarine samples.

5.6- Factors Controlling Algae Growth

The above data suggest that there is no one factor which determines algal growth patterns, but that each of the factors considered (sediment type and size; river flow; air temperature; water nutrient concentrations) potentially affects algal growth in the estuary. The primary factor controlling algal growth is mean grain size (Figure 4.7). Regression analysis of mean grain size of surface sediment samples and LOI% using log transformed data shows a strong negative correlation ($p<0.001$; $N=62$; $R^2 = 0.74$). This relationship is further confirmed by examining the grain size and LOI% data from cores L2 and R2. This relationship can be explained partially by Jin *et al* (2005) who found that in sediments of similar composition the adsorption rates for phosphates was doubled while nitrate adsorption tripled in higher clay/lower sand concentrations (Table 5.2).

Properties	Sediments	
	East Taihu Lake	Wuli Lake
TP (mg kg^{-1})	451.3	819.2
TN (mg kg^{-1})	686.3	2190.5
Organic carbon (%)	1.87	3.16
CEC (meq 100 g^{-1})[2]	13.33	22.15
Grain size (μm)		
Clay, <4	10.80	13.35
Silt, 4–63	76.86	84.50
Sand, 63–500	12.20	2.14
Major element (%)		
SiO_2	66.93	67.74
Al_2O_3	11.63	12.38
Fe_2O_3	5.15	4.92
MnO	0.11	0.14
CaO	1.37	0.97

Table 5.2- Grain size distribution, chemical compositions and nutrient concentrations for different trophic sediments (Jin *et al*, 2005).

The nutrient concentrations from the water samples suggest a link with algal growth. The areas where the highest N and P concentrations were measured are in areas of high algal growth. However, this is based on a set of samples collected on one day only and requires further investigation, and consistent algal growth is also observed in the areas with the lowest observed nutrient concentrations, at L3 and R4. These data suggest that, while nutrients are important for the growth of algae in an area, the size of sediment, and therefore the rate of adsorption, is a much more important factor in determining the areas where algae can grow, as evidenced by the areas of low LOI% observed in the coarsest sediments near the mouth of the estuary.

Limitations of this study include the necessity to use data collected over different timescales and resolutions, such as comparing algal cover (annual measurement) with river flow data (daily data, aggregated seasonally) and water chemistry and sediment (point samples). Only a few water samples were available. Hence, determining the controls on algal growth requires careful analysis. For example, seasonal weather patterns also play a partial role in controlling algal growth. As detailed in Section 5.4 there is some correlation between spring temperature and algal growth. However, for a more detailed view of this relationship longer data sets for algal cover are required. Additionally, while seasonal flow variations do not appear to impact year to year algal growth, the impact that predicted flow rates have on deposition around the estuary does. As these flow rates directly control the amount and size of sediment being deposited in each area, it could be said that flow is a controlling factor in algal growth.

Following this study, it is clear that there are many ways in which the study of factors controlling algae growth can be improved. Most notably, the water nutrient data used in this study provides only a snapshot of the conditions that exist in the waters of the Ythan estuary. From Domburg *et al* (1998) we know that N and P input into the estuary has changed noticeably since 1960. For a much clearer picture of how this controls algae growth, continuous monitoring of water chemistry in the estuary, particularly in area which exhibit annual algae growth should be undertaken. Similarly, the recording of algal cover and locations on a smaller monthly or seasonal scale would also provide a much clearer picture of the growth patterns in the Ythan.

Chapter 6- Conclusions

The findings of this study highlight the impact that different anthropogenic and natural factors have on algal growth in the Ythan Estuary, Aberdeenshire. Using data from sediment and water samples taken in the field, the areas which are most at risk of eutrophication were established. Further observations were made using past temperature and flow conditions to try and establish the reasons for annual variance in algal growth.

The key findings of this study included an observed negative correlation between grain size and LOI% in the estuary. As shown in Figures 4.5 and 4.8, the greatest LOI% is seen in samples where mean grain size is below 100μm. Quantitative analysis of the LOI% data, along with the results shown in Figure 5.2, show a weak correlation between LOI% and algae growth, though this can be somewhat skewed by moisture content in samples, as described in Hoskins (2002). A weak negative correlation was found between average daily maximum spring temperatures and algal growth in the same year, while there was no calculable correlation between flow and algal growth, though the reliability of these results could be improved by monitoring seasonal algal biomass. Nutrients were observed in their highest concentrations in areas where there was the greatest influence of fresh water, highlighting the important of the salinity gradient in the Ythan. Various hypotheses were made based on the available literature regarding how each of these factors impacts algae growth. Figure 6.1 shows the extent to which each controls the growth of algae in the estuary.

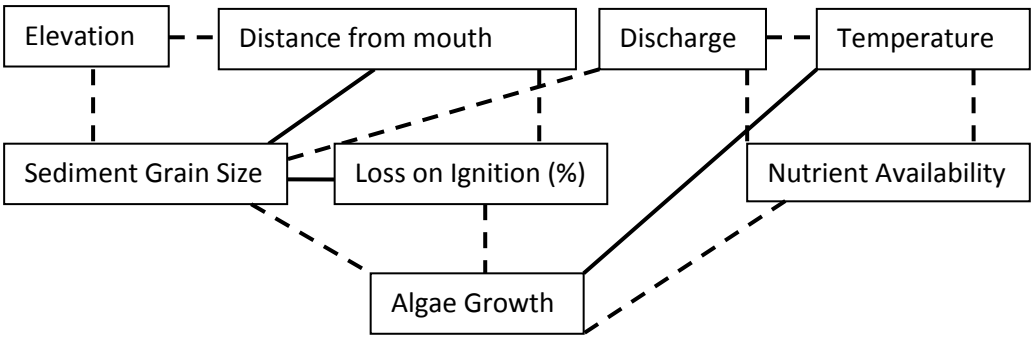

Figure 6.1- Links between observed factors in the Ythan Estuary. Dotted line denotes weak correlation, bold line denotes strong correlation.

It should be noted that the results contained in this study are only a snapshot of the active processes in the estuary, and therefore not representative of the full impact that any of these factors are likely to have. In order to better understand these factors more work needs to be done. To better understand variance in annual algal growth, total algae cover should be quantified for each year. With longer data on algae cover, a more representative study on the effect of discharge and temperature can be undertaken, allowing a more in-depth analysis of the observed correlations between algae growth and spring temperatures. For data on how depositional environments and controls impact the growth of algae in the Ythan, dating of sediment cores would allow an estuary-wide study on deposition rates. Finally, year-round monitoring of nutrient concentrations entering the estuary would allow a better understanding of how these affect annual variance in algal cover.

References

- Allen, G.P. Salomon, J.C. Bassoullet, P. Du Penhoat, Y. de Grandpré. C. (1980)- *Effects of tides on mixing and suspended sediment transport in macrotidal estuaries,* Sedimentary Geology, Vol 26, Issues 1-3, pp.69-90

- Balls, P.W. Macdonald, A. Pugh, K. Edwards, A.C. (1995)- *Long-term nutrient enrichment of an estuarine system: Ythan, Scotland (1958–1993),* Environmental Pollution, Vol 90, Issue 3, pp. 311-321

- Baxter, M.S. Farmer, J.G. McKinley, I.G. Swan, D.S. Jack, W. (1981)- *Evidence of the unsuitability of gravity coring for collecting sediment in pollution and sedimentation rate studies,* Environmental Science and Technology, Vol 15, pp. 843-846

- Beuselinck, L. Govers, G. Poesen, J. Degraer, G. Froyen, L. (1998)- *Grain-size analysis by laser diffractometry: comparison with the sieve-pipette method,* Catena, Vol 32, Issues 3-4, pp.193-208

- Boesch, D.F. (2002) - *Challenges and opportunities for science in reducing nutrient over-enrichment of coastal ecosystems*, Estuaries and Coasts, Vol 25, Issue 4, pp.886-900

- Boesch, D.F. (2002) – *Causes and consequences of nutrient over-enrichment of coastal waters,* International seminar on nuclear war and planetary emergencies, 26th session, World Scientific Publishing.

- Bolam, S.G. Fernandes, T.F. Read, P. Raffaelli, D. (2000) - *Effects of macroalgal mats on intertidal sandflats: an experimental study*, Journal of Experimental Marine Biology and Ecology, Vol 249, Issue 1, pp.123-137

- Cameron, W.M. Pritchard, D.W. (1963)-*Estuaries*. In Hill, M.N. (ed): *The Sea*, John Wiley and Sons, Vol 2, pp.306 – 324

- Cardoso, P.G. Leston, S. Grilo, T.F. Bordalo, M.D. Crespo, D. Raffaelli, D. Pardal, M.A (2010) - *Implications of nutrient decline in the seagrass ecosystem success,* Marine Pollution Bulletin, Vol 60, Issue 4, pp.601-608

- Carpenter, S.R. Caraco, N.F. Correll, D.L. Howarth, R.W. Sharpley, A.N. Smith, V.H. (1998)- *Nonpoint Pollution of Surface Waters with Phosphorus and Nitrogen,* Ecological Applications, Vol. 8, Issue 3, pp. 559-568

- Childers, D.L. McKellar, H.N. (1987)- *A simulation of saltmarsh water column dynamics,* Ecological Modelling, Vol 36, Issues 3-4, pp.211-238

- Childers, D.L. McKellar, H.N. Dame, R.F. Sklar, F.H. Blood, E.R. (1993)- *A Dynamic Nutrient Budget of Subsystem Interactions in a Salt Marsh Estuary,* Estuarine, Coastal and Shelf Science, Vol 36, Issue 2, pp.105-131

- Christiansen, T. Wiberg, P.J. Milligan, T.G. (2000)- *Flow and Sediment Transport on a Tidal Salt Marsh Surface*, Estuarine, Coastal and Shelf Science, Vol 50, Issue3, pp.315-331

- Cloern, J.E. (2001) - *Our evolving conceptual model of the coastal eutrophication problem,* Marine Ecology Progress Series, Vol 210, pp.223-253
- Czuba, J.A. Straub, T.D. Curran, C.A. Landers, M.N. Domanski, M.M. (2014)- *Comparison of fluvial suspended-sediment concentrations and particle-size distributions measured with in-stream laser diffraction and in physical samples,* Water Resources Research, AGU Publications
- D'Elia, C.F. Sanders, J.G. Boynton, W.R (1986)- *Nutrient enrichment studies in a coastal plain estuary: phytoplankton growth in large-scale, continuous cultures*, Canadian Journal of Fisheries and Aquatic Sciences, Vol 43, pp. 397-406
- Dawson, M. (1987)- *Sediment size variation in a braided reach of the Sunwapta River, Alberta, Canada,* Earth Surface Processes and Landforms, Vol 13, pp.699-618
- Dennsion, W.C. and Abal, E.G. 1999. Moreton Bay Study: A Scientific Basis for the Healthy Waterways Campaign, South East Queensland Water Quality Management Strategy, pp. 245
- Domburg, P. Edwards, A.C. Sinclair, A.H. Wright, G.G. Ferrier, R.C. (1998) *Changes in fertilizer and manurial practices during 1960-1990: Implications for N and P inputs to the Ythan catchment, NE Scotland*, Nutrient Cycling in Agroecosystems, Vol 52, pp.19-29
- Dronkers, J. (1986)- *Tidal asymmetry and estuarine morphology,* Netherlands Journal of Sea Research, Vol20, Issues 2-3, pp.117-131
- Ferguson, R.I. Cudden, J.R. Hoey, T.B. Rice, S.P. (2006)- *River system discontinuities due to lateral inputs: generic styles and controls*, Earth Surface Processes and Landforms, Vol 31, Issue 9, pp.1149-1166
- Flindt, M.R. Pardal, M.A. Lillebøb, A.I. Martins, I. Marques, J.C. (1999) - *Nutrient cycling and plant dynamics in estuaries: A brief review*, Acta Oecologica, Vol 20, Issue 4, pp.237-248
- Gale, S.J. Hoare, P.J. (1991)- *Quaternary sediments- petrographic methods for the study of unlithified rocks,* Belhaven Press, London
- Gallagher, D. L. Dietrich, A. M. Reay, W. G. Hayes, M. C. Simmons, G. M. (1996)- *Ground Water Discharge of Agricultural Pesticides and Nutrients to Estuarine Surface Water,* Groundwater Monitoring & Remediation, Vol 16, Issue 1, pp.118–129
- Grabowski, R.C. Droppo, I.G. Wharton, G. (2011) - *Erodibility of cohesive sediment: The importance of sediment properties*, Earth-Science Reviews, Vol 105, pp.101-120
- Green, D.R. (2005)- *Applying geospatial technologies to weedmat monitoring and mapping: the Ythan Estuary, NE Scotland*, Coastal and Marine Geospatial Technologies, Chpt 15
- Hoskins, B. (2002)- *Organic Matter by Loss on Ignition* , University of Maine

- Hull, S.C. (1987) - *Macroalgal mats and species abundance: a field experiment*, Estuarine, Coastal and Shelf Science, Vol 25, Issue 5, pp.519-532
- Jackson, D. (1986)- *A manually operated core sampler suitable for use on fine particulate sediments,* Estuarine, Coastal and Shelf Science, Vol 23, pp.419-421
- Jin, X. Wang, S. Pang, Y. Zhao, H. Zhou, X. (2005)- *The adsorption of phosphate on different trophic lake sediments, Colloids and Surfaces*, Physicochemical and Engineering Aspects, Vol 254, Issues 1–3, pp.241-248
- Karunarathna, H. Reeve, D. Spivack, M. (2008)- *Long-term morphodynamic evolution of estuaries: An inverse problem,* Estuarine, Coastal and Shelf Science, Vol 77, Issue 3, pp.385-395
- Kelly, W.E. Gularte, R.C. (1981)- *Erosion Resistance of Cohesive Soils,* Journal of the Hydraulics Division, Vol 107, Issue 10, pp.1211-1224
- Madsen, A.T. Murray, A.S. Andersen, T.J. Pejrup, M. Breuning-Madsen, H. (2005)- *Optically stimulated luminescence dating of young estuarine sediments: a comparison with 210Pb and 137Cs dating*, Marine Geology, Vol 214, Issues 1–3, pp.251-268
- Maier, G. Nimmo-Smith, R. J. Glegg, G. A. Tappin, A. D. Worsfold, P. J. (2009)- *Estuarine eutrophication in the UK: current incidence and future trends,* Aquatic Conservation: Marine and Freshwater Ecosystems, Vol 19, pp. 43–56
- Maroulis, J.C. Nanson, G.C. (1996)- *Bedload transport of aggregated muddy alluvium from Cooper creek, central Australia: A flume study*, Sedimentology, Vol 43, Issue 5, pp.771-790
- Melillo, J. M. Naiman, R. J. Aber, J. D. Linkins, A. E. (1984)- *Factors Controlling Mass Loss and Nitrogen Dynamics of Plant Litter Decaying in Northern Streams,* Bulletin of Marine Science, Vol 35, Issue 3, pp.341-356
- Montel, Y. Oudot, C. (1988)- *A high sensitivity method for the determination of nanomolar concentrations of Nitrate and Nitrite in seawater with a technicon autoanalyzer II,* Journal of Marine Chemistry, Vol 24, Issues 3-4, pp.239-252
- Nielsen, N. Nielsen, J. (2002)- *Vertical Growth of a Young Back Barrier Salt Marsh, Skallingen, SW Denmark,* Journal of Coastal Research, Vol 18, Issue 2, pp.287-299
- Officer, C.B. (1981)- *Physical dynamics of estuarine suspended sediments,* Marine Geology, Vol 40, Issues 1-12, pp.1-14
- Persson, G. Jansson, M. (1988)- *Phosphate Uptake and Utilization by Bacteria and Algae,* From: Phosphorous in Freshwater systems, Springer, pp.177-189
- Pihl, L. Svenson, A. Moksnes, P.O. Wennhage, H. (1999) - *Distribution of green algal mats throughout shallow soft bottoms of the Swedish Skagerrak archipelago in relation to nutrient sources and wave exposure*, Vol 41, Issue 4, pp.281-294

- Pugh, K.B. (1993)- *The nutrient status of the Ythan catchment and estuary,* North East River Purification Board, Technical Report 93/1
- Raffaelli, D. (1999) - *Nutrient enrichment and trophic organisation in an estuarine food web*, Acta Oecologica, Vol 20, Issue 4, pp.449-461
- Raffaelli, D.G. Raven, J.A. Poole, L.J. (1998)- *Ecological impact of green macroalgal blooms,* Oceanography and Marine Biology, Issue 36, pp.97-125
- Rennie, A.F. Hansom, J.D. (2011)- *Sea level trend reversal: Land uplift outpaced by sea level rise on Scotland's coast,* Geomorphology, Vol 125, pp. 193-202
- Rice, S.P. Kiffney, P. Greene, C. Pess, G. (2008)- *The ecological importance of tributaries and confluences,* in-River Confluences, Tributaries and the Fluvial Network, John Wiley, pp.209
- Rice, S. Ferguson, R.I. Hoey, T. (2006)- *Tributary control of physical heterogeneity and biological diversity at river confluences,* Canadian Journal of Fisheries and Aquatic Sciences, vol. 63, pp.2553-2566
- Rice, S. (1998) - *Which tributaries disrupt downstream fining along gravel-bed rivers?* Geomorphology, Vol 22, Issue 1, pp.39-56
- Schlager, W. (1993)- *Accommodation and supply—a dual control on stratigraphic sequences,* Sedimentary Geology, Vol 86, Issues 1–2, pp. 111-136
- Sheffield, A.T. Healy, T.R. McGlone, M.S. (1995)- *Infilling Rates of a Steepland Catchment Estuary, Whangamata, New Zealand,* Journal of Coastal Research, Vol 11, Issue 4, pp.1294-1308
- Shennan, I. Peltier, W.R. Drummond, R. Horton, B. (2002) *Global to local scale parameters determining relative sea-level changes and the post-glacial isostatic adjustment of Great Britain*, Quaternary Science Reviews, Vol 21, Issues 1–3, pp. 397-408
- SNH (1996)- *Coastal processes and management of Scottish Estuaries III,* Scottish Natural Heritage Review, No. 52
- Stove, G.C. (1978)- *The hydrography, circulation and sediment movements of the Ythan Estuary*, PhD Thesis (unpublished), University of Aberdeen
- Temmerman, S. Moonen, P. Schoelynck, J. Govers, G.Bouma, T.J. (2012)- *Impact of vegetation die-off on spatial flow patterns over a tidal marsh,* Geophysical Research Letters, Vol 39, Issue 3
- Tolhurst, T.J. Black, K.S. Shayler, S.A. Mather, S. Black, I. Baker, K. Paterson, D.M. (1999)- *Measuring the in situ Erosion Shear Stress of Intertidal Sediments with the Cohesive Strength Meter (CSM),* Estuarine, Coastal and Shelf Science, Vol 49, Issue 2, pp. 281-294

- Uncles, R.J. Stephens, J.A. Smith, R.E. (2002)- The dependence of estuarine turbidity on tidal intrusion length, tidal range and residence time, Continental Shelf Research, Vol 22, Issues 11-13, pp.1835-1856

- Valle-Levinson, A. (ed, 2010)- Contemporary Issues in Estuarine Physics, Cambridge University Press

- Vanni, M.J. Renwick, W.H. Headworth, J.L. Auch, J.D. Schaus, M.H. (2001)- *Dissolved and particulate nutrient flux from three adjacent agricultural watersheds: A five-year study,* Biogeochemistry, Vol 54, Issue 1, pp. 85-114

- Vleeschouwer, F. Chambers, F.M. Swindles, G.T. (2010)- *Coring and sub-sampling of peatlands for palaeoenvironmental research,* Mires and Peat, Vol 7

- Widdows, J. Brinsley, M. Elliott, M. (1998) - *Use of in situ flume to quantify particle flux*. In: Black, K. S, Paterson, D. M and Cramp, A. (eds) *Sedimentary Processes in the Intertidal Zone*, Geological Society, London, Special Publications, Vol 139, pp.85-97

- Wrath, W.F. (1936)- *Contamination and compaction in core sampling,* Science, Vol 84, pp.537-538

Appendices

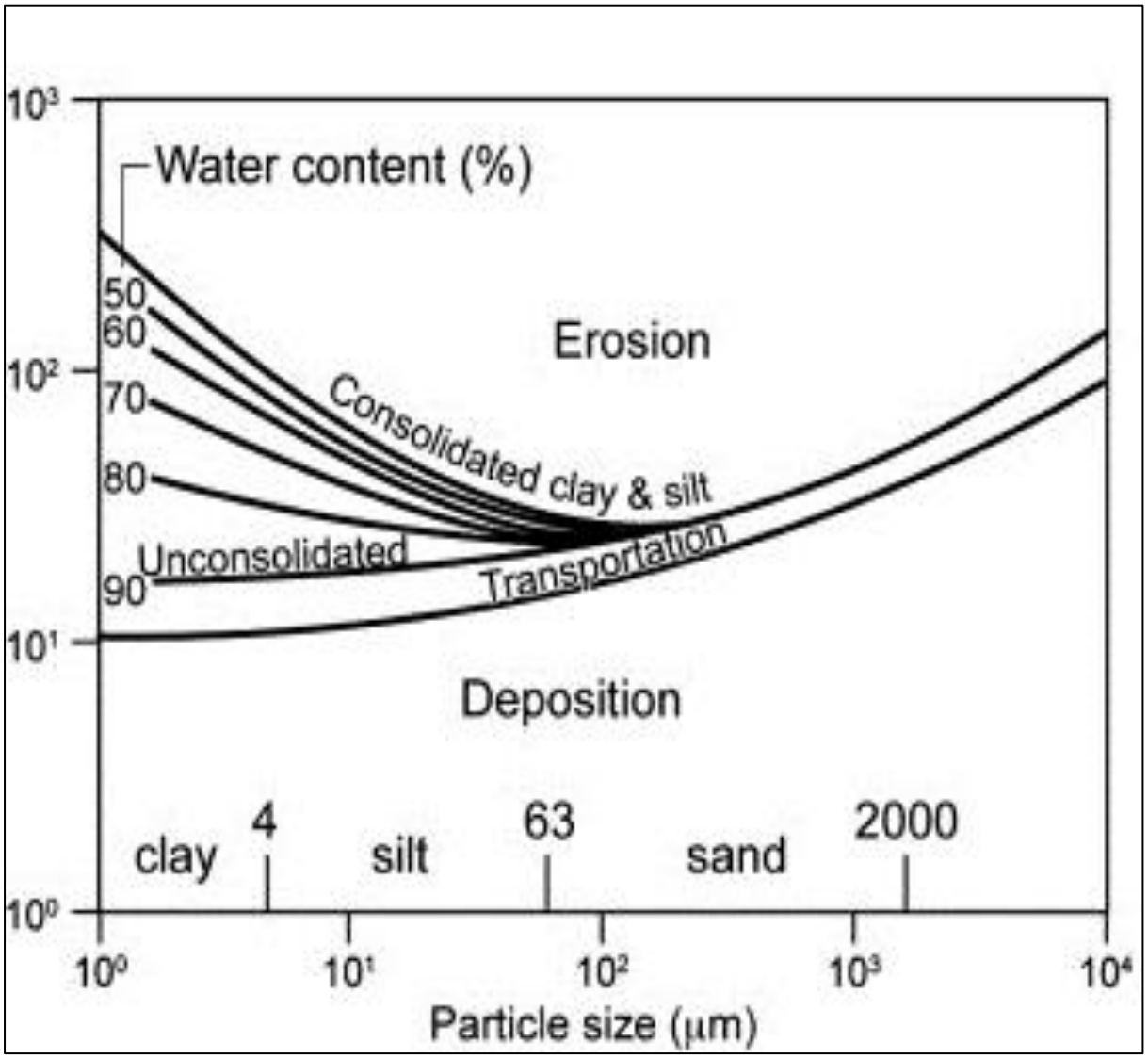

Appendix 1- Postma diagram of particle size vs velocity (Grabowski et al, 2011).

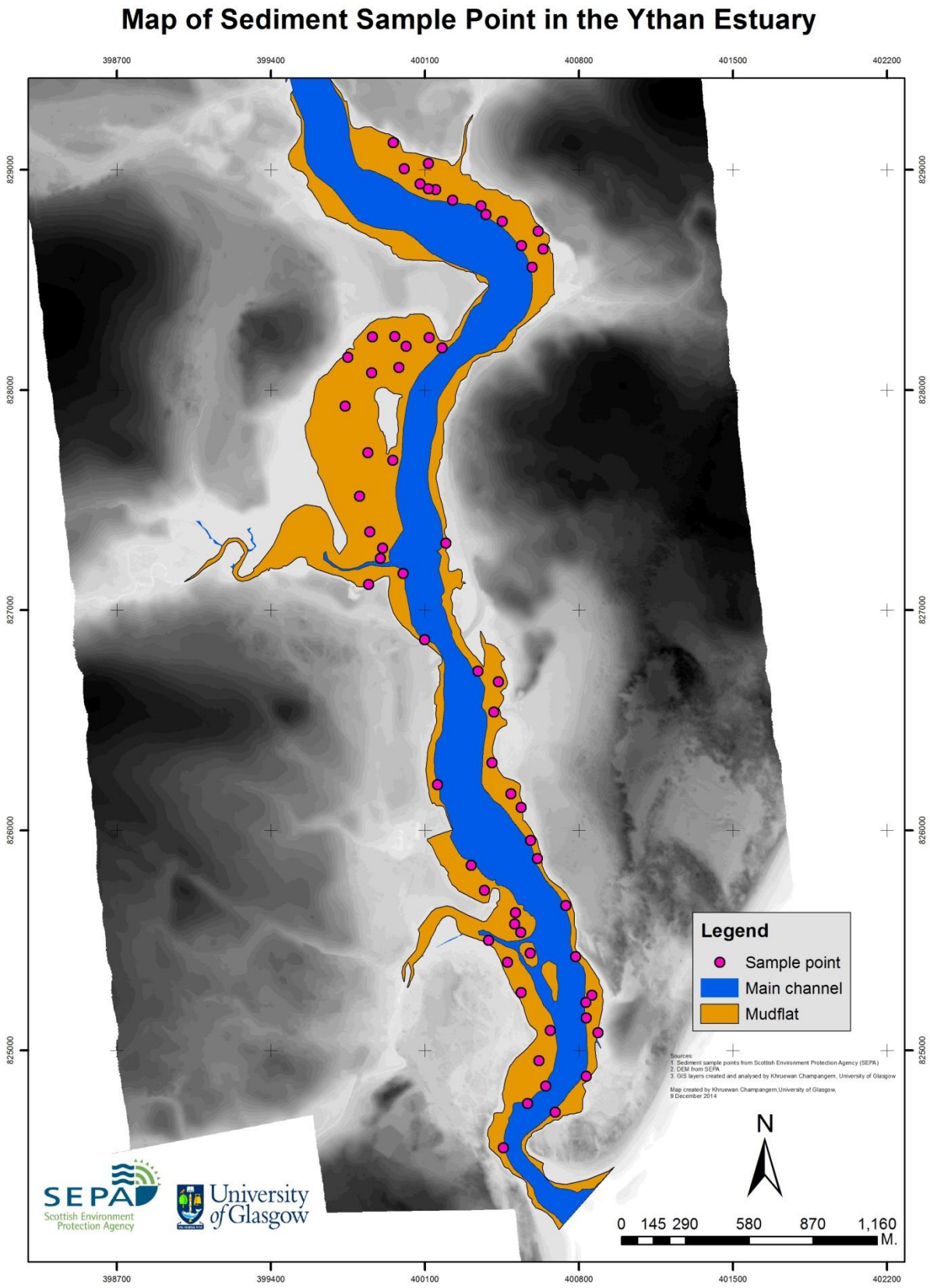

Appendix 2- Sediment Sample Locations. Locations provided by SEPA (file SEPA STATIONS from Clare Scanlan).

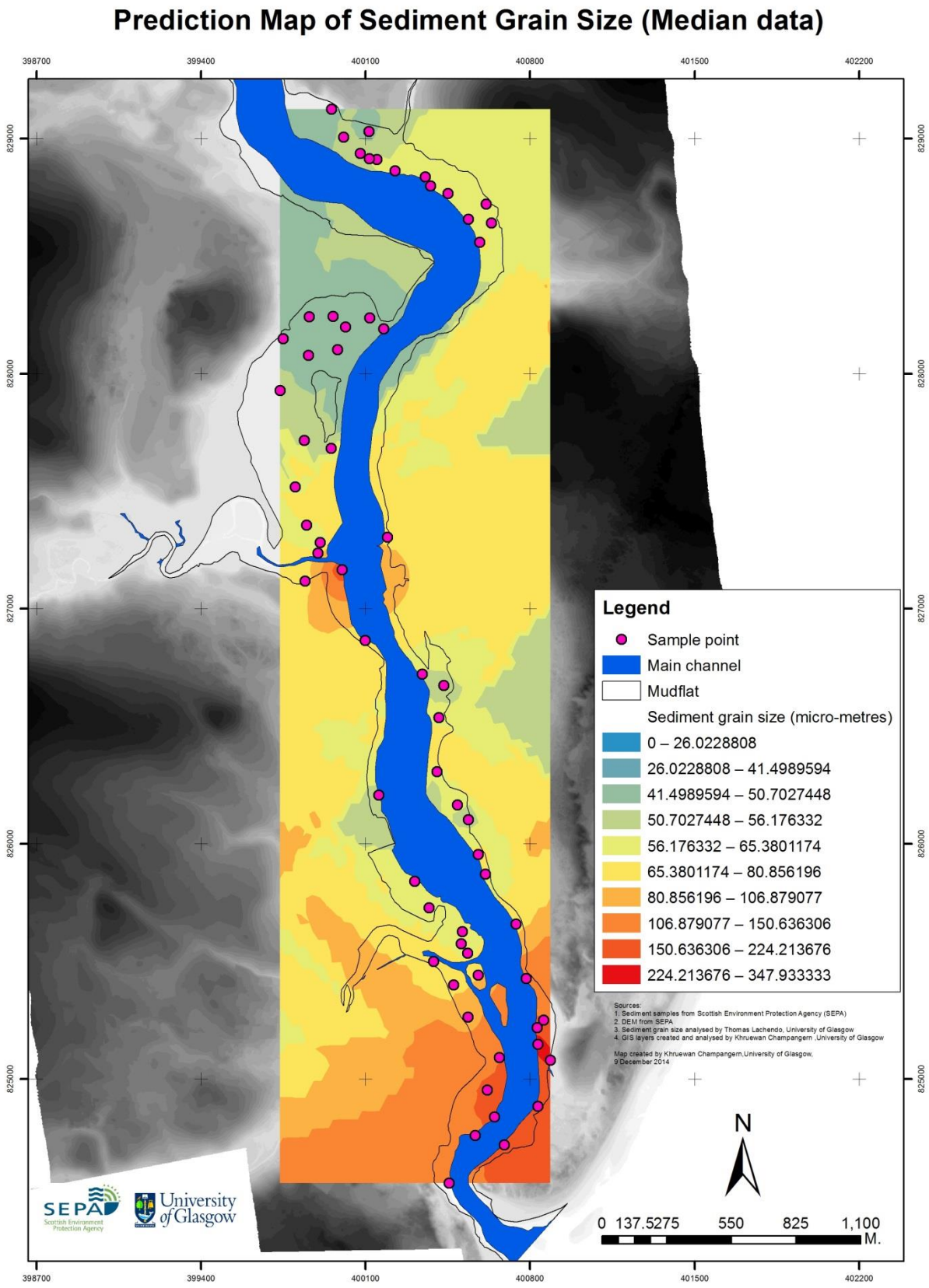

Appendix 3- Median grain size of surface sediment samples interpolated using kriging.

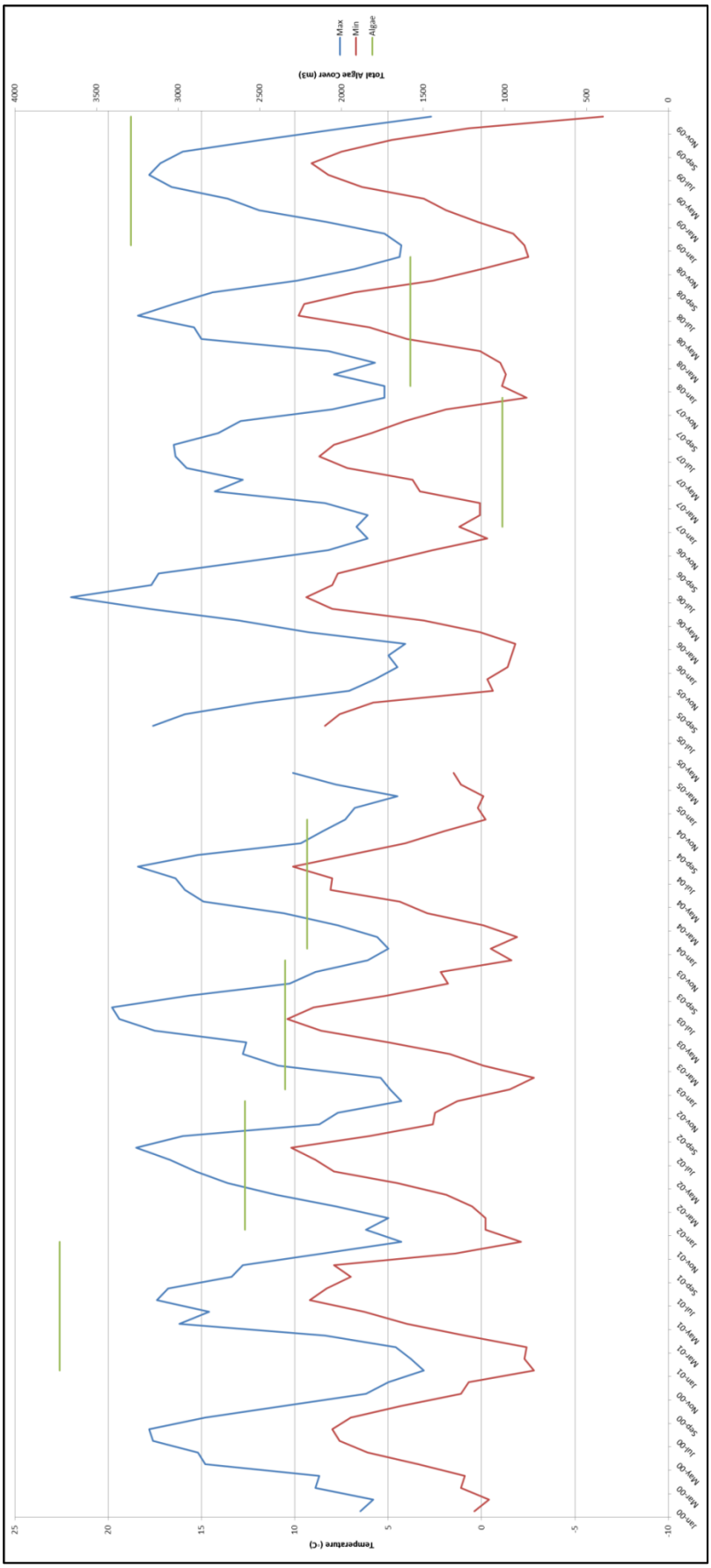

Appendix 4- Monthly Max and Min temperature vs Algae Cover.

Temperature	Spring Max	Summer Max	Autumn Max	Winter Max	Spring Min	Summer Min	Autumn Min	Winter Min
R2 Value	-0.76	-0.25	0.16	-0.10	-0.72	-0.28	0.28	0.21
P Value	0.05	0.59	0.73	0.84	0.07	0.54	0.55	0.65
Flow	Spring		Summer		Autumn		Winter	
R2 Value	0.489		-0.269		-0.505		0.148	
P Value	0.265		0.559		0.248		0.752	

Appendix 5- Pearson correlation coefficient and p-value for Flow and Temperature vs. Algae Growth.

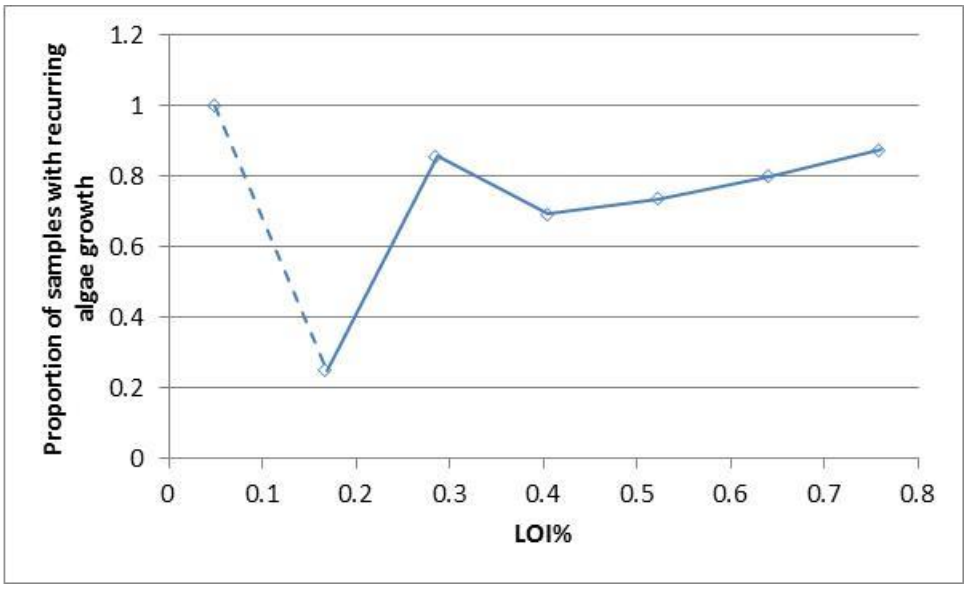

Appendix 6 - Proportion of samples with recurring algal growth as a function of LOI% (see Figure 5.2).